



University of  
Massachusetts  
Amherst

## **Advancing Aquatic Biodiversity and Relative Abundance Monitoring: Employing Environmental DNA (eDNA) to Assess Diadromous Fish Populations and Ecosystem Health**

Item Type	Dissertation (Open Access)
Authors	Garner, James
Rights	Attribution-NonCommercial-NoDerivatives 4.0 International
Download date	2026-05-11 01:59:08
Item License	<a href="http://creativecommons.org/licenses/by-nc-nd/4.0/">http://creativecommons.org/licenses/by-nc-nd/4.0/</a>
Link to Item	<a href="https://hdl.handle.net/20.500.14394/57386">https://hdl.handle.net/20.500.14394/57386</a>

Advancing Aquatic Biodiversity and Relative Abundance  
Monitoring: Employing Environmental DNA (eDNA) to Assess  
Diadromous Fish Populations and Ecosystem Health

A Dissertation Presented

By

James Graham Garner

Submitted to the Graduate School of the  
University of Massachusetts Amherst in partial fulfillment  
of the requirements for the degree of

DOCTOR OF PHILOSOPHY

September 2025

Environmental Conservation

© Copyright by James G. Garner 2025  
All Rights Reserved

# Advancing Aquatic Biodiversity and Relative Abundance Monitoring: Employing Environmental DNA (eDNA) to Assess Diadromous Fish Populations and Ecosystem Health

A Dissertation Presented

By

JAMES GRAHAM GARNER

Approved as to style and content by:

\_\_\_\_\_

Adrian Jordaan, Co-Chair

\_\_\_\_\_

Michelle Staudinger, Co-Chair

\_\_\_\_\_

Allison H. Roy, Member

\_\_\_\_\_

Jeremy Andersen, Member

\_\_\_\_\_

Paige Warren, Department Head,  
Environmental Conservation

\_\_\_\_\_

Kristina Stinson, Graduate Program Director,  
Environmental Conservation

# DEDICATION

This dissertation is dedicated to my dogs, Goats and Tango. You were more than companions—you were my anchors, my shadows, my strength when I was weak. Goats, you carried me as far as you could on this journey, and it turns out that it was all the way to the finish line. Your gentle, attentive love helped me weather some of the hardest days, and I will always be grateful for every moment we shared. Tango, to imagine a better companion is impossible. You were an extension of my being, and your steady presence gave me the strength to take the first step on this path. You both left too soon, but your spirits carried me forward. I will always love you, sweet Trangus and lil' buddy.

Finally, this dissertation is dedicated to my family: Jim, Debbie, and Jordan. Without your unwavering love and support, this journey would not have been possible. Dad, your integrity and work ethic inspires me daily to be better. Mom, your warmth and playfulness have shown me how to not take things too seriously, and to persist even when times are tough. Jor, your brilliance and empathy have always been a shining beacon to me for what might be possible if I apply myself. I am so grateful for the life you have helped me lead. I will not let your love and kindness go to waste.

# ACKNOWLEDGEMENTS

No one accomplishes anything on their own. Mentors, collaborators, colleagues, friends, family, my partner, and my pets all contributed to this five-year effort in different ways. I would like to thank my Co-Advisors Dr. Adrian Jordaan and Dr. Michelle Staudinger for believing in me. Adrian, your willingness to help me with anything at the drop of a hat, standards for scientific excellence, and your supportive, fun lab environment helped maintain my sanity and positive disposition throughout this experience. Michelle, your professionalism, generosity, and unwavering support inspired confidence in me every step along the way. You always pushed me to look, think, and dig deeper, and to produce the best quality science I could. Both of your mentorship and guidance have been invaluable to me, and I look forward to a career of collaboration with you both.

Next I would like to sincerely thank my committee members. Dr. Allison Roy, and Dr. Jeremy Andersen. Allison, your lab group, lab meetings, and lab in general were a second home to me. You were the first person I reached out to when I started this journey. Your support, community, feedback, and kindness helped make my experience at UMass Amherst so special. Jeremy, without your generosity, patient explanations, and laboratory support, literally none of this dissertation would have been possible. I aspire to be the kind, collaborative, professional, and excellent scientist you both are. Thank you from the bottom of my heart.

I would also like to thank my first professional collaborators during this whole PhD process: the Diadromous Fisheries Team of Biologists and Biological Technicians at the Massachusetts Division of Marine Fisheries (MA DMF). Brad Chase, the leader of the

Diadromous Fisheries Team, was the first person to believe in and support me on this journey. Your letters of support for both my roles at the JRWA and here at UMass Amherst helped me start this journey. Your belief in me, and your willingness to have your team help me collect water samples throughout the 2021 diadromous fish runs will be a debt I can never repay, and a mark of pride I carry with me throughout my life. I cannot thank you enough for your kindness and support. John Sheppard, without your dedicated, meticulous attention to detail and professionalism, this project would not have been possible. I am honored to call you a friend and colleague. Thank you for all the hard work you put in to help make this project not only possible, but excellent. Trevor Burns, I know how hard you worked to make the samples you collected for me the best you possibly could. I was so grateful and happy to know a friend was out there helping every day, sending me updates. I am honored for your help and friendship, thank you, brother. Sarah Turner, your leadership when I was your Biological Technician, and your willingness to help will always be appreciated. Thank you for being a part of my success. Ben Gahagan, your knowledge and experience were invaluable to this project, thank you for all of your help, and see you at lab meeting. Ed and Jimmy - y'all are the best, and have always helped me stay sane, either with fond memories, or fun plans. It has been a true privilege to collaborate with such a diverse and inspiring group of project partners throughout the course of this PhD. Working alongside you has been one of the most rewarding and meaningful aspects of this journey.

Next, I would like to thank the members of the “eDNA Ecology Club”, a group of dedicated undergraduate researchers I had the absolute honor of mentoring, working with, and watching grow as professionals and scientists. Without your hard work, none of this

would have been possible, thank you from the bottom of my heart, and know you will always have an exemplary reference, a colleague, and friend in me. Thank you Gwynne Hayes (the OG), Eva Kozol, Gwen Church, Anya Quaglietta, Lexi Lattanzio, Nina Balagula, and Lea Luetjens.

I would like to thank the members of the Jones River Watershed Association (JRWA). I learned what it meant to be the steward of a truly special place during my time at the Landing. I will never forget the feelings associated with doing everything we could with so little, trying to do so much. I will always be grateful to the JRWA, its board, and its members for their belief in me, and the work we were able to do together. It is my genuine hope that the research presented here might be useful to you and your mission and might help in winning you some much-deserved grant funding in the future.

I wouldn't have made it this far without the support of my lab community. I would like to thank the Roy, Jordaan, and Staudinger lab groups. Y'all were my family here at UMass, and I am so lucky to have the privilege of knowing each and every one of you. Thank you, Abhishek Kumar, Alexa Hershberger, Amy Teffer, Anna Baynes, Ayla Skorupa, Ben Gahagan, Doug Bishop, Elsa Goerig, Jackie Stephens, Jenny Rogers, Julia Vineyard, Julian Burgoff, Kate Abbott, Katrina Zarella Smith, Lian Guo, Matt Devina, Sez Guitart, Shelby Truckenbrod, and Stefanie Farrington for your friendship and support.

I would also like to thank my amazing broader community of friends and colleagues here at UMass Amherst: John Swenson, Jamie Stoll, Nadia Fernandez, Blair Bentley, Estefany Argueta, Kate Buckman, Ethan Rutledge, Beth Rogers, Cosmo Laviola, Ayo O'Uhuru, David Ferris, Nargis Mirzaie, Roisin Kirby, Lena Fletcher, Laura Hitchcock, and Katrina

Phillips. Y'all made UMass fun, and I hope I get to keep having fun with all of you for a long while yet.

Some are silver and others gold. I would like to thank whichever one of those means old friends, without whom I would not have been able to navigate half of the code, mapping, and hurdles that come with a second round of grad school. Thank you Nick Ray, Drew Trlica, Karina Scavo Lord, Nate Fuller, Dan Hall, Paul Tanner, Will Caffry, Fauve, Atlas, Solenne, Scott Leathers, Pat Whetsel, JJ Sullivan, Joe Pelayo, and Sarah Pelayo.

Finally, I would like to thank my partner, Linnea Winter. You have been my calm harbor in every storm. You have shown me the meaning of what it is to be seen and loved fully. I cannot fathom the odds (detection probability - lol) that I was lucky enough to find you, and luckier still that you would love me. This dissertation would not exist without your unwavering support. Thank you so much for being you, your love, and your support. You have my heart.

# ABSTRACT

## Advancing Aquatic Biodiversity and Relative Abundance Monitoring: Employing Environmental DNA (eDNA) to Assess Diadromous Fish Populations and Ecosystem Health

SEPTEMBER 2025

JAMES GRAHAM GARNER, B.A., UNIVERSITY OF COLORADO, BOULDER

M.S., BOSTON UNIVERSITY

Ph.D., UNIVERSITY OF MASSACHUSETTS AMHERST

Directed by: Professor Adrian Jordaan and Professor Michelle Staudinger

Environmental DNA (eDNA) analyses allow for the detection of species by isolating and analyzing genetic material shed into the environment. Despite their growing use, eDNA methods remain constrained by uncertain detection probabilities, limited calibration with traditional monitoring, signal variability, and inconsistent methods. This dissertation explores the functional application of eDNA for ecological monitoring and fisheries management across three complementary studies. In Chapter Two, I used eDNA metabarcoding to assess aquatic vertebrate and diadromous fish biodiversity after the Elm Street Dam removal in the Jones River watershed. From 2020 to 2021, species richness declined at downstream sites, while upstream sites gained richness but lost functional diversity. Multivariate statistical analyses revealed significant temporal and spatial differences in community composition, consistent with early-stage ecological restructuring. In Chapter Three, I developed mechanistic and statistical models to

estimate river herring abundance across three connected ponds using log-transformed eDNA concentrations from ten synchronized sampling events. A single electronic resistivity fish counter in the most downstream pond served as an anchor for calibration. eDNA concentrations tracked two-day and cumulative fish counts well (site-level  $R^2 = 0.94$ ). Predictive accuracy declined in a watershed-scale linear model ( $R^2 = 0.58$ ), but improved when a linear mixed model was used that accounted for basin volume and distance from the e-count station ( $R^2 = 0.76$ ). I then developed a mechanistic model incorporating site-specific scaling based on hydrological distance, basin surface area, and DNA decay. The best-performing models, using uniform sensitivity-scaled exponents ( $\alpha = 0.01$ ) at site ( $R^2 = 0.98$ ) and watershed ( $R^2 = 0.97$ ) scales demonstrated eDNA's potential to estimate fish abundance at sites unsampled by traditional methods using a single traditional anchor count. In Chapter Four, I compared eDNA quantitative polymerase chain reaction (qPCR) estimates with four traditional fish relative abundance monitoring methods across seven case studies. eDNA aligned closely with resistivity counters, electrofishing, and video surveys, but not fyke nets. A multispecies occupancy model highlighted higher detection certainty for eDNA approaches and exposed traditional method-specific detection biases. Together, these studies demonstrate eDNA's utility for scalable, quantitative ecological monitoring, advancing data-driven frameworks for biodiversity assessment and resource management in aquatic ecosystems.

TABLE OF CONTENTS

DEDICATION ..... iv

ACKNOWLEDGEMENTS ..... v

ABSTRACT ..... ix

LIST OF TABLES ..... xv

LIST OF FIGURES ..... xvii

CHAPTER 1.....17

INTRODUCTION.....17

Dissertation Objectives.....22

CHAPTER 2.....25

ENVIRONMENTAL DNA METABARCODING REVEALS RAPID AQUATIC  
COMMUNITY SHIFTS AND DIADROMOUS FISH RECOLONIZATION  
FOLLOWING MAINSTEM DAM REMOVAL .....25

Introduction.....25

Methods .....28

    Study Area and Site Selection .....28

    eDNA Sample Collection and Storage.....29

    eDNA Filtration and Extraction .....30

    Metabarcoding and Bioinformatics .....30

Data Analysis .....32

    Assessing Sampling Effort.....32

    Year to Year Assessment of Locations Upstream and Downstream of the Former Dam  
    .....34

    Species Richness, Evenness, and Community Composition (Alpha and Beta  
    Diversity).....34

    Functional Diversity Trait Data .....36

Substrate-Specific Trait Responses to Dam Removal .....	39
Results.....	39
Assessing Sampling Effort.....	40
Year to Year Assessment of Locations Upstream and Downstream of the Former Dam	
.....	40
Species Richness, Evenness, and Community Composition (Alpha and Beta	
Diversity).....	40
Functional Diversity Trait Data .....	44
Substrate-Specific Trait Responses to Dam Removal .....	46
Discussion .....	47
Disturbance and species turnover .....	48
Diadromous Species Turnover Following Dam Removal .....	51
eDNA use in monitoring biodiversity.....	54
A path forward.....	55
CHAPTER 3.....	79
ENVIRONMENTAL DNA FOR FISHERIES MANAGEMENT: ENHANCING	
ABUNDANCE MONITORING WITH SPATIAL, TEMPORAL, AND	
ENVIRONMENTAL INSIGHTS.....	79
Introduction.....	79
Methods .....	81
Study System.....	81
Electronic Herring Counter Data Collection.....	82
eDNA Sample Collection.....	82
Environmental Data Collection .....	83
eDNA Filtration .....	83
DNA Extraction .....	84
DNA Sample Preparation.....	84
qPCR Assay Design .....	85
Conversion of C <sub>q</sub> Values .....	86
Calibrating eDNA and Traditional Methods .....	86
Spatial, Biological, and Environmental Effects .....	88

Mechanistic Allocation of Fish Abundance from eDNA in a Hydrologically Connected Pond System.....	89
Results.....	92
Calibrating eDNA and Traditional Methods .....	92
Spatial, Biological, and Environmental Effects .....	93
Mechanistic Allocation of Fish Abundance from eDNA in a Hydrologically Connected Pond System.....	94
Discussion .....	96
 CHAPTER 4.....	 113
 TOWARDS A UNIFIED APPROACH FOR FISHERIES ABUNDANCE ESTIMATION: INTEGRATING EDNA AND TRADITIONAL METHODS THROUGH DETECTION PROBABILITY .....	 113
Introduction.....	113
 Methods .....	 116
Study Areas and Study Species .....	116
Traditional Monitoring Methods .....	118
Electronic Herring Counter: River Herring.....	118
Video Monitoring: River Herring .....	118
Electrofishing: American Shad.....	119
Fyke Nets: Rainbow Smelt.....	119
Environmental DNA Methods.....	119
eDNA Sample Collection.....	119
eDNA Processing and Analysis .....	120
Statistical Analyses .....	122
Data Preparation .....	122
Relative Abundance Estimation Using Bayesian Hierarchical Models.....	123
Detection Probability Estimation Using Bayesian Occupancy Models.....	124
Comparison of Detection Probabilities.....	125

Results.....	127
Relative Abundance Calibration Using Bayesian Hierarchical Models .....	127
Detection Probability Estimation Using Bayesian Occupancy Models.....	128
Site-Specific Comparisons of Detection Probabilities .....	129
Frequentist Validation of Detection Relationships .....	130
Discussion .....	131
Calibration and Detection .....	131
Monitoring and Management .....	133
Future Research .....	136
CHAPTER 5.....	153
CONCLUSIONS .....	153
Collaborators and Stakeholder Engagement.....	157
Foundation for future research .....	157
Lessons Learned .....	157
eDNA: from black box to repeatable science.....	159
Future Research.....	160
BIBLIOGRAPHY .....	165

## LIST OF TABLES

Table	Page
2.1. Rarefaction modeling results for 19 sites in the Jones River watershed, including estimated species richness, fraction of sampling effort required to reach asymptotic richness, and estimated number of field samples needed to reach rarefaction asymptote per year and cumulatively.....	58
2.2. Site-level observed species richness across spatial and temporal scales in the Jones River watershed.....	59
2.3. Site-level diadromous species richness across temporal scales in the Jones River watershed.....	60
2.4: Site-level detection frequency of aquatic species across years and stream positions in the Jones River watershed.....	61
2.5. Conservation and invasion status of selected fish species detected in the Jones River watershed.....	63
2.6. PERMANOVA results comparing functional trait and taxonomic community composition across sites and years in the Jones River watershed.....	64
2.7. Results of Wilcoxon rank-sum tests comparing functional diversity metrics across sites and years in the Jones River watershed.....	65
3.1. Basin volumes and distances from fish counter. Volume and spatial data for four ponds and pools near the fish counter in the Monument River Watershed, Massachusetts, USA.....	102
3.2. qPCR assay components for river herring detection. Gene target, synthetic gene block, primer sequences, and probe used for species-specific detection of river herring (alewife and blueback herring) targeting the ND2 mitochondrial gene.....	102
3.3. Summary of model performance metrics across sites, temporal windows, and scaling approaches.....	103

3.4. Sampling and amplification success across sites. Total number of sampling dates and number of successful amplifications (in at least one of two replicates) per site during the 2021 river herring monitoring period.....	104
3.5. Correlation strength and statistical significance of eDNA-based relative abundance estimates across trial temporal sampling windows. R <sup>2</sup> values and associated p-values for correlations between eDNA signal and fish counts across increasing temporal sampling windows (3, 6, and 9 days).....	104
3.6. Best-performing temporal bin models for predicting eDNA signal.....	105
3.7. Effect sizes and significance of predictors in a multiple linear regression model estimating log-transformed 2-day fish counts.....	105
3.8. AIC model selection and performance metrics for predicting 2-day binned river herring counts.....	106
4.1. Abundance metrics used in eDNA monitoring and fisheries management.....	139
4.2. Bayesian hierarchical model results calibrating eDNA abundance to traditional fish monitoring methods.....	141
4.3. Site-level detection probabilities for eDNA versus traditional fish monitoring methods using Bayesian hierarchical occupancy models.....	142
4.4. Estimates of eDNA detection probabilities when traditional methods fail, based on empirical and Bayesian models. Empirical and Bayesian estimates of eDNA detection probabilities when traditional methods fail to detect a species.....	142
4.5. Bayesian model comparisons evaluating the relationship between eDNA and traditional detection methods, with and without site-level effects.....	143
4.6. Statistical comparisons between eDNA and traditional detection methods using logistic regression, chi-squared tests, and t-tests.....	143

## LIST OF FIGURES

Figure	Page
2.1. Map of the Jones River Watershed, in Southeastern Massachusetts. ....	66
2.2. Rarefaction curves comparing upstream and downstream communities across years. ....	67
2.3. Site-specific rarefaction curves for four representative locations with complete sampling in 2020 and 2021. ....	68
2.4. Non-metric multidimensional scaling (NMDS) plots visualizing aquatic vertebrate community composition across upstream and downstream sites in the Jones River watershed based on eDNA metabarcoding data. ....	69
2.5. Non-metric multidimensional scaling (NMDS) plots showing patterns in diadromous fish community composition across upstream and downstream sites in the Jones River watershed based on eDNA metabarcoding data. ....	70
2.6. Violin plots showing multivariate dispersion (distance to centroid) for diadromous fish communities in the Jones River watershed, based on eDNA metabarcoding data and Bray–Curtis dissimilarities. ....	71
2.7. Comparison of functional diversity metrics across upstream and downstream communities in the Jones River watershed (2020–2021). ....	72
2.8. Functional diversity metrics across years (2020 vs. 2021) within downstream, upstream, and watershed-wide communities. ....	73
2.9. Taxonomic heat trees of aquatic vertebrate communities detected via eDNA metabarcoding across the Jones River watershed in 2020 (A.), 2021 (B.), and both years combined (C.). ....	74
2.10. Taxonomic heat trees of aquatic vertebrate communities detected via eDNA metabarcoding at downstream sites in the Jones River watershed for 2020 (A.), 2021 (B.), and both years combined (C.). ....	75
2.11. Taxonomic heat trees of aquatic vertebrate communities detected via eDNA metabarcoding at upstream sites in the Jones River watershed for 2020 (A.), 2021 (B.), and both years combined (C.). ....	76

2.12. Changes in functional richness across upstream and downstream mainstem sites of the Jones River between 2020 and 2021, categorized by substrate-associated trait groups.....	77
2.13. Community Weighted Mean (CWM) trait values for substrate-associated species in upstream and downstream mainstem sites of the Jones River, 2020–2021.....	78
3.1. Map of the Monument River watershed. Red dots signify sampling locations for the upstream reaches of the watershed. Northmost sampling location was the outflow of Little Herring Pond into Great Herring Pond.....	107
3.2. Map of downstream sampling locations within the Monument River watershed.....	108
3.3. Proportional allocation of river herring across three connected ponds over time based on mechanistic model outputs.....	109
3.4. Comparison of predicted fish counts and eDNA concentrations across three connected ponds over time using two mechanistic scaling approaches.....	110
3.5. Temporal alignment of log-transformed eDNA gene copy equivalent (GCE) scores (green lines) and binned two-day fish count totals (orange lines) across four monitoring locations during the 2021 spring migration season.....	111
3.6. Cumulative log-transformed eDNA gene copy equivalent (GCE) scores (green lines) and cumulative fish counts (orange lines) across four sampling locations during the 2021 spring migration season.....	112
4.1. Map of the seven paired eDNA and traditional survey methods throughout coastal Massachusetts.....	144
4.2. Temporal alignment of log-transformed eDNA gene copy equivalent (GCE) scores (green lines) and traditional fish counts (orange lines) targeting river herring (alewife ( <i>Alosa pseudoharengus</i> ) and blueback herring ( <i>Alosa aestivalis</i> )) during the 2021 spring migration season at two locations within the Massachusetts waters.....	145
4.3. Temporal alignment of log-transformed eDNA gene copy equivalent (GCE) scores (green lines) and traditional fish counts (orange lines) targeting American shad ( <i>Alosa sapidissima</i> ) during the 2021 spring sampling season at two locations within the North and South River watersheds.....	146

4.4. Temporal alignment of log-transformed eDNA gene copy equivalent (GCE) scores (green lines) and traditional fish counts (orange lines) during the 2021 spring spawning season at three coastal Massachusetts rivers.....	147
4.5. Comparison of eDNA and Traditional Fish Proportions of Detection Across Sites and Traditional Methods.....	148
4.6. Comparison of Detection Probabilities and Credible Interval Widths Between eDNA and Traditional Sampling Methods.....	149
4.7. Site-Specific Comparison of Detection Probabilities and Credible Interval Widths for eDNA vs. Traditional Sampling Methods.....	150
4.8. Comparison of Detection Probabilities and Credible Interval Widths for eDNA vs. Traditional Sampling Methods. Boxplots comparing detection probabilities (panel A.) and 95% credible interval widths (panel B).....	151
4.9. Posterior Distribution of eDNA-Based Abundance Estimates Posterior distribution plot for eDNA.....	152

# CHAPTER 1

## INTRODUCTION

Humans and ecosystems are fundamentally connected (Johnson, 2010); the “One Health” concept describes how human mental and physical health, safety, and well-being are closely tied to access to clean water, healthy aquatic habitats, biodiverse natural spaces, and sustainable fisheries (Destoumieux-Garzón et al., 2018; Masterson, 2019).

Biodiversity, including species richness, evenness, abundance, genetic diversity, and functional variety, is fundamental to the structure, resilience, and long-term sustainability of ecosystems (Helfrich, 2005; Gamfeldt, 2008). Ecosystems with higher biodiversity often provide higher quality essential resources (e.g. food and shelter) and play a key role in ecosystem services, including regulation and provisioning (Gouletquer, 2014).

Human land use has significantly transformed Earth's ecology for millennia, reshaping biodiversity, ecosystems, and climate (Ellis, 2021). Freshwater and coastal ecosystems have been disproportionately affected around the world by anthropogenic activities, with habitat degradation, hydrologic modification, and species loss representing some of the most persistent ecological consequences (Carpenter et al., 2011). In the northeastern United States, centuries of development have led to the cumulative loss of habitat complexity and longitudinal connectivity, resulting in reduced resilience of river ecosystems and diminished ecosystem services (Mattocks et al., 2017; Wohl et al., 2019). In riverine systems, human-induced changes, such as land-use conversion, pollution, channelization, and the widespread construction of dams, have fragmented ecological networks and disrupted the natural flow regime, impairing biological connectivity and the flux of energy and materials (Poff et al., 1997).

New England has the highest density of dams in the United States, with over 14,000 structures, many dating back to early industrialization (Magilligan et al., 2017; Abbott 2023). Massachusetts alone harbors more than 3,000 dams, yet fewer than 10% of watersheds where dams have been removed have been studied for their ecological recovery (Bellmore et al., 2017). Despite being built for diverse purposes (e.g., hydropower, drinking water supply, flood control, navigation), the ecological and potential human infrastructure impacts of most dams are large. As dams age, the risk of failure increases due to construction deficiencies, inadequate maintenance, and increasingly extreme weather events (Lane, 2007). Many have now reached the end of their technical and economic utility, creating a pressing need for decisions about rehabilitation, modernization, or removal (Dobrinkova et al., 2020). Dams profoundly disrupt stream connectivity by altering the natural flow regime, including the magnitude, frequency, duration, timing, and rate of change of flows, fragmenting critical habitats, obstructing sediment transport, impairing floodplain dynamics, and blocking the migratory pathways and life cycles of diadromous (migratory) fishes, (Poff et al., 1997; Freeman et al., 2003; Graf, 2003; Barbarossa et al., 2020). These aging barriers now block nearly 90% of the habitat that diadromous fish historically accessed (Magilligan et al., 2016; Chapman et al., 2020; Roy et al., 2018).

Diadromous is an umbrella term for anadromous and catadromous life histories; anadromous fish species live the bulk of their lives in marine environments and move into freshwater habitats to complete and repeat their life cycles, while catadromous species exhibit the opposite to complete their life cycles (Bloom & Lovejoy, 2014).

Diadromous fishes function as keystone species across the diverse habitats they occupy.

Diadromy provides several distinct ecological advantages (Bloom & Lovejoy, 2014): anadromy allows species to take advantage of the higher productivity of marine environments for feeding and growth as juveniles and adults, while spawning in freshwater. These spawning events often result in numbers great enough to satiate predators in a system, and give those that make it through the springtime gauntlet the time and resources they need to develop enough to migrate back out to the ocean (Bloom & Lovejoy, 2014). These migrations are also beneficial to the ecosystems they occur within, as they are the source of one of the largest nutrient exchanges between ecosystem types (bringing marine nutrients to freshwater systems, and vice versa) in the natural world (Doughty et al., 2016; Oullet et al., 2022). However, these advantages come at a cost, as both strategies require species to undergo energetically expensive physiological adaptations to transition between freshwater and marine environments, managing the metabolic demands of osmoregulation in response to shifting salinity levels (Delgado & Ruzzante., 2020). Unfortunately, these advantageous migrations have been interrupted by an enduring legacy of human infrastructure (dams and culverts) that dramatically reshaped these watersheds.

After two and a half centuries of compounding habitat loss, habitat degradation, and overfishing, diadromous species like river herring, which rely on connected riverine habitats, have declined to historic lows (Hare et al., 2021). The path forward for diadromous species recovery has become increasingly clear, and improving stream connectivity through barrier removal has been identified as critical to recovering these species and restoring them as healthy, functional keystone members of the multiple ecosystems they inhabit (Goode., 1880; Waldman., 2013; Hare et al., 2021).

The path to dam removal is not simple. Restoration projects often require significant financial investment, and the ability to identify specific species that stand to benefit or are at risk from proposed actions can strengthen grant applications and help attract the resources needed to implement large-scale ecological recovery (Riche et al., 2018; Brenton et al., 2023). There remains much to understand about ecological response to dam removal in general, and researchers are still refining methods on how to effectively measure and understand related ecological impacts (Abbott et al., 2024). Monitoring ecosystem biodiversity metrics to inform, prioritize, and assist with understanding baseline conditions and assisting in raising restoration funding via traditional methods is often a time and resource expensive undertaking (Díaz-Ferguson et al. 2014). Therefore, novel, rapid, accessible, and standardized biomonitoring approaches are needed for the conservation and assessment of ecological integrity to prevent added human disturbance in sensitive natural habitats (Dudgeon et al. 2006; Huang, 2006). Moreover, effective resource management and policy development often requires relevant, real-time data. Recently, environmental DNA (eDNA) has emerged as a novel tool capable of measuring species richness, evenness, and relative abundance at a given location and time from environmental samples derived from water, sediment, and air (Carraro et al., 2021). This technique has the potential to offer a scalable, non-invasive, and cost-effective alternative to traditional survey methods for biodiversity assessment and ecological monitoring.

Since its origins in the 1980s and 1990s detecting bacterial and phytoplankton communities in marine environments, eDNA has shown potential to improve biodiversity and conservation science. Unlike traditional surveys that require specialized equipment (e.g., boats, nets) and extensive labor, eDNA offers an efficient and scalable alternative

(Ogram, Sayler, & Barkay, 1987). Over time, eDNA techniques, laboratory protocols, and field sampling equipment have become more developed, and reagent costs have continuously decreased over time. With modern equipment and streamlined protocols, results can become available *in situ* and *ex situ* after a matter of hours (Bailiff & Karl 1991; Weinbauer, Fuks, & Peduzzi, 1993; Paul, Kellog, & Jiang, 1996; Díaz-Ferguson et al. 2014; Evans et al. 2017; Stoeckle et al. 2020). The sample collection and the sample filtration are relatively straightforward, although both can be prone to contamination if care is not taken and protocols are not followed. However, the downstream processes associated with environmental DNA are complex, context specific, and not clearly outlined for those looking to use this tool in an applied real-world setting. At each point, including sample collection, dozens of individual choices are required. From the volume of water chosen to sample, to filter material, to filter pore size, to eDNA technique to choose (Quantitative Polymerase Chain Reaction (qPCR), metabarcoding using next generation sequencing (NGS) technology, among many more), to which genes, genetic primers and probes, and what DNA extraction and library prep kits to purchase, carrying out an entire eDNA survey from start to finish is no simple task (Roussel et al., 2015; Yates et al 2019). Each decision has a long list of scientific references available to help disseminate options, but they lack consistency, often providing different and sometimes even conflicting feedback (Miya, 2022). The field lacks standardization and functional approaches to implementation are still needed (Cristescue et al., 2018).

Despite methodological hurdles, eDNA metabarcoding enables detection of any organism that inhabits—and sheds DNA into—a given environment, provided that genomic reference sequences and corresponding DNA barcodes have been developed and included

in curated databases. eDNA methods have the potential to address a range of ecologically and biologically meaningful questions, including species presence, relative abundance, and spatiotemporal distribution patterns (Carraro et al., 2024; Yates et al., 2021). These insights can support the detection of rare, endangered, invasive, or otherwise important species, help estimate shifts in species ranges, identification of life history events such as migration or spawning, and the monitoring of ecosystem health, biodiversity, and trophic interactions (Beng & Corlett, 2020). The current and future applications of this technology are limited only by the ability to interpret these genetic blueprints (within their associated environmental contexts) and translate them into meaningful conservation action. To realize this potential, we must not only continue refining the tools and methods, but also ensure they are accessible to those best positioned to use them: conservation organizations, nonprofit groups, graduate students, Tribal communities, school programs, and local, state, and federal agencies.

### **Dissertation Objectives**

The goal of this dissertation was to evaluate the use of environmental DNA (eDNA) as a quantitative ecological monitoring tool by assessing how eDNA concentration, detection probability, and biological inference were influenced by spatial, temporal, and methodological factors across connected freshwater systems. Chapter 2 used eDNA metabarcoding to assess changes in biodiversity and community composition of vertebrate and diadromous fish species in the Jones River watershed following the removal of the medium-sized, mainstem Elm Street Dam in Southeastern Massachusetts. By analyzing spatial (upstream vs. downstream) and temporal (2020 vs. 2021) patterns in eDNA data, this chapter provides insight into early ecological responses to dam removal.

Rarefaction analyses were also used to evaluate the sampling effort required to effectively characterize species richness in a post-restoration context, offering guidance for future monitoring design. Chapter 3 builds on the prior investigation by developing and testing models to estimate river herring relative abundance from eDNA data in a connected freshwater system. Specifically, this chapter: 1) Evaluated the relationship between log-transformed eDNA concentrations and both two-day and cumulative fish passage counts using linear and linear mixed models. 2) Assessed whether incorporating spatial covariates such as basin surface area and hydrological distance from a traditional fish counting station improves eDNA-based abundance predictions across a watershed. 3) Constructs a nested mechanistic model that incorporates site-specific scaling factors based on surface area, distance, and expected DNA transport and degradation dynamics. 4) Generates spatially explicit fish abundance estimates at unsampled locations using only eDNA data and a single validated downstream e-count station. 5) Compares the performance of mechanistic and statistical modeling approaches, demonstrating the utility of both sensitivity-scaled and surface area scaled mechanistic models for extending eDNA-based inference across complex aquatic networks. In Chapter 4, seven studies were used to evaluate eDNA qPCR-based relative abundance estimate calibrations against four commonly used fisheries survey methods (fyke nets, video, resistivity counters, and electrofishing). Using both Bayesian and frequentist approaches, a unified framework centered on detection probability was developed to provide a shared source of uncertainty across methods. By quantifying variation in detection bias across species, methods, and environments, this chapter advances the use of detection probability as a critical metric for selecting and integrating monitoring approaches. Collectively, these

four chapters showcase practical applications of eDNA in ecosystem management by providing scalable, data-driven frameworks for biodiversity monitoring, abundance estimation, and long-term ecological assessment in aquatic systems.

Data—information—is the foundation upon which our society and understanding of the world are built. It fuels everything from economic systems to ecological insight, shaping both global infrastructure and scientific discovery (Buckland, 2017; Wolff, 2016). This Dissertation provides tools and knowledge to gather eDNA data necessary to understand the ecosystems to which we are inextricably linked—and, in doing so, helps to justify and secure support for future restoration.

## **CHAPTER 2**

### **Environmental DNA Metabarcoding Reveals Rapid Aquatic Community Shifts and Diadromous Fish Recolonization Following Mainstem Dam Removal**

#### **Introduction**

Dam removal is an increasingly employed river restoration strategy in the United States and is gaining global momentum as a management approach to increase the resilience of aquatic ecosystems (Foley et al., 2017). Dams fundamentally alter riverine ecosystems by modifying natural flow regimes, changing sediment transport dynamics, fragmenting aquatic habitats, and disrupting longitudinal connectivity (Bednarek, 2001; Poff et al. 1997). Dam removal generally leads to rapid geomorphological and hydrological recovery, followed by more gradual ecological responses, including shifts in aquatic community composition and biodiversity (Foley et al., 2017). Reconnecting upstream and downstream habitats post-dam removal has been linked to improved fish passage, increased habitat availability, and restoration of natural sediment transport processes (Bellmore et al., 2017). Despite these benefits, fewer than 10% of dam removals have been subject to long-term (defined here as more than one year) post-removal monitoring, leaving substantial knowledge gaps regarding ecosystem recovery trajectories and biodiversity responses at site-specific and watershed scales (Bellmore et al., 2019).

Biodiversity is a critical component of ecosystem function and resilience, encompassing species richness, evenness, and genetic diversity (Ney and Helfrich, 2005; Gamfeldt,

2008). Aquatic biodiversity, particularly vertebrate communities, plays a vital role in ecosystem services such as nutrient cycling, habitat provisioning, and food web stability (Gouletquer, 2014). However, monitoring aquatic biodiversity is often constrained by logistical challenges, including the need for specialized equipment, high costs, and the invasive nature of traditional sampling methods (Díaz-Ferguson et al., 2014). Traditional monitoring methods vary by taxa and often require multiple techniques—such as electrofishing, gill netting, and trap netting—to capture the full diversity present within ecosystems. Furthermore, biodiversity baselines are incomplete or nonexistent in many regions like undeveloped or developing nations, or in remote habitats (Meyer, 2015; Amano, 2013). These limitations highlight the need for more cost-effective, scalable, and noninvasive methods for biodiversity assessments, especially in the context of environmental restoration and management.

Environmental DNA (eDNA) metabarcoding has emerged as a novel tool for high-resolution biodiversity monitoring (Miya, 2022). Initially developed for detecting bacterial and phytoplankton communities, eDNA techniques have since been applied to a wide range of taxa, including fish, amphibians, and invertebrates (Ogram, Saylor, & Barkay, 1987; Bailiff & Karl, 1991; Weirbauer, Fucks, & Peduzzi, 1993; Paul, Kellog, & Jiang, 1996; Evans et al., 2017; Stoeckle et al., 2020). Compared to traditional fishery monitoring methods like electrofishing and beach seine surveys, eDNA metabarcoding offers increased sensitivity for detecting rare and cryptic species, requires fewer resources for sample collection, provides a single platform through which a comprehensive assessment of species richness and presence can be gained, and allows for broad spatial

and temporal monitoring with reduced disturbance to aquatic ecosystems (Andres et al., 2020).

eDNA metabarcoding has been used to track diadromous fish species presence before dam removal, as well as after recolonization of newly accessible habitats following dam removals; for example, eDNA was used at the Elwha River and Bloede Dam systems to detect river herring and salmonids at low densities (Duda et al., 2021; Huang et al., 2023). eDNA has the potential to complement traditional monitoring techniques by providing an early-warning system for detecting migratory species returning to restored habitats, as well as track the presence of non-native species following dam removals (Duda et al., 2021). Additionally, the integration of eDNA with socio-environmental analyses has highlighted its role in assessing ecosystem health and informing dam management decisions. For example, by using eDNA metabarcoding to provide pre-removal biodiversity baselines that can help demonstrate ecological benefits to local communities that can be used to strengthen public support and inform stakeholder engagement strategies during the restoration planning process (Fernandez et al., 2022). Despite these potential uses, key challenges remain for applying eDNA to dam removal monitoring. This includes distinguishing true ecological change from background variability, linking detection signals to upstream recolonization dynamics, and developing scalable frameworks for assessing biodiversity and functional recovery across entire watersheds. Advancements in modeling approaches, such as the use of Michaelis-Menten saturation models to estimate species richness and detect sampling sufficiency, as well as eDNA-based detection probability, are recent first steps to improving eDNA monitoring and management strategies (Carraro et al., 2024; Xu et al., 2023; Miya, 2022).

eDNA metabarcoding has also been increasingly applied to functional diversity assessments, providing insights into ecosystem function beyond taxonomic richness. By integrating trait-based analyses with eDNA-based species inventories, researchers can assess how functional diversity indices (e.g., functional richness, functional dispersion, and functional divergence) respond to environmental changes (Cantera et al., 2024; Condachou et al., 2023). These trait-based methods would allow for tracking shifts in functional diversity indices as well as shifts in traits associated with habitat preference across different years post-dam removal, offering a deeper understanding of ecological recovery patterns beyond species-level detection (Dalongeville et al., 2022; Pereira et al., 2021).

This study compared the effectiveness of eDNA metabarcoding to assess patterns in biodiversity, community shifts, and functional diversity in a coastal watershed following a critical dam removal. Specific objectives were to: (1) assess the sampling effort necessary to effectively estimate species richness from eDNA metabarcoding data at the dam removal site through rarefaction analyses, and (2) evaluate shifts in species richness, evenness, functional diversity, and composition of aquatic vertebrate and diadromous fish communities upstream and downstream of the former dam across multiple years. Results provide insights into the effectiveness of eDNA metabarcoding for aquatic biodiversity monitoring and contribute to a broader understanding of ecosystem changes following dam removal at a watershed scale.

## **Methods**

### **Study Area and Site Selection**

The Jones River watershed, situated in southeastern Massachusetts, USA, drains approximately 77.69 km and discharges into Kingston Bay at coordinates 41.997795, -70.709569, ultimately connecting to the Gulf of Maine and the Atlantic Ocean. This region falls within the Northeastern Coastal Zone ecoregion, characterized by coastal pine barren, temperate broadleaf, and mixed forests. The watershed's geology is predominantly shaped by glacial activity, featuring glacial till, outwash plains, and stratified drift deposits overlying metamorphic and igneous bedrock. Land use within the watershed is a mosaic of suburban residential areas, agricultural lands—including cranberry bogs—and forested zones, reflecting a landscape influenced by both natural processes and human activities. The watershed is a Hydrologic Unit Code 10 (HUC 10) scale watershed, and features diverse aquatic habitats, including headwater lakes, dammed impoundments, tributaries, and mainstem riverine environments. The headwaters originate at Silver Lake, a 259 hectare lake that served as a water supply for the region from 1904 to present.

The Elm Street dam, located approximately eight km upstream of the river's mouth, was removed in November of 2019 to restore connectivity and improve aquatic habitat to Silver Lake. Sampling sites were distributed across 19 locations within the watershed, selected based on upstream (n=11) or downstream (n=8) proximity to the former dam, habitat variability (e.g., riffles, pools), and restoration efforts. Six tributary and two mainstem sites were selected downstream of the former dam, and five tributary, four mainstem, and two lake sites were selected upstream of the former dam (Figure 2.1).

### **eDNA Sample Collection and Storage**

Duplicate, 500-mL water samples and a single field blank sample were collected once a month at each of the 19 sites during February, April, May, and June from 2020 to 2023, following protocols established by Holmes et al. (2021). Sampling at each site was conducted over a single 24-hour period whenever possible or across two consecutive sampling dates. Samples were placed in sealed Ziploc bags to prevent contamination, stored on ice, and then frozen at -20°C. Samples were filtered within 2 weeks of collection. Samples were thawed overnight in 50-liter coolers arranged to prevent contact between samples, with cooler lids slightly open for optimal temperature control.

### **eDNA Filtration and Extraction**

Water samples were filtered following guidelines outlined in Ficetola et al. (2008) using 47 mm, 0.8 µm nitrocellulose filters (Whatman, part number: 7188-004) and a vacuum pump system (Cole Palmer, part number: 07532-40) in the Elkington Laboratory at UMass Amherst, a controlled environment free of target organisms. Filtration equipment was sterilized with 10% bleach, rinsed with distilled water, and dried in a sterile hood. Filters were folded and stored in sterilized microcentrifuge tubes containing 95% ethanol and frozen at -80°C until DNA extraction was performed. Filters from replicate samples were pooled before analysis. DNA was extracted using Qiagen DNeasy Blood and Tissue Kits with negative laboratory controls to monitor contamination. Laboratory and processed field blank samples were included with samples delivered to the sequencing facility to control for and detect potential contamination.

### **Metabarcoding and Bioinformatics**

The 12S nuclear ribosomal gene region was targeted to identify vertebrate specific communities following protocols by Riaz et al. (2011). Library preparation and sequencing were performed at the University of Maine's eDNA Epscore laboratory using the Illumina MiSeq platform (2×300 bp paired-end reads). A MiSeq Reagent Kit v3 (600 cycle) was used with a 5% PhiX spike-in as a control. Raw sequence reads were quality-checked using FastQC v0.11.7 (Andrews, 2010) and MultiQC v1.14 (Ewels et al., 2016). Bioinformatic processing was conducted with QIIME2 v2021.4 (Bolyen et al., 2019) on the Ohio Supercomputing Center platform (OSC, 1987). Taxonomic assignment used the National Center for Biotechnology Information (NCBI) nucleotide database, and sequences with a confidence score below 98% were removed. Amplicon sequence variants (ASVs) assigned to the same species were consolidated. Field and laboratory blanks from the 2022 and 2023 sampling seasons returned positive detections across multiple freshwater and marine vertebrate taxa, many overlapping with potential target species, and thus those years were excluded from analyses to maintain data integrity.

Detected DNA sequences were checked against a second online reference using the National Center for Biotechnology Information (NCBI) nucleotide sequence database to ensure species assignment accuracy. For each species detected, classes were linked to each record. Results were filtered by class, retaining only those hits that were of interest to this project (classes included: Agnatha, Osteichthyes, Amphibia, and Reptilia). Species detections were assigned a confidence score during the bioinformatic process. Species with a confidence score of less than 98% were removed from the final results. For each species detection, a "true detection" threshold of 100 read counts was chosen based on personal communications with the UME eDNA Epscore lab, and detections falling below

the 100 read count threshold were removed from final results. This QA/QC process resulted in a “cleaned” and final version of our metabarcoding results, and were used in subsequent analyses (Cantera et al., 2019; Holmes et al., 2022).

Data was grouped at the annual scale (2020 and 2021), as well as the combined year scale (2020 + 2021) to assess the biodiversity metrics for the Jones River watershed. Temporal groups were used across spatial analyses, such as upstream and downstream of the Elm Street dam removal site.

## **Data Analysis**

### **Assessing Sampling Effort**

Rarefaction curves were generated to assess sampling adequacy and species richness saturation using the rarecurve function in vegan R package (Oksanen et al., 2007), implemented in R version 4.3.2 using RStudio. A step size of 10 was used, and curves were plotted to evaluate asymptotic trends across sites and location categories. Sites with curves that failed to reach an asymptote were flagged for potential under-sampling.

Site-specific species richness was estimated using a combination of direct species counts and rarefaction modeling. Observed species richness was calculated for each site by determining the number of unique species present across all sampling events within a given site.

To estimate expected species richness and evaluate whether sampling effort was sufficient to capture the full taxonomic diversity at each site, the rarefy() function in the vegan R package (Oksanen et al., 2007) was applied using individual site-based rarefaction analyses. The rarefaction approach accounts for differences in sample sizes

and provides a standardized estimate of species richness at a given level of sampling effort. For each site, rarefaction was computed using a cumulative species detection matrix, summing presence-absence (or in the case for eDNA metabarcoding analyses, detection-non detection) scores across lab and field replicates, assuming detections were greater than the QA/QC threshold. The maximum observed sample size at each site was used as the reference point for rarefied richness estimation.

For sites where rarefaction curves did not reach an asymptote, a nonlinear Michaelis-Menten saturation model was applied to estimate the theoretical maximum species richness ( $S_{\max}$ ) and interpolate the required sampling effort (Colwell & Coddington, 1994). This model, which follows the form:

$$S = \frac{S_{\max} \cdot N}{K + N}$$

where  $S$  is the estimated species richness at sample size  $N$ ,  $S_{\max}$  is the asymptotic species richness, and  $K$  is the half-saturation constant, was fitted using nonlinear least squares regression. The model was parameterized with an initial estimate of  $S_{\max}$  as the maximum observed richness and  $K$  as the median observed sample size.

Presence-absence (or as is the case with eDNA metabarcoding, “detection-non-detection”) data, and outputs from rarefaction and Michaelis-Menten saturation models were used to assess sampling effort sufficiency across sites in separate and combined years. First, sampling effort was quantified by calculating the total number of species observations at each site across 16 sampling events (two field replicates per month across

four months over two years). For each site, the needed number of *species observations* to reach the plateau, and the estimated species richness ( $S_{\max}$ ) were recorded based on model outputs. The efficiency of sampling effort was calculated using three metrics: number of observations per species = (species observations / estimated species richness); the fraction of total effort required = (species observations / actual species observations); and the percentage of total effort needed = ((species observations / actual species observations) \* 100). Finally, the total number of field samples required to achieve total species richness was estimated by multiplying the fraction of total effort by the total number of field sampling events, which was 8 samples per year and 16 for cumulative years (Table 2.1). This approach allowed for an evaluation of whether sampling coverage was sufficient at each site and how sampling effort requirements varied spatially and temporally across the watershed.

### **Annual Assessment of Locations Upstream and Downstream of the Former Dam**

#### *Species Richness, Evenness, and Community Composition (Alpha and Beta Diversity)*

Species richness was calculated using the phyloseq package in R at multiple temporal scales. First, richness was determined for each unique combination of site, month, and year based on presence-absence data. To summarize annual trends, the monthly presence-absence data were aggregated by year (Table 2.2, Supplementary Table 2.1A), marking a species as present in a given year if detected in any monthly sample within that year.

Similarly, overall species richness per site for the entire study period (2020–2021) was calculated by aggregating across all sampling events, marking species as present if they were detected in any month of either year. These analyses were conducted using

Operational Taxonomic Unit (OTU) matrices aggregated by year and habitat categories

(site, upstream, downstream, and whole watershed) via the phyloseq package. Species richness, evenness, beta diversity metrics, and functional diversity were assessed across all predetermined spatial and temporal scales.

Beta diversity analyses were conducted to evaluate differences in community composition across multiple spatial and temporal scales. A site-by-species matrix (19 sites  $\times$  species detected) was constructed using presence-absence data derived from eDNA read counts, and Bray-Curtis dissimilarities were calculated using the *vegdist* function in the *vegan* R package. Non-metric Multidimensional Scaling (NMDS) ordinations were performed on these dissimilarity matrices to visualize community composition patterns and potential temporal shifts in species assemblages across individual years (2020 vs. 2021) and cumulatively. Ellipses representing 95% confidence intervals were estimated around each assemblage group's centroid. Additionally, aquatic vertebrate and diadromous fish community composition were evaluated for upstream and downstream locations across individual and cumulative years.

To evaluate spatial and temporal variation in aquatic vertebrate and diadromous fish assemblages, a series of PERMANOVA (Permutational Multivariate Analysis of Variance) tests using Bray–Curtis dissimilarity matrices were performed, constructed from site-level presence–absence data. Monthly eDNA metabarcoding detections were pooled by site to generate matrices summarizing total species composition for all aquatic vertebrates as well as a subset representing only diadromous fishes. Comparisons were conducted across upstream and downstream site groupings and between years, resulting in six pairwise PERMANOVA tests per group: within-group temporal comparisons, whole-watershed temporal comparisons, and upstream vs. downstream comparisons. All

analyses were conducted using site-level group matrices aggregated from all site-by-month observations within each category.

To visualize the relative abundance of taxonomic groups within aquatic communities detected across the Jones River watershed, we generated taxonomic heat tree plots using the Metacoder R package (Foster et al., 2017). Mean community composition was estimated using log-transformed read count scores derived from eDNA metabarcoding data. These scores were aggregated across taxonomic levels, and visualized from the Kingdom node (center) through to the species level (outermost nodes), with edge thickness corresponding to the number of reads and color representing  $\log_{10}$  mean read count intensity. Three separate plots were generated to illustrate differences in community structure at multiple spatial scales: 1) all sites across all sampling dates (full watershed view); 2) downstream sites only, pooled across 2020 and 2021, and; 3) upstream sites only, pooled across 2020 and 2021. These visualizations allowed for efficient comparison of species- and genus-level representation across different sections of the watershed and provided insight into the spatial distribution of taxa at fine and coarse taxonomic resolution.

#### *Functional Diversity Trait Data*

Functional diversity, defined as the range and distribution of species traits within an ecological community, was assessed using multiple trait-based metrics. Functional trait data were compiled from established sources, including Frimpong & Angermeier (2009), FishBase (Humphries et al., 2023), and the USGS FiCli database (Krabbenhof et al., 2020). Only traits related to habitat preferences and trophic guilds were retained, and only species with complete trait data were included. A full trait list is provided in Table

S3. Trait data were extracted and processed using the dplyr package in R (Wickham et al., 2023) and aligned with the operational taxonomic unit (OTU) table from the phyloseq object to ensure consistency in species representation between taxonomic and trait-based analyses.

All numeric trait values were standardized using z-score transformation (mean = 0, SD = 1) with the scale() function in R to ensure comparability and to prevent traits with large ranges from dominating the analysis. Traits exhibiting zero or near-zero variance were removed to reduce multicollinearity and ensure robust ordination. Beta dispersion analysis (PERMDISP) was conducted using the vegan package in R to verify the assumption of multivariate homogeneity of variance prior to group comparisons.

To reduce trait dimensionality while preserving ecological signal, Principal Component Analysis (PCA) was applied to the species-by-trait matrix, retaining axes that explained at least 95% of cumulative variance. The “Cailliez” correction was applied in dbFD() to correct for non-Euclidean trait distances (Laliberté & Legendre, 2010). This approach enabled clear characterization of trait space and species positioning within it.

To test whether community-weighted trait composition differed across spatial (upstream vs. downstream) and temporal (2020 vs. 2021) gradients, we performed permutational multivariate analysis of variance (PERMANOVA) using Bray-Curtis dissimilarities derived from site-level trait composition matrices. Bray-Curtis dissimilarity was chosen for its suitability in community-level data, as it accounts for both species presence-absence and abundance differences. Grouping variables (location and year) were tested using 999 permutations in the adonis2() function in vegan (Oksanen et al., 2007).

Because upstream sites spanned a broader range of habitat types than downstream sites, a

representative subset of upstream and downstream sites was selected to meet PERMANOVA assumptions of balanced group sizes. Downstream sites included (from most downstream to upstream): Kingston Harbor, Smelt Brook, Landing Road, Halls Brook, First Brook, Third Brook, and Elm Street Downstream. Upstream sites included Elm Street Upstream, Furnace Brook, Sylvia Place Downstream, Wapping Road, Foxworth Lane, Jones River Brook, and Grove Street. Each group included three mainstem and four tributary sites.

To quantify broader functional diversity (FD), several indices were computed using the `dbFD()` function in the `FD` package (Laliberté et al., 2014), including: Functional Richness (`FRic`): Volume of occupied trait space; Functional Divergence (`FDiv`): Degree to which species diverge from the trait centroid; Functional Dispersion (`FDis`): Mean distance of species from the centroid; and Community-Weighted Means (`CWMs`): Relative trait values weighted by read count abundance, capturing dominant traits per community. Community-weighted mean (`CWM`) trait values were calculated by weighting trait scores by species' relative abundances (read counts) at each site, producing a trait composition matrix used in multivariate and univariate comparisons.

To test for differences in FD metrics across spatial and temporal groups, Wilcoxon rank-sum tests (Mann-Whitney U) were applied, due to non-normal distributions and small group sizes. This non-parametric approach ensured robust inference.

PERMANOVA analyses were conducted to assess differences in community-weighted functional trait composition across spatial (upstream vs. downstream) and temporal (2020 vs. 2021) gradients (Table 2.6). Functional trait composition was evaluated using Bray-Curtis dissimilarity on site-level functional trait matrices, with comparisons including

within-habitat temporal differences (upstream and downstream separately), watershed-wide temporal shifts, and spatial differences between upstream and downstream communities in 2020, 2021, and across both years combined (Table 2.6). PERMANOVA results focused solely on Bray-Curtis dissimilarity scores for species presence absence resulted in the same results, therefore both are reported.

### *Substrate-Specific Trait Responses to Dam Removal*

To evaluate potential trait-based ecological responses to dam removal, species were grouped based on substrate preference into two categories: 1) Sand/Muck-preferring species, including benthic taxa and specialists associated with fine substrates such as sand and organic muck; and 2) Hard-bottom-preferring species, comprising taxa that prefer coarser substrates such as gravel, cobble, or boulder. This grouping was used to assess whether shifts in sediment dynamics presumed to result from dam removal (i.e., reduced fine sediment deposition upstream and increased sediment accumulation downstream) influenced habitat-specific community trait assemblages. For this analysis, only mainstem sites likely to experience sediment redistribution were included. Downstream sites were Elm Street Downstream, Landing Road, and Kingston Harbor; upstream sites were Elm Street Upstream, Wapping Road, and Foxworth Lane. For each trait group, separate Bray-Curtis dissimilarity matrices and PCA reductions were computed, and PERMANOVA was used to assess whether sediment-associated trait composition differed between locations and years.

All analyses were conducted in R version 4.2.2 (R Core Team, 2022)

## **Results**

## **Assessing Sampling Effort**

Rarefaction curves for upstream and downstream sites exhibited asymptotic trends, suggesting adequate sampling to approach species saturation (Table 2.1; Figure 2.2).

However, site-specific curves showed variability, with some locations (e.g., 2020 samples from Furnace Brook) not reaching a plateau (Figures 2.3, 2.4).

The estimated number of species observations needed to reach asymptote ranged from 12 to 102 observations. Estimated species richness values ranged between 15 to 32 per site, and closely aligned with observed values. The estimated number of field samples needed to reach the rarefaction plateau and detect total species richness ranged between one and three for individual years, and two to four for combined year sampling. All values for the estimated amount of effort needed to adequately detect total species richness were  $< 1$ , and each site's actual sampling effort surpassed the estimated number of field samples required for species accumulation to reach saturation. This indicated that actual sampling effort was greater than what was needed at any given site across all year categories (Table 2.1, Figure 2.2).

## **Annual Assessment of Locations Upstream and Downstream of the Former Dam**

### *Species Richness, Evenness, and Community Composition (Alpha and Beta Diversity)*

In 2020, upstream sites had a species richness of 27, while downstream sites had a species richness of 36. By 2021, upstream species richness increased to 34, while downstream richness decreased to 33 species. Cumulatively, downstream sites had a combined species richness of 44 species, and upstream sites had a combined richness of 40 total species (Table 2.2). For diadromous species, richness was comparable between

upstream and downstream regions in both years, but when years were combined, downstream sites had higher species richness than upstream sites (Table 2.3).

NMDS ordination highlighted differentiation between upstream and downstream community compositions (Figure 2.5). Downstream sites exhibited greater dispersion in ordination space, while upstream sites clustered more tightly. NMDS ordination suggested no differences in diadromous fish communities across upstream and downstream sites.

PERMANOVA analyses revealed significant temporal and spatial structuring of both aquatic vertebrate and diadromous fish communities across the Jones River watershed (Table 2.6). For aquatic vertebrates, taxonomic composition was significantly different between 2020 and 2021 within both downstream ( $R^2 = 0.137$ ,  $p = 0.001$ ) and upstream sites ( $R^2 = 0.156$ ,  $p = 0.001$ ), and across all sites within the watershed ( $R^2 = 0.140$ ,  $p = 0.001$ ). Spatial differences between upstream and downstream communities were also detected across all sites ( $R^2 = 0.025$ ,  $p = 0.002$ ) and within 2020 ( $R^2 = 0.064$ ,  $p = 0.001$ ), though not in 2021 ( $R^2 = 0.02$ ,  $p = 0.24$ ). Diadromous fish communities exhibited even stronger spatiotemporal structuring, with significant temporal differences observed in downstream ( $R^2 = 0.317$ ,  $p = 0.001$ ), upstream ( $R^2 = 0.329$ ,  $p = 0.001$ ), and across watershed scale comparisons ( $R^2 = 0.317$ ,  $p = 0.001$ ). Spatial contrasts between upstream and downstream diadromous assemblages were significant across all sites combined ( $R^2 = 0.024$ ,  $p = 0.035$ ) and in 2020 ( $R^2 = 0.044$ ,  $p = 0.032$ ), but not in 2021 ( $R^2 = 0.02$ ,  $p = 0.27$ ).

Total species richness for the Jones River watershed was 50 species. Total species richness was highest in 2020 with 40 unique species detected, declining to 38 species in

2021. Similarly, mean species richness across all sites declined from 16.4 in 2020 to 14.9 in 2021 (Table 2.2). Across all sites and years (2020–2021), species richness varied considerably, with the most downstream site, Kingston Harbor exhibiting the highest richness (N = 34) and the next most downstream tributary site Smelt Brook the lowest (N = 15) (Table 2.2). Several common and one catadromous species were detected across all sites, including American eel (*Anguilla rostrata*), bluegill (*Lepomis macrochirus*), chain pickerel (*Esox niger*), fallfish (*Semotilus corporalis*), golden shiner (*Notemigonus crysoleucas*), pumpkinseed sunfish (*Lepomis gibbosus*), rock bass (*Ambloplites rupestris*), tessellated darter (*Etheostoma olmstedii*), and white sucker (*Catostomus commersonii*) (Table 3). Mean relative read counts (percent contributions of total read counts across all samples) were used to weight nodes, highlighting taxa with high abundances (e.g., Perciformes, Cypriniformes) (Figure 2.6).

Ten diadromous species native to Massachusetts were detected in the Jones River watershed, with diadromous species richness varying significantly across sites and years (Tables 2.3 and 2.4). In 2020, all ten diadromous species were present, whereas in 2021, Atlantic tomcod (*Microgadus tomocod*) was absent (N=9). Mean diadromous species richness across all annual sampling events declined from 2.3 in 2020 to 1.8 in 2021 (Table 2.2 and 2.3). The cumulative mean number of diadromous species detected across all sites and sampling events was 2.04.

Non-metric multidimensional scaling (NMDS) analysis revealed distinct clustering of sites by year, indicating compositional differences between 2020 and 2021 post-dam removal (Figure 2.2). NMDS ordination of fish communities in upstream versus downstream locations of the Elm Steet dam revealed non-significant clustering (Figure

2.7). However, upstream sites clustered more tightly than did downstream sites. NMDS ordination of diadromous fish communities in the Jones River watershed across combined years (2020 and 2021) revealed no significant patterns or overlap (Figure 2.8). Metacoder heat tree visualizations revealed distinct patterns in community composition and relative taxon abundance across the Jones River watershed. At the watershed scale (and at the family taxonomic resolution) in 2020, Salmonids, Clupeids, Centrarchids, Percids, Anguillids, and Esocids dominated. In 2021, we saw similar patterns, but with larger contributions from Sygnathids, Petromyzontids, and Cyprinids, and smaller contributions from Gasterostids, Gadids, Pholids, and Paralichthids. Comparisons between upstream and downstream sites highlighted spatial variation in dominant taxa. Downstream communities exhibited higher relative abundances of diadromous species, including blueback herring (*Alosa aestivalis*) and rainbow smelt (*Osmerus mordax*), as well as coastal taxa such as Atlantic silverside (*Menidia menidia*) and mummichog (*Fundulus heteroclitus*) (Figure 2.5, middle panel). In contrast, upstream sites were dominated by resident freshwater species including golden shiner (*Notemigonus crysoleucas*), fallfish (*Semotilus corporalis*), brown bullhead (*Ameiurus nebulosus*), and multiple sunfish and perch taxa (Figure 2.5, right panel). Overall, community composition displayed both taxonomic diversity and spatial structuring, with diadromous and estuarine-affiliated species contributing more heavily to downstream assemblages and freshwater taxa prevailing upstream.

No state or federally listed endangered species were detected above QA/QC validation thresholds. However, multiple native and diadromous Species of Greatest Conservation Concern (MA SGCN) and state-classified invasive, non-native, and introduced species

were identified (Table 2.5). When the invasive common carp sequence was BLASTED against the National Center for Biotechnological Information database (NCBI), Amplicon Sequence Variant (ASV) sequences came back as 100% match for common carp. When the banded darter ASV was checked, it came back as a 96% match, with a 100% match reported for swamp darter (*Etheostoma fusiforme*) - a species known to be native to the Jones River watershed. A heat tree plot was generated to visualize species evenness throughout the Jones River watershed (Figure 2.6). Taxa that were consistently present across multiple sites included yellow perch, bluegill, golden shiner, rock bass, brook trout, tessellated darter, and American eel.

#### *Functional Diversity Trait Data*

PERMANOVA and Bray-Curtis temporal comparisons within downstream sites showed no significant differences in functional trait composition between 2020 and 2021 ( $R^2 = 0.04$ ,  $F = 0.52$ ,  $p = 0.79$ ). However, functional trait composition in upstream sites exhibited a significant shift between years ( $R^2 = 0.20$ ,  $F = 3.06$ ,  $p < 0.001$ ), indicating interannual variation in upstream functional trait and community structure. At the watershed scale, temporal comparisons did not reveal significant differences in functional trait composition between years ( $R^2 = 0.03$ ,  $F = 0.84$ ,  $p = 0.57$ ).

Spatial comparisons between upstream and downstream communities were not significant in either 2020 ( $R^2 = 0.06$ ,  $F = 0.79$ ,  $p = 0.80$ ) or 2021 ( $R^2 = 0.08$ ,  $F = 1.05$ ,  $p = 0.44$ ), suggesting no strong differentiation in functional trait composition along the upstream-downstream gradient in either year. When combining data across years, upstream and downstream differences remained non-significant ( $R^2 = 0.03$ ,  $F = 0.84$ ,  $p = 0.53$ ), further indicating a lack of spatial structuring in functional trait or community

composition across the watershed. These results suggest that temporal variability in functional trait composition is more pronounced in upstream habitats, whereas downstream communities and watershed-wide functional trait structures remained relatively stable across years. Spatial differentiation in functional trait composition between upstream and downstream sites was not detected at either the annual or combined-year scale.

Significant differences in functional richness (FRic) were detected for upstream sites between 2020 and 2021 ( $W = 66, p < 0.001$ ), and for watershed-wide comparisons ( $W = 152, p < 0.001$ ), indicating a significant decrease in the breadth of ecological roles present in upstream and overall watershed communities over time. In contrast, richness did not significantly differ between downstream sites across years ( $W = 20, p = 0.06$ ), nor did it vary between upstream and downstream sites in either year or when data were combined across both years ( $p > 0.05$  for all comparisons).

Significant differences in functional divergence (FDiv) were observed in year-to-year comparisons at the watershed scale ( $W = 16, p < 0.001$ ), as well as within upstream ( $W = 10, p = 0.04$ ) and downstream ( $W = 0, p = 0.03$ ) sites (Table 2.7). These results suggest shifts in the distribution of species within trait space over time, particularly within the upstream and watershed-wide contexts. A significant difference in divergence was also found when comparing upstream and downstream sites across years ( $W = 196, p = 0.01$ ), but not within years ( $W=20, p = 0.06$  and  $W=18, p = 0.16$  for 2020 and 2021, respectively). In contrast, functional dispersion (FDis) showed no significant differences in any spatial or temporal comparisons ( $p > 0.05$  for all tests). This suggests that while the total volume of functional space occupied (FRic) and the clustering of species within

that space (FDiv) varied over time, the overall spread of species within the occupied space remained relatively stable.

### *Substrate-Specific Trait Responses to Dam Removal*

PERMANOVA analyses revealed that substrate-associated traits exhibited divergent patterns of response to dam removal, with trait groups linked to depositional (muck and sand) compared to erosional (gravel and boulder) substrates showing distinct temporal and spatial dynamics. For muck/sand-associated traits, the model explained a higher proportion of functional trait variation, though the effect was not statistically significant ( $R^2 = 0.35$ ,  $F = 1.44$ ,  $p = 0.36$ ). Notably, downstream communities exhibited pronounced increases in functional richness for sand- and muck-preferring taxa from 2020 to 2021 (Figure 2.12A, left panel), aligning with predictions of increased sediment availability following dam removal. This increase was particularly evident in the downstream group, which more than tripled in trait richness over the study period, although the "Elm Street Downstream" site showed more muted change (Figure 2.1). At the same time, community-weighted mean (CWM) trait values for benthic and muck-associated taxa increased or remained elevated across both years (Figure 2.13A), suggesting persistent habitat suitability for fine-sediment-adapted species in downstream depositional zones. Upstream communities also exhibited changes in sand/muck-associated richness, but these shifts were less consistent. "All Upstream" sites showed a sharp increase in functional richness between years (Figure 2.12A, right panel), while the Elm Street Upstream site experienced a notable decline, highlighting spatial heterogeneity in trait responses. Correspondingly, upstream CWM values for benthic traits remained high across years, while muck and sand trait values increased between 2020 and 2021 (Figure

2.13A), suggesting localized expansion of fine sediment–associated taxa in upstream reaches potentially influenced by upstream deposition or indirect effects of altered flow conditions.

In contrast, hard bottom–associated traits (gravel, cobble, and boulder) exhibited less overall temporal and spatial variability. PERMANOVA analyses explained a smaller portion of trait variation ( $R^2 = 0.22$ ,  $F = 0.73$ ,  $p = 1.00$ ), suggesting little ecological restructuring of rocky substrate specialists during the study period. Functional richness of these traits remained relatively stable across sites, with only minor interannual increases observed (Figure 2.12B). Notably, "Elm Street Upstream" exhibited no change in richness between years, while both "All Upstream" and "All Downstream" groups showed modest gains. CWM trait values for cobble and gravel remained consistently high across sites and years, indicating persistent trait dominance (Figure 2.13B). The only substantial change was an increase in boulder-preferring taxa at upstream sites in 2021, (Figure 2.13B).

## **Discussion**

eDNA monitoring revealed clear spatial and temporal variation in community composition across the Jones River watershed. High detection sensitivity allowed for the identification of subtle shifts in functional diversity, rare species presence, and differences in native and non-native species distributions. Notably, eDNA-based metrics captured patterns consistent with ecological restructuring across multiple spatial scales—from localized habitat changes near the former dam site to broader variation across the watershed. While causality cannot be confirmed without pre-removal data and longer-term post-removal data, the observed changes align with expected outcomes of increased

longitudinal connectivity and demonstrate the utility of eDNA for characterizing early post-restoration dynamics (Bellmore et al., 2019).

### **Disturbance and species turnover**

The Jones River Watershed Association initiated the removal of the Elm Street dam in 2019 with goals of restoring connectivity and enhancing biodiversity throughout the watershed (Personal communication, *JRWA Board of Directors*). Patterns in diversity and species distributions reveal a complex early response to this restoration action during the first two years post-removal. Following the Elm Street dam removal, the decline in species richness from 2020 to 2021 across most sites, along with significant temporal differences in community composition at both upstream and downstream locations, and the spatial differences observed between reaches in 2020, could be interpreted as an initial ecological degradation, but requires additional evidence to discriminate causal effects from stochastic ones. Alternatively, these patterns may align with established ecological theory, which predicts elevated species turnover in riverine systems following large-scale disturbances, with communities gradually transitioning toward a new equilibrium (Muha et al., 2021). Changes to natural flow regimes can trigger cascading ecological effects (Poff et al., 1997), particularly in systems undergoing abrupt transitions. The resulting reorganization phase (Holling and Gunderson, 2002) reflects a period of flux, where biotic communities respond to shifting hydrology, sediment transport, and novel habitat availability. Given the dynamic nature of this stage, observed species shifts, both upstream and downstream, are part of an expected, variable process rather than fixed trends, with ecosystem structure continuing to evolve until a new stable state is reached. Similar short-term declines in richness have been observed in other dam

removal studies, where ecosystem recovery occurs over multiple years as habitat stabilizes and species redistribute (Bellmore et al., 2019).

The diminishing spatial differentiation between upstream and downstream assemblages following dam removal could be a consequence of sediment-mediated functional homogenization occurring throughout the Jones River watershed. The 2019 removal of the Elm Street Dam triggered the downstream migration of impounded sediments, which had accumulated over decades. These sediments, sourced from the watershed's glacially derived sandy aquifers (Persky, 1993) and exacerbated by winter sanding practices from upstream cranberry operations (Davenport & Schiffhauer, 2000; McCanty et al., 2021), progressively altered habitat structure and substrate composition in both upstream and downstream reaches.

Functional trait and community composition analyses revealed complex and spatially divergent responses, with clear evidence of both localized habitat restructuring and broader ecological filtering. While species richness increased in upstream reaches between 2020 and 2021, functional richness declined significantly. This decoupling suggests colonization by functionally redundant generalist species following improved connectivity, consistent with patterns observed in other systems (Baiser & Lockwood, 2011). These generalists may have replaced or outcompeted functionally unique taxa, resulting in a narrower array of ecological roles despite higher species counts.

Trait-level patterns offer further insight potentially associated with sediment-driven and other physical changes to the system. Functional richness associated with nearly all substrate preferences (benthic, muck, sand, gravel, cobble, boulder) showed no trend across the combined mainstem between 2020 and 2021. Subtle increases were detected

and should be monitored over longer time frames to determine if recovery is gradual. For example, sand-preferring species increased in both upstream and downstream sites. Fine sediment enrichment due to impoundment scouring and downstream deposition, as well as continued sand inputs from upstream cranberry bog operations, may support recruitment of sand-preferring taxa in the upper watershed in future years (Baiser and Lockwood, 2011; barabossa et al., 2020; Davenport and Schiffhauser., 2000; McCanty *et al.*, 2021).

However, within the formerly impounded upstream reach, trait responses were more heterogeneous. Sand- and muck-preferring species exhibited non-significant declines between 2020 and 2021, possibly signaling a loss of depositional habitats as fine sediments migrated downstream. Simultaneously, boulder-preferring taxa increased in this reach, supporting the interpretation that dam removal exposed coarser, previously buried substrates—possibly restoring legacy habitats. Intriguingly, muck-preferring species also increased upstream over time despite the loss of fine sediment, a pattern that may reflect localized retention zones, sampling noise, or turnover in taxa with shared habitat affinities. This unexpected result merits further investigation using sediment data.

The significant decline in upstream functional richness also coincided with the loss of functionally unique species such as four-toed salamanders (*Hemidactylium scutatum*) and fallfish (*Semotilus corporalis*), detected in 2020 but absent in 2021. Their disappearance may indicate ecological filtering due to missed detections resulting from potentially low abundances, altered flow regimes, sediment shifts, vegetation changes, or trophic restructuring (Biggs et al., 2020). Overall, these results suggest that upstream

communities are undergoing functional homogenization, driven by both trait convergence and species turnover.

Taxonomic homogenization has been widely documented in post-disturbance systems (Ticiani et al., 2022), with functional responses exhibiting high variability. Some systems exhibit convergence and reduced resilience (Buisson et al., 2013), while others show trait divergence or resilience-driven expansion (Mouton et al., 2020; Jones et al., 2022). Our findings emphasize that taxonomic and functional changes are not always correlated (Baiser & Lockwood, 2011), and that examining both dimensions is essential to understanding ecosystem response to large-scale restoration actions like dam removal.

### **Diadromous Species Turnover Following Dam Removal**

Prior to the 2019 removal of the Elm Street Dam, agency surveys and volunteer herring counts (Mass Wildlife, JRWA, pers. comm.) showed the diadromous fish community in the upper Jones River watershed was highly constrained, with upstream records limited to only a few species—American eel, brook trout, sea lamprey, and river herring relative to the species diversity found post dam removal using eDNA methods. The fish ladder at the dam, an Alaskan Steeppass, was poorly suited to species with lower burst swimming capacity or unique passage behaviors and had an estimated efficiency of fish passage below 30% (Brown et al., 2013; Silva et al., 2017). Consequently, species such as American shad and rainbow smelt, which require moderate to low velocities for upstream migration, were not detected above the dam prior to its removal (Noonan et al., 2012; Castro-Santos et al., 2009).

eDNA monitoring following dam removal revealed immediate and substantial expansion of diadromous species richness and distributions. In both 2020 and 2021, diadromous

taxa—including alewife (*Alosa pseudoharengus*), blueback herring (*Alosa aestivalis*), American eel (*Anguilla rostrata*), American shad (*Alosa sapidissima*), white perch (*Morone americana*), rainbow smelt (*Osmerus mordax*), sea lamprey (*Petromyzon marinus*), and brook trout (*Salvelinus fontinalis*)—were detected in multiple combinations across all eleven upstream monitoring sites. This shift from four species with limited upstream access to eight detected across the entire watershed suggests rapid recolonization and expanded connectivity. These differences reflected both increasing species richness and altered assemblage structure, as several species (e.g., American shad, rainbow smelt) appeared in 2021 that were undetected upstream in 2020. Spatial differences between upstream and downstream sites were also significant in 2020 but diminished by 2021, suggesting a trend toward community convergence as recolonization progressed.

These findings are consistent with prior studies, such as in the Patapsco River, where river herring rapidly recolonized upstream habitats following the Bloede Dam removal (Huang et al., 2023). The persistence and expansion of diadromous species in the Jones River, despite interannual variation and broader ecosystem restructuring, indicates that restored connectivity supported functional migration routes for multiple taxa (Pess et al., 2014; Pess et al., 2024). There are also potential cascading ecological benefits of dam removal. For example, increased fish passage may aid the recolonization of native freshwater mussels, which rely on diadromous fish as hosts for larval dispersal (Haag & Warren, 1998). Additionally, the movement of anadromous species upstream may reintroduce marine-derived nutrients (MDN) into freshwater food webs, enhancing productivity and supporting ecosystem recovery (Naiman et al., 2002).

However, the expansion of connectivity can also introduce ecological risks. Dam removals and climate change are known to open pathways for non-native and invasive species by facilitating range shifts and reducing dispersal barriers (Abbott et al., 2024). Common carp (*Cyprinus carpio*) and banded darter (*Etheostoma zonale*) were not historically detected in the Jones River watershed based on MassWildlife and JRWA records, nor were they observed during the 2020 sampling year. While banded darter detections were likely bioinformatic misassignments, common carp was detected in 2021 at an upstream tributary site (Sylvia Place, connected to Furnace Brook). This detection occurred in habitat consistent with carp preferences—slow currents, weedy margins, and soft substrates in lower river reaches and marshes (Frimpong & Angermeier, 2009; Takeuchi et al., 2002). While dam removal can restore natural processes and benefit native biodiversity, it may also inadvertently enable the spread of invasive species previously restricted by barriers (Bellmore et al., 2019; Daniels et al., 2023). The detection of common carp post-dam removal emphasizes the sensitivity of eDNA methods and the importance of ongoing monitoring and context-aware management strategies that weigh both the benefits and potential unintended consequences of restored connectivity.

Post-removal recovery trajectories remain context-dependent. Hydrologic conditions, land use, and legacy sediment influence the speed and scope of biotic recovery (Foley et al., 2017; Fields et al., 2021). Process-based restoration (e.g., hydrologic connectivity) may occur rapidly, but form-based and assemblage-level recovery often unfolds over decades (McHenry & Pess, 2008). Whether the recolonization observed in the Jones River represents full recovery or early stages of a longer-term transition remains

uncertain, but the rapid reappearance of multiple diadromous taxa—and early warning signs of invasive species expansion—reflect an ecosystem in active flux and underscore the need for adaptive, evidence-based restoration monitoring that incorporates eDNA and traditional means of biodiversity assessment.

### **eDNA use in monitoring biodiversity**

In the Jones River watershed, eDNA metabarcoding revealed clear spatial and temporal shifts in community composition, including upstream recolonization by diadromous species and divergent patterns in richness and functional diversity. The method also detected rare taxa and broader community restructuring with minimal ecological disturbance, highlighting its value for watershed-scale biomonitoring. Rarefaction results showed that less than 30% of the total sampling effort was needed to capture most taxa at each site, demonstrating eDNA's potential to reduce monitoring costs while maintaining analytical robustness. These findings underscore the importance of optimizing sampling design and standardizing protocols to enhance the efficiency and reproducibility of future eDNA applications.

Despite its strengths, eDNA metabarcoding has limitations. Non-detections do not equate to confirmed absence, as false negatives are common, especially when compared to targeted techniques like qPCR or ddPCR (Cristescu et al., 2018; Miya, 2022).

Conversely, false positives can also arise due to tag-jumping, cross-contamination, or amplification of degraded DNA from transient or dead organisms, potentially leading to erroneous ecological conclusions (Goldberg et al., 2016; Deiner et al., 2017). Advancing the utility of eDNA will require integrating species-specific shedding rates,

environmental covariates, and occupancy models to improve detection accuracy and ecological inference (Mauvisseau et al., 2019).

Additionally, contamination and preservation remain critical challenges. In this study, two years of metabarcoding data were excluded due to laboratory contamination, with marine and mammalian DNA—unlikely to have originated in the field—detected in both field and lab blanks. Sample preservation methods also varied across years: Longmire’s solution was used in 2020–2021, while 95% ethanol was used in 2022–2023 due to supply constraints. Longmire’s solution is generally more effective at preserving DNA integrity for metabarcoding and minimizing degradation and contamination risk, whereas ethanol, though widely used, has been linked to greater variability in DNA retention and higher contamination potential (Turner et al., 2014; Williams et al., 2017).

Taken together, these findings reinforce the need for rigorous contamination controls and protocol standardization in eDNA workflows. Establishing dedicated pre- and post-PCR lab spaces, implementing multiple negative controls, and adhering to consistent decontamination practices are essential steps to ensure reliable, reproducible results—especially in sensitive applications such as restoration monitoring.

### **A path forward**

Effective restoration evaluation requires clearly defined objectives, robust baseline data, well-designed studies, and long-term monitoring—paired with a willingness to adapt and learn from setbacks (Kondolf, 1995). Multidisciplinary, sustained research is essential for assessing the ecological consequences of dam removal and guiding informed management decisions (McHenry & Pess, 2008; Wagner & Moore, 2023). Although the

loss of two years of data due to contamination was a significant limitation, this study's two consecutive years of high-quality eDNA monitoring provide a critical foundation for long-term ecological assessment in the Jones River watershed. These data represent the first watershed-wide record of post-removal fish community structure and offer an essential baseline for tracking the magnitude, direction, and duration of ecological change (Hansen & Hayes, 2012).

Looking ahead, several key developments could enhance the role of eDNA monitoring in evaluating restoration outcomes. Establishing centralized, open-access data repositories would enable state and federal agencies, tribal nations, NGOs, researchers, and community science networks to track biodiversity changes across multiple watersheds, fostering large-scale assessments of ecological recovery. This collaborative infrastructure would support cumulative learning across regions, facilitate meta-analyses, and improve the generalizability of restoration science. Standardizing protocols across institutions will further improve data comparability, transparency, and equity in ecosystem monitoring.

In the Jones River, a ten-year post-removal resurvey in 2030 would provide essential data on community stabilization, functional resilience, and long-term recolonization trajectories. Integrating eDNA data with traditional monitoring methods (e.g., electrofishing, video surveys) could offer a more holistic understanding of how ecological networks respond to restored connectivity. Notably, this study already documented the reappearance of multiple diadromous species and directional shifts in functional diversity within two years of dam removal—evidence of rapid ecological response that would have been difficult to capture using conventional surveys alone.

Beyond its scientific value, eDNA metabarcoding offers a scalable and cost-effective tool for conservation practitioners. When paired with effective communication strategies, eDNA data can support evidence-based storytelling to secure funding, engage local communities, and promote stewardship across watersheds (Erete et al., 2016; Lyon et al., 2020; Stolper et al., 2016; Riche et al., 2017; Brenton et al., 2023). By embedding eDNA into long-term restoration frameworks, practitioners can improve the detection of early ecological change, refine adaptive management, and maximize the ecological and social return on investment of dam removal projects.

In sum, this study demonstrates that eDNA monitoring is a sensitive and practical tool for detecting species expansions, shifts in diversity, and community restructuring following dam removal.

## Tables

Table 2.1. Rarefaction modeling results for 19 sites in the Jones River watershed, including estimated species richness, fraction of sampling effort required to reach asymptotic richness, and estimated number of field samples needed to reach rarefaction asymptote per year and cumulatively. Cumulative estimated sample numbers were generated from rarefaction curves for 2020 and 2021 combined per site, not from adding individual years. All sites had 16 field samples (8 per year), and rarefaction curves indicated sampling sufficiency at all locations. Rarefaction modeling estimated the minimum number of samples required to reach near-asymptotic species richness per site per year. “Fraction of effort” reflects the proportion of the 16 total samples needed to achieve this threshold.

Watershed Position	Site No.	Site Name	Est. Species Richness	Fraction of Effort Needed	Estimated Samples		
					2020	2021	Combined
Downstream	1	Kingston Harbor	32	0.27	3	2	4
	2	Smelt Brook	15	0.16	2	1	3
	3	Landing Road	24	0.20	2	1	3
	4	Halls Brook	17	0.16	2	1	3
	5	First Brook	19	0.13	1	1	2
	6	Second Brook	17	0.19	1	1	3
	7	Third Brook	20	0.12	2	1	2
	8	Elm Street	22	0.21	2	1	3
<b>Former Dam Location</b>							
Upstream	9	Elm Street Up	22	0.17	2	1	3
	10	Furnace Brook	20	0.20	2	1	3
	11	Sylvia Place	20	0.21	2	1	3
	12	Sylvia Place Up	19	0.16	2	1	3
	13	Wapping Road	22	0.23	2	1	4
	14	Foxworth Lane	23	0.21	2	1	3
	15	Grove Street	21	0.17	2	1	3
	16	Pine Brook	19	0.21	2	1	3
	17	Jones River	18	0.18	2	1	3
	18	Silver Lake	22	0.20	2	1	3
19	Tubbs Brook	19	0.18	2	1	3	
		Average	21	0.19	2	1	3

Table 2.2. Site-level observed overall vertebrate species richness across spatial and temporal scales in the Jones River watershed. Aquatic species richness values are reported by site (ordered from downstream to upstream), including site code, habitat type, relation to the Elm Street Dam removal site, and mean monthly richness across in 2020, 2021, and cumulatively. Site codes and habitat classifications align with field collection metadata. Cumulative richness reflects species detected across all sampling months in both years.

<b>Overall Vertebrate Species Richness</b>								
<b>Jones River Watershed</b>			<b>2020</b>		<b>2021</b>		<b>Combined</b>	
<b>Watershed Position</b>	<b>Site No.</b>	<b>Site Name</b>	<b>Richness</b>	<b>Mean</b>	<b>Richness</b>	<b>Mean</b>	<b>Richness</b>	<b>Mean</b>
Downstream	1	Kingston Harbor	30	16.8	18	9.3	34	13.0
	2	Smelt Brook	13	9.3	9	5.3	15	7.3
	3	Landing Road	20	11.0	15	6.7	25	9.1
	4	Halls Brook	16	9.5	8	5.0	17	7.6
	5	First Brook	14	6.5	12	5.3	19	5.9
	6	Second Brook	11	6.0	14	6.5	17	6.3
	7	Third Brook	17	12.3	13	5.8	20	9.0
	8	Elm Street	19	12.3	14	7.0	22	9.6
<b>Former Dam Location</b>								
Upstream	9	Elm Street Up	21	12.8	17	8.8	22	10.8
	10	Furnace Brook	18	11.3	14	7.0	22	9.2
	11	Sylvia Place	17	12.5	15	8.3	21	10.4
	12	Sylvia Place Up	16	10.0	11	5.0	19	7.5
	13	Wapping Road	19	13.3	15	8.3	22	10.8
	14	Foxworth Lane	20	13.0	16	6.5	23	9.8
	15	Grove Street	19	10.0	13	6.0	21	8.0
	16	Pine Brook	17	12.8	7	5.0	20	10.2
	17	Jones River	16	10.0	14	7.8	18	8.7
	18	Silver Lake	18	11.5	15	6.5	25	9.0
	19	Tubbs Brook	15	12.8	13	7.3	19	10.0
		Watershed Total	40	16.4	38	14.9	50	21.1

Table 2.3. Site-level diadromous species richness across temporal scales in the Jones River watershed. Diadromous fish species richness is reported for each sampling site from downstream to upstream, with site code, habitat type, and relationship to the Elm Street Dam removal site. Richness is presented for each year and cumulatively, alongside mean monthly richness. Diadromous species include anadromous and catadromous fishes detected by eDNA metabarcoding. Totals reflect unique species detected across all sampling dates per year and cumulatively.

<b>Diadromous Species Richness</b>								
<b>Jones River Watershed</b>			<b>2020</b>		<b>2021</b>		<b>Combined</b>	
<b>Watershed Position</b>	<b>Site No.</b>	<b>Site Name</b>	<b>Richness</b>	<b>Mean</b>	<b>Richness</b>	<b>Mean</b>	<b>Richness</b>	<b>Mean</b>
Downstream	1	Kingston Harbor	8	4.5	6	4.7	8	4
	2	Smelt Brook	1	1	1	1	1	0.9
	3	Landing Road	4	2.5	2	1.5	4	1.9
	4	Halls Brook	4	1.5	2	1.3	4	1.4
	5	First Brook	2	2	3	1.8	3	1.9
	6	Second Brook	2	1	2	1.3	2	1
	7	Third Brook	5	3	2	2	5	2.3
	8	Elm Street	4	2.8	6	3.3	6	2.6
<b>Former Dam Location</b>								
Upstream	9	Elm Street Up	6	3.3	6	3	6	3.1
	10	Furnace Brook	5	2.7	4	2.3	6	2.5
	11	Sylvia Place	4	2.5	3	1.8	5	2.1
	12	Sylvia Place Up	4	2	2	1	4	1.4
	13	Wapping Road	5	3.3	6	3	6	3.1
	14	Foxworth Lane	5	3	3	1.7	5	2.1
	15	Grove Street	5	2.3	4	2	6	2.1
	16	Pine Brook	3	1.8	1	1	3	1.5
	17	Jones River	3	1.3	3	2	4	1.7
	18	Silver Lake	5	2.5	3	1.7	6	1.9
	19	Tubbs Brook	1	1	3	1.3	3	1.1
	Watershed	10	2.32	9	1.8	10	2.04	

Table 2.4. Site-level detection frequency of aquatic species across years and stream positions in the Jones River watershed.

Common Name	Genus	Species	Total Sites Detected			Upstream Sites Detected			Downstream Sites Detected		
			2020	2021	Cumulative	2020	2021	Cumulative	2020	2021	Cumulative
Alewife	<i>Alosa</i>	<i>pseudoharengus</i>	15	11	16	9	7	9	6	4	7
American eel	<i>Anguilla</i>	<i>rostrata</i>	19	19	19	11	11	11	8	8	8
American gizzard shad	<i>Dorosoma</i>	<i>cepedianum</i>	0	1	1	0	0	0	0	1	1
American shad	<i>Alosa</i>	<i>sapidissima</i>	8	4	9	6	2	6	2	2	3
Atlantic herring	<i>Clupea</i>	<i>harengus</i>	1	3	4	0	1	1	1	2	3
Atlantic menhaden	<i>Brevoortia</i>	<i>tyrannus</i>	1	3	3	0	0	0	1	3	3
Atlantic silverside	<i>Menidia</i>	<i>menidia</i>	1	1	1	0	0	0	1	1	1
Atlantic tomcod	<i>Microgadus</i>	<i>tomcod</i>	1	0	1	0	0	0	1	0	1
Banded darter	<i>Etheostoma</i>	<i>zonale</i>	0	4	4	0	2	2	0	2	2
Banded killifish	<i>Fundulus</i>	<i>diaphanus</i>	0	1	1	0	1	1	0	0	0
Black crappie	<i>Pomoxis</i>	<i>nigromaculatus</i>	10	4	13	7	1	7	3	3	6
Blueback herring	<i>Alosa</i>	<i>aestivalis</i>	10	6	10	5	2	5	5	4	5
Bluegill	<i>Lepomis</i>	<i>macrochirus</i>	19	19	19	11	11	11	8	8	8
Brook trout	<i>Salvelinus</i>	<i>fontinalis</i>	11	12	15	6	9	10	5	3	5
Brown bullhead	<i>Ameiurus</i>	<i>nebulosus</i>	10	8	13	7	6	9	3	2	4
Bullfrogs	<i>Lithobates</i>	<i>catesbeianus</i>	1	0	1	1	0	1	0	0	0
Chain pickerel	<i>Esox</i>	<i>niger</i>	19	0	19	11	0	11	8	0	8
Common carp	<i>Cyprinus</i>	<i>carpio</i>	0	1	1	0	1	1	0	0	0
Common shiner	<i>Luxilus</i>	<i>cornutus</i>	4	0	4	2	0	2	2	0	2
Eastern newt	<i>Notophthalmus</i>	<i>viridescens</i>	0	1	1	0	1	1	0	0	0
Fallfish	<i>Semotilus</i>	<i>corporalis</i>	19	0	19	11	0	11	8	0	8
Four-toed salamander	<i>Hemidactylium</i>	<i>scutatatum</i>	2	0	2	2	0	2	0	0	0
Fourspine stickleback	<i>Apeltes</i>	<i>quadracus</i>	1	1	2	0	0	0	1	1	2
Golden shiner	<i>Notemigonus</i>	<i>crysoleucas</i>	19	19	19	11	11	11	8	8	8
Grass pickerel	<i>Esox</i>	<i>americanus</i>	0	17	17	0	11	11	0	6	6
Grubby sculpin	<i>Myoxocephalus</i>	<i>aenaeus</i>	1	0	1	0	0	0	1	0	1
Hickory shad	<i>Alosa</i>	<i>mediocris</i>	1	0	1	0	0	0	1	0	1
Largemouth bass	<i>Micropterus</i>	<i>salmoides</i>	17	12	18	11	8	11	6	4	7

Table 2.4. Site-level detection frequency of aquatic species across years and stream positions in the Jones River watershed.

Common Name	Genus	Species	Total Sites Detected			Upstream Sites Detected			Downstream Sites Detected		
			2020	2021	Cumulative	2020	2021	Cumulative	2020	2021	Cumulative
Mummichog	<i>Fundulus</i>	<i>heteroclitus</i>	2	3	3	0	1	1	2	2	2
Ninespine stickleback	<i>Pungitius</i>	<i>pungitius</i>	1	0	1	0	0	0	1	0	1
Northern green frog	<i>Lithobates</i>	<i>clamitans</i>	1	0	1	0	0	0	1	0	1
Northern pipefish	<i>Syngnathus</i>	<i>fuscus</i>	0	1	1	0	0	0	0	1	1
Painted turtle	<i>Chrysemys</i>	<i>picta</i>	5	3	5	4	2	4	1	1	1
Pumpkinseed sunfish	<i>Lepomis</i>	<i>gibbosus</i>	19	16	19	11	10	11	8	6	8
Rainbow smelt	<i>Osmerus</i>	<i>mordax</i>	5	2	5	3	1	3	2	1	2
Redbreast sunfish	<i>Lepomis</i>	<i>auritus</i>	7	0	7	2	0	2	5	0	5
Rock bass	<i>Ambloplites</i>	<i>rupestris</i>	19	15	19	11	9	11	8	6	8
Rock gunnel	<i>Pholis</i>	<i>gunnellus</i>	1	1	2	0	0	0	1	1	2
Sea lamprey	<i>Petromyzon</i>	<i>marinus</i>	4	5	7	4	4	6	0	1	1
Sea raven	<i>Hemitripterus</i>	<i>americanus</i>	0	1	1	0	0	0	0	1	1
Smallmouth bass	<i>Micropterus</i>	<i>dolomieu</i>	8	1	8	6	1	6	2	0	2
Striped sea-bass	<i>Morone</i>	<i>saxatilis</i>	1	1	1	0	0	0	1	1	1
Summer flounder	<i>Paralichthys</i>	<i>dentatus</i>	0	1	1	0	0	0	0	1	1
Swamp darter	<i>Etheostoma</i>	<i>fusiforme</i>	0	1	1	0	0	0	0	1	1
Tessellated darter	<i>Etheostoma</i>	<i>olmstedii</i>	18	19	19	11	11	11	7	8	8
Two-lined salamander	<i>Eurycea</i>	<i>bislineata</i>	13	8	15	9	5	10	4	3	5
White perch	<i>Morone</i>	<i>americana</i>	2	2	4	2	2	4	0	0	0
White sucker	<i>Catostomus</i>	<i>commersonii</i>	19	10	19	11	9	11	8	1	8
Winter flounder	<i>Pseudopleuronectes</i>	<i>americanus</i>	2	0	2	0	0	0	2	0	2
Yellow perch	<i>Perca</i>	<i>flavescens</i>	19	16	19	11	10	11	8	6	8
<b>Watershed Totals Aquatic Species</b>			40	38	50	27	34	40	36	33	44
<b>Watershed Totals Diadromous Species</b>			10	9	10	8	8	8	8	8	9

Table 2.5. Conservation and invasion status of selected fish species detected in the Jones River watershed. Each species is evaluated for inclusion on the Massachusetts Species of Greatest Conservation Need (MA SGCN) list, as well as its classification as invasive, non-native, or introduced within Massachusetts. Species considered “non-native” or “introduced” are present in the region but not historically native. Status values are based on state conservation databases and regional ecological assessments. Presence of a “Y” indicates confirmed status. “?” denotes a species with uncertain or regionally variable status.

<b>Common Name</b>	<b>MA SGCN?</b>	<b>Invasive</b>	<b>Non-Native</b>	<b>Introduced</b>
Alewife	Y	-	-	-
American eel	Y	-	-	-
American shad	Y	-	-	-
Banded darter	-	-	?	-
Black crappie	-	-	-	Y
Blueback herring	Y	-	-	-
Brook trout	Y	-	-	-
Common carp	-	Y	-	-
Common shiner	Y	-	-	-
Fallfish	Y	-	-	-
Largemouth bass	-	-	Y	-
Rock bass	-	-	Y	-
Sea lamprey	Y	-	-	-
Smallmouth bass	-	-	-	Y
Swamp darter	Y	-	-	-
Tessellated darter	Y	-	-	-
White sucker	Y	-	-	-

Table 2.6. PERMANOVA results comparing functional trait and taxonomic community composition across sites and years in the Jones River watershed. Results of PERMANOVA analyses evaluating differences in community-weighted functional trait composition, full aquatic vertebrate taxonomic composition, and diadromous fish composition using Bray–Curtis dissimilarity matrices. Comparisons include temporal shifts within upstream and downstream sites (2020 vs. 2021), overall watershed-wide temporal shifts, and spatial differences between upstream and downstream communities for each year and across both years. All analyses were conducted on site-level matrices using all monthly sampling events within each site, then aggregated into group matrices for analysis.

Comparison	Functional Trait Composition			Aquatic Vertebrates			Diadromous Fishes		
	R <sup>2</sup>	F	p	R <sup>2</sup>	F	p	R <sup>2</sup>	F	p
Downstream: 2020 v. 2021	0.04	0.52	0.79	0.14	9.24	0.001	0.32	27.4	0.001
Upstream: 2020 v. 2021	0.20	3.06	<0.001	0.16	14.9	0.001	0.33	39.6	0.001
All Sites: 2020 v. 2021	0.03	0.84	0.57	0.14	22.9	0.001	0.32	65.9	0.001
2020: Upstream v. Downstream	0.06	0.79	0.80	0.06	4.81	0.001	0.04	3.27	0.032
2021: Upstream v. Downstream	0.08	1.05	0.44	0.02	1.38	0.24	0.02	1.50	0.267
All Sites: Upstream v. Downstream	0.03	0.84	0.53	0.03	3.59	0.002	0.02	3.43	0.035

Table 2.7. Results of Wilcoxon rank-sum tests comparing functional diversity metrics across sites and years in the Jones River watershed. Wilcoxon rank-sum tests were used to assess group differences in three functional diversity metrics: Functional richness (FRic) measures the total volume of trait space occupied by species in a community, representing the breadth of ecological roles. Functional divergence (FDiv) describes the degree to which species are distributed toward the edges of the trait space (i.e., niche differentiation), while functional dispersion (FDis) captures the mean distance of species to the community’s trait centroid, indicating trait spread. Comparisons span temporal differences within upstream and downstream sites, overall year-to-year shifts, and spatial contrasts between upstream and downstream sites for each year and across both years combined. W = Wilcoxon test statistic. Analyses were performed using community-weighted means of trait values at the site level across all sampling months.

<b>Comparison</b>	<b>Richness</b>		<b>Divergence</b>		<b>Dispersion</b>	
	<b>W</b>	<b>p-value</b>	<b>W</b>	<b>p-value</b>	<b>W</b>	<b>p-value</b>
Downstream: 2020 v. 2021	20	0.06	0	0.03	10	1
Upstream: 2020 v. 2021	66	<0.001	10	0.04	40	0.58
All Sites: 2020 v. 2021	152	<0.001	16	<0.001	85	0.71
2020: Upstream v. Downstream	18	0.16	50	0.06	41	0.38
2021: Upstream v. Downstream	36	0.72	46	0.16	42	0.33
All Sites: Upstream v. Downstream	116	0.67	196	0.01	168	0.14

## Figures

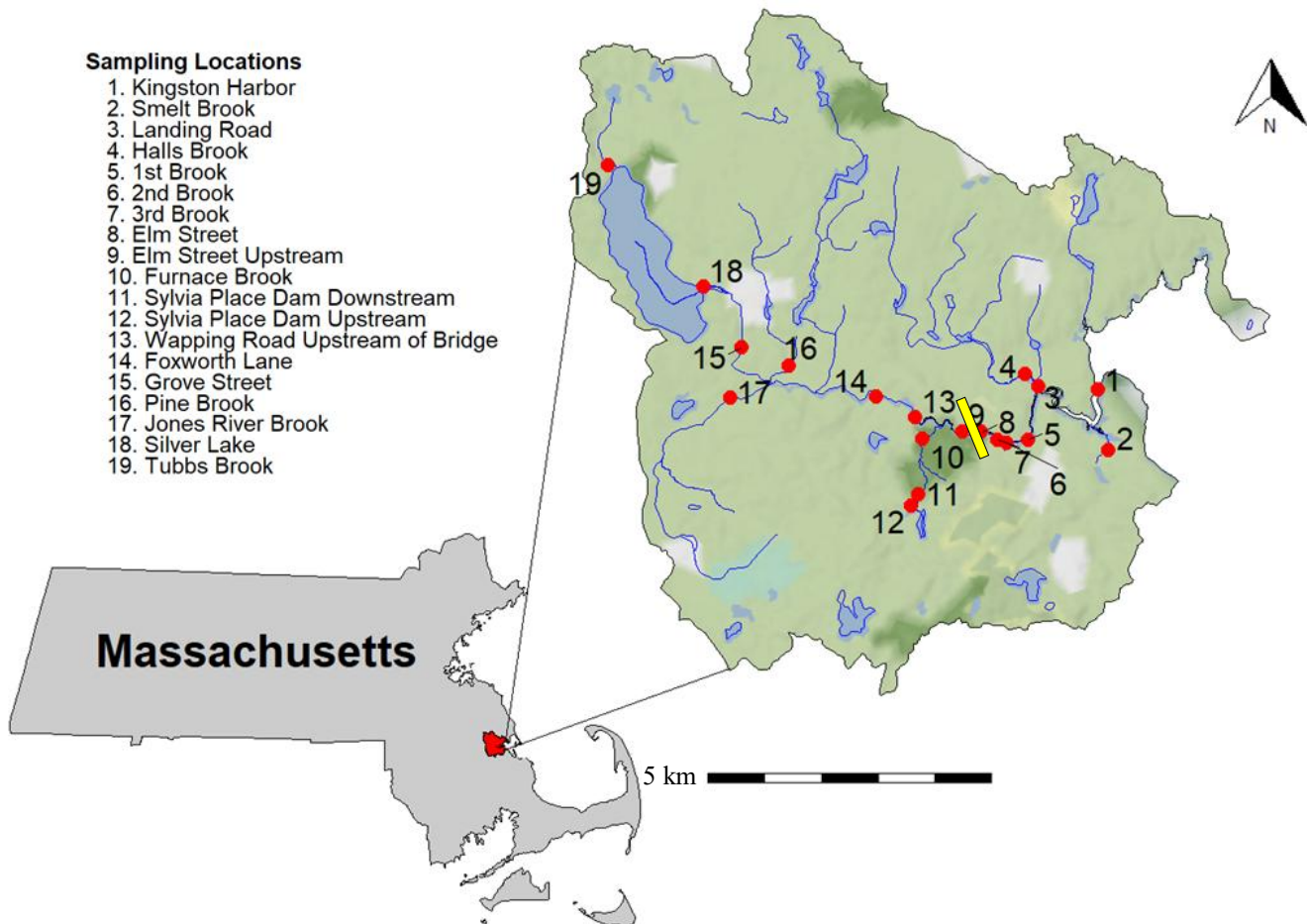


Figure 2.1. Map of the Jones River Watershed, in Southeastern Massachusetts. Red dots represent the 19 sampling locations, numbered from most downstream (1) to upstream (19). The yellow bar represents the location of the Elm Street dam removal in November 2019.

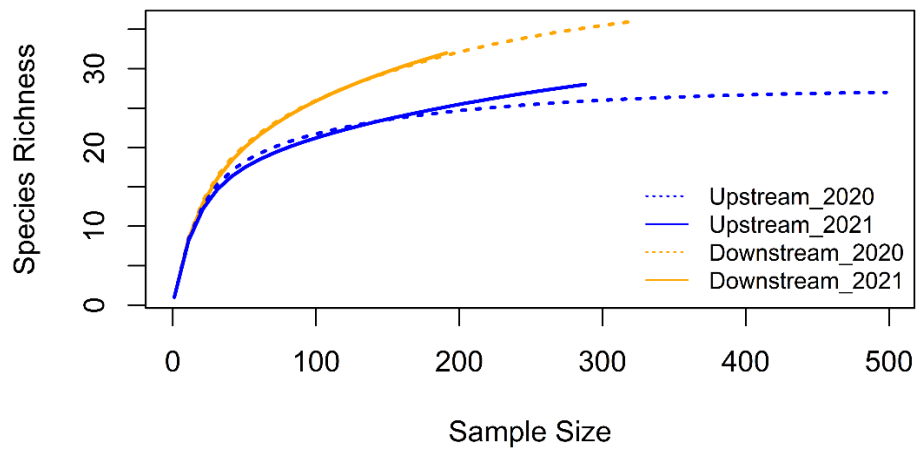


Figure 2.2. Rarefaction curves comparing upstream and downstream communities across years. Rarefaction curves depicting species richness as a function of sample size for upstream and downstream eDNA sampling locations in the Jones River watershed, shown separately for 2020 (dashed lines) and 2021 (solid lines).

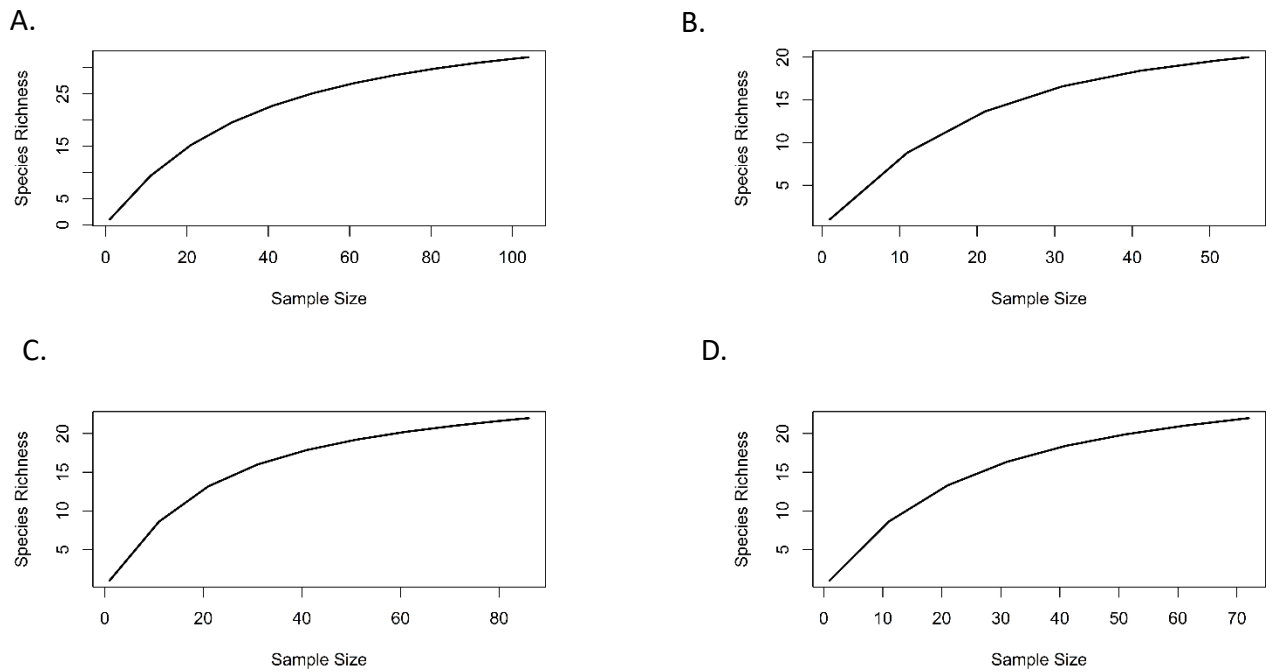


Figure 2.3. Site-specific rarefaction curves for four representative locations with complete sampling in 2020 and 2021. Rarefaction curves for four key sampling locations: A. Kingston Harbor (KH), B. Furnace Brook (FB), C. Wapping Road (WR), and D. Silver Lake (SL) within the Jones River watershed. Curves were generated using the `rarecurve()` function in *vegan* to evaluate species richness accumulation and sampling adequacy for each site across both years (2020 and 2021 combined). The x-axis represents sample size, and the y-axis represents the cumulative number of detected species. Sites where curves failed to plateau were flagged for potential undersampling and further evaluated using Michaelis-Menten saturation models.

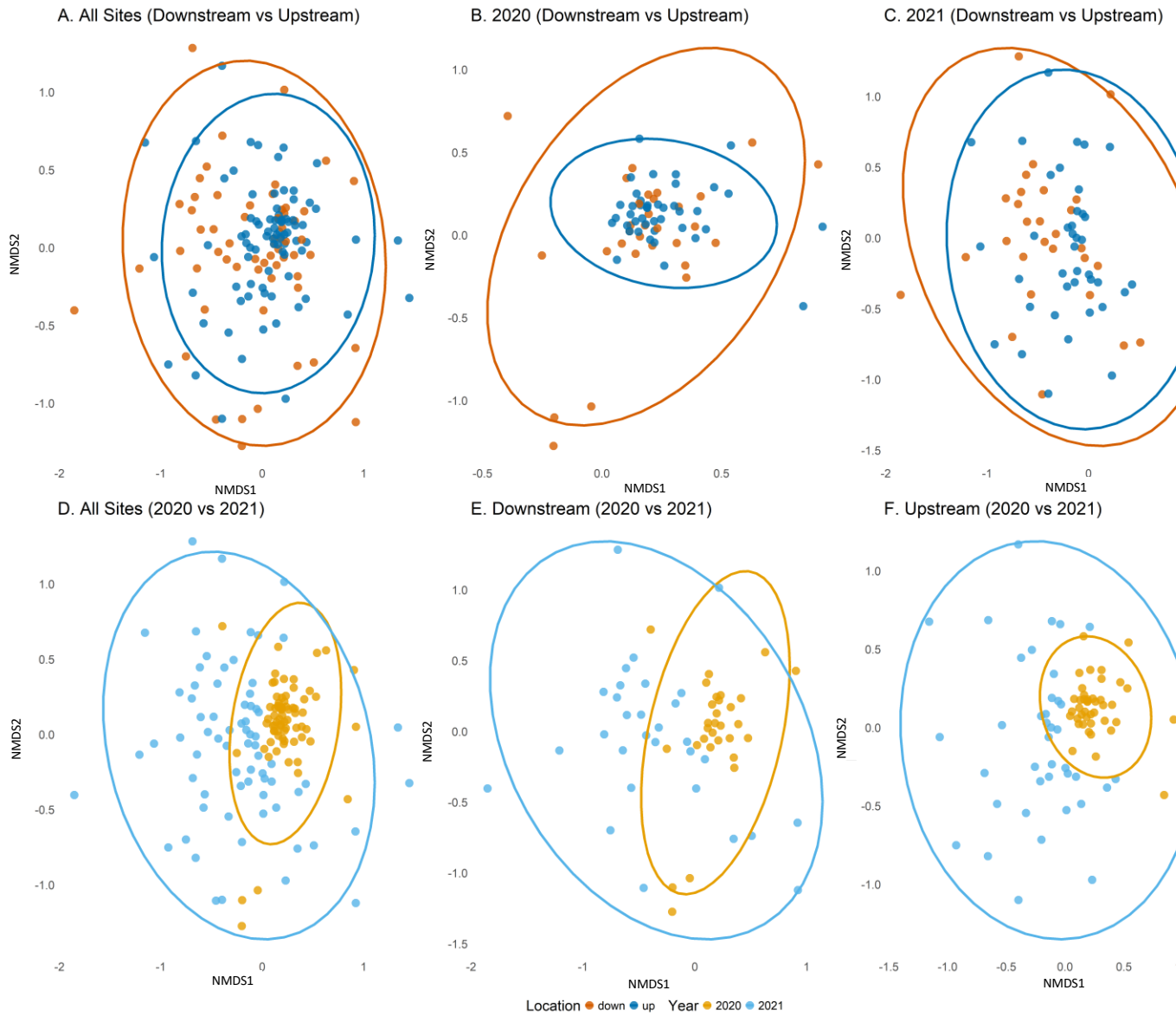


Figure 2.4. Non-metric multidimensional scaling (NMDS) plots visualizing aquatic vertebrate community composition across upstream and downstream sites in the Jones River watershed based on eDNA metabarcoding data. Plots are grouped by spatial and temporal comparisons using Bray–Curtis dissimilarity on presence-absence matrices. Each point represents a site-by-month sampling event, and ellipses indicate 95% confidence intervals for group centroids. (A–C) Compare upstream (blue) vs. downstream (orange) communities for all sites combined A., only 2020 samples B., and only 2021 samples C. (D–F) Show temporal comparisons between 2020 (gold) and 2021 (blue) across all sites D., downstream sites only E., and upstream sites only F.

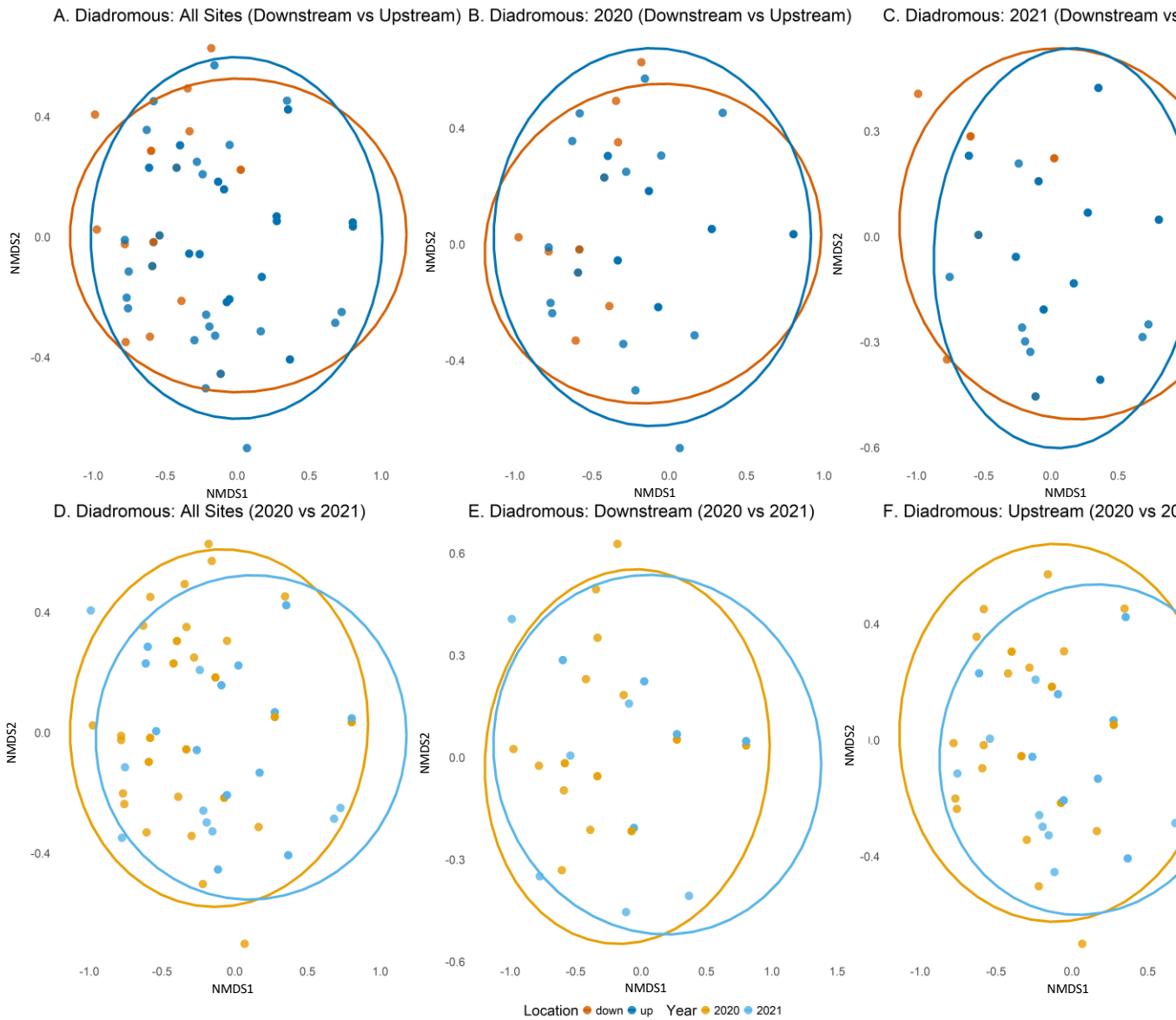


Figure 2.5. Non-metric multidimensional scaling (NMDS) plots showing patterns in diadromous fish community composition across upstream and downstream sites in the Jones River watershed based on eDNA metabarcoding data. NMDS was performed using Bray–Curtis dissimilarity on presence-absence matrices of diadromous species. Each point represents a site-by-month sampling event, with ellipses indicating 95% confidence intervals around group centroids. Panels A–C display spatial comparisons between upstream (blue) and downstream (orange) reaches for all sites A., 2020 only B., and 2021 only C.. Panels D–F illustrate temporal comparisons between 2020 (gold) and 2021 (blue) for all sites D., downstream sites only E., and upstream sites only F.

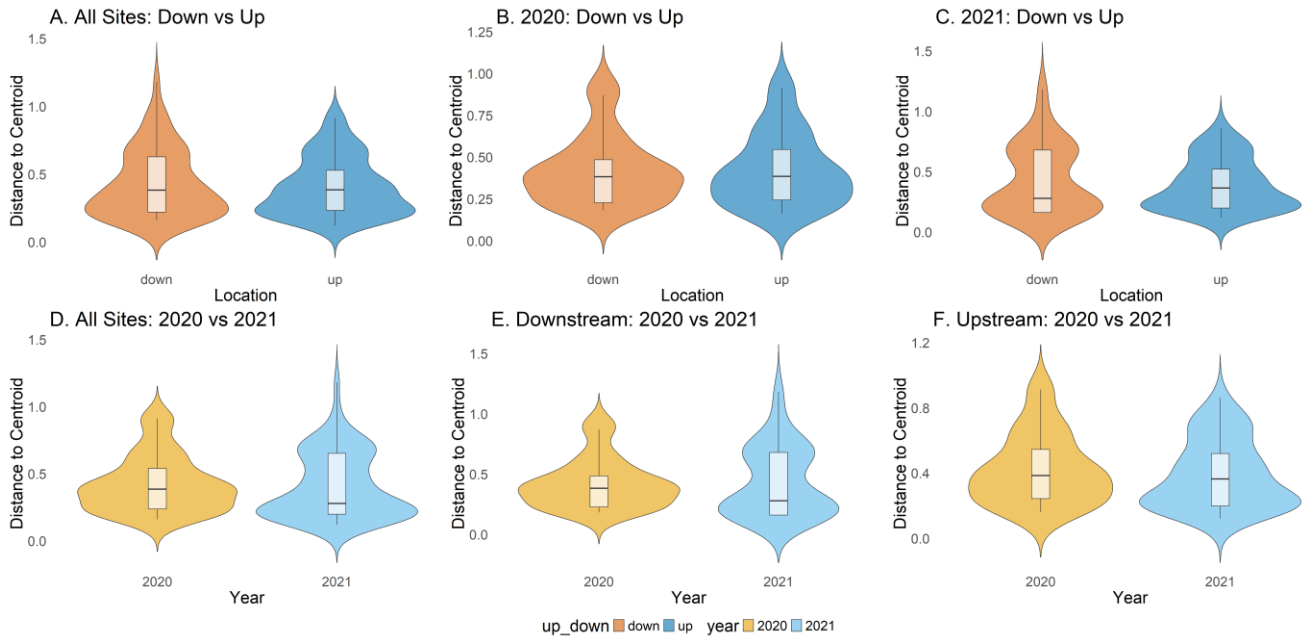


Figure 2.6. Violin plots showing multivariate dispersion (distance to centroid) for diadromous fish communities in the Jones River watershed, based on eDNA metabarcoding data and Bray–Curtis dissimilarities. Dispersion values were calculated from site-by-month presence-absence matrices and reflect within-group variability. Comparisons are shown between upstream (blue) and downstream (orange) reaches for all sites A., 2020 B., and 2021 C., and between years (2020 = gold; 2021 = blue) for all sites D., downstream sites E., and upstream sites F. Larger dispersion in upstream communities (especially in 2020) suggests ongoing ecological turnover and colonization following dam removal.

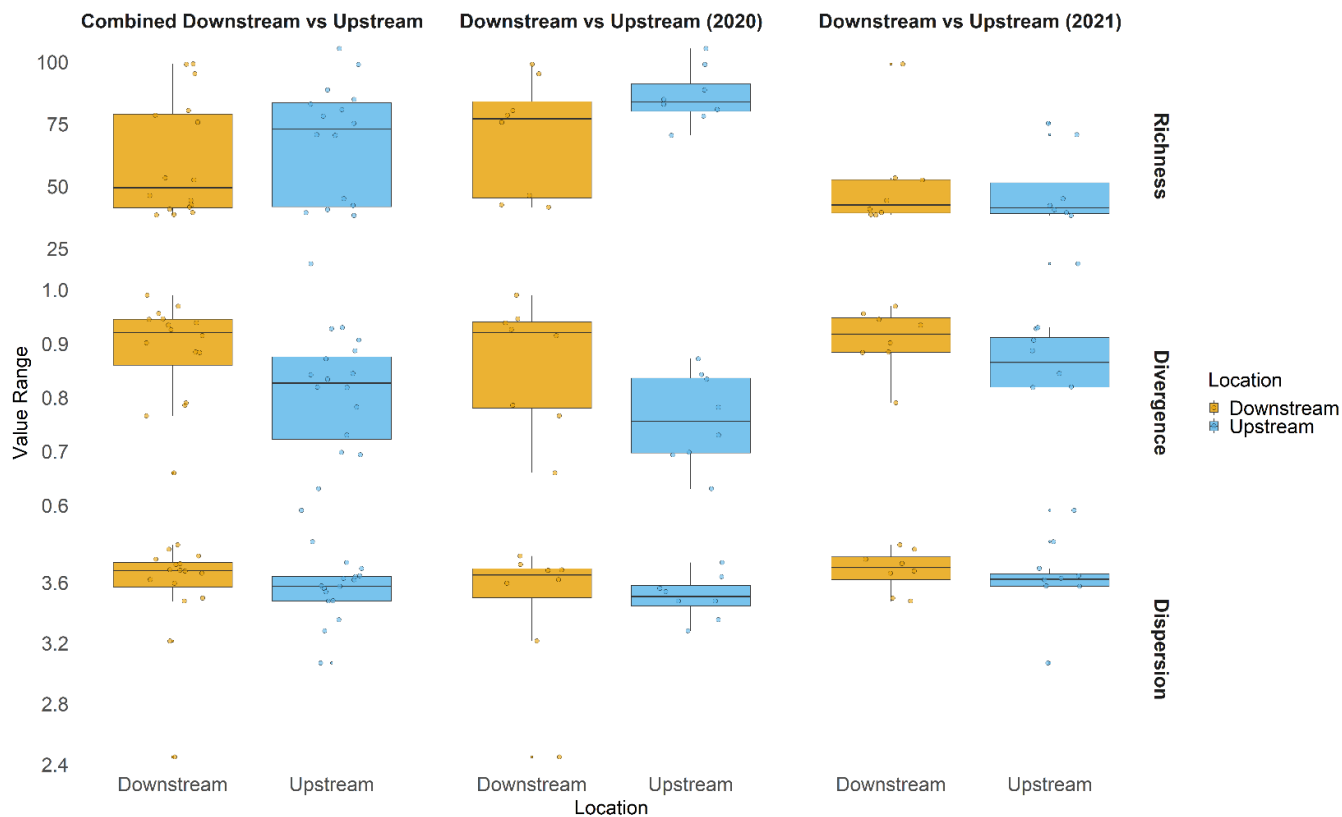


Figure 2.7. Comparison of functional diversity metrics across upstream and downstream communities in the Jones River watershed (2020–2021). Boxplots displaying functional richness (top row), functional divergence (middle row), and functional dispersion (bottom row) for upstream (blue) and downstream (orange) sites, grouped by combined years (left column), 2020 (center column), and 2021 (right column). These trait-based metrics were calculated using community-weighted trait matrices derived from standardized habitat and trophic traits. Statistical differences between upstream and downstream communities for each metric and time period were assessed using Wilcoxon rank-sum tests due to non-normal data distributions.

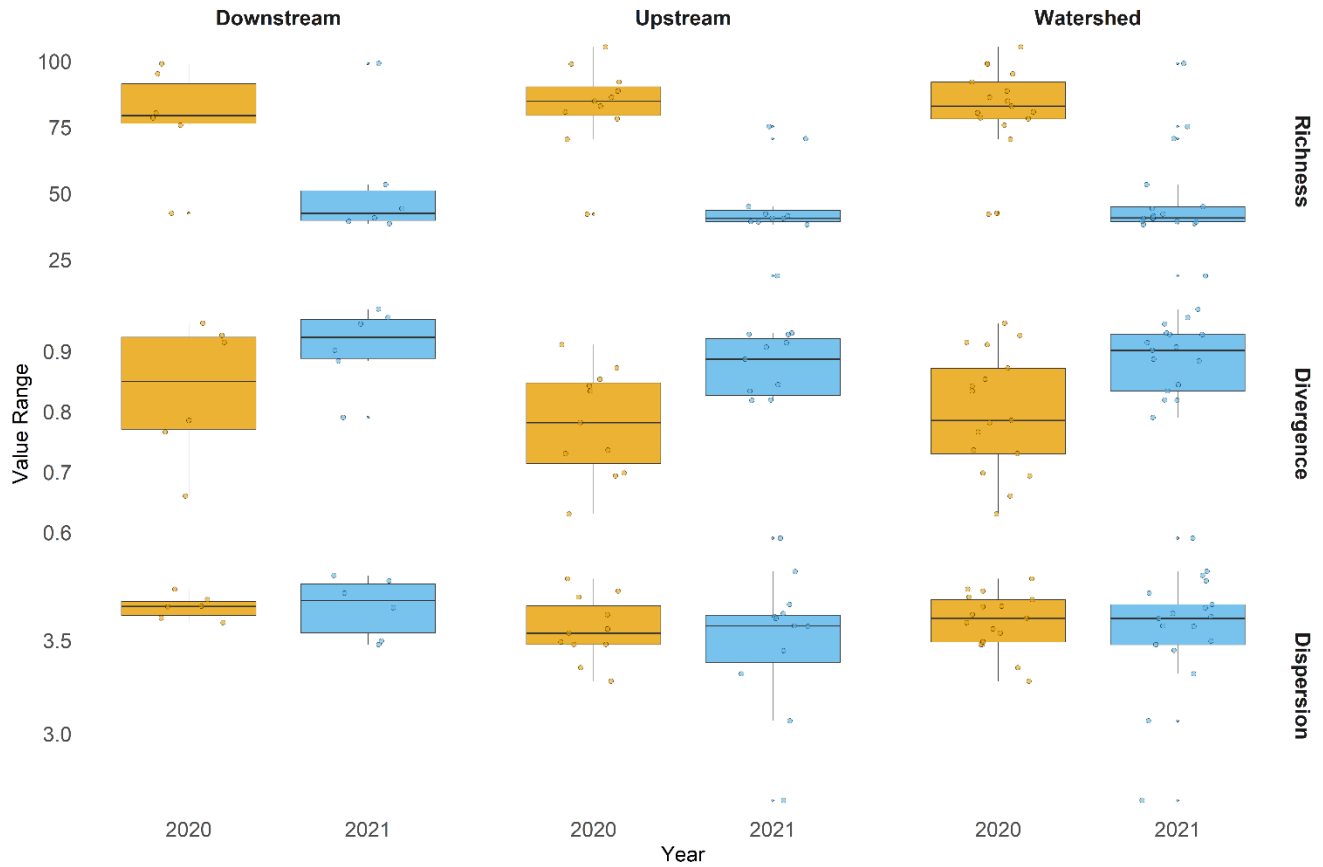


Figure 2.8. Functional diversity metrics across years (2020 vs. 2021) within downstream, upstream, and watershed-wide communities. Boxplots showing functional richness (top row), functional divergence (middle row), and functional dispersion (bottom row) for 2020 (gold) and 2021 (blue) across three spatial categories: downstream (left column), upstream (center column), and the entire watershed (right column). Functional trait metrics were calculated using community-weighted trait matrices derived from standardized habitat and trophic traits. Differences between years were assessed using Wilcoxon rank-sum tests to evaluate temporal trends in trait expression following dam removal. Results reveal interannual variation in trait composition across locations, suggesting dynamic changes in community structure during early ecological recovery.

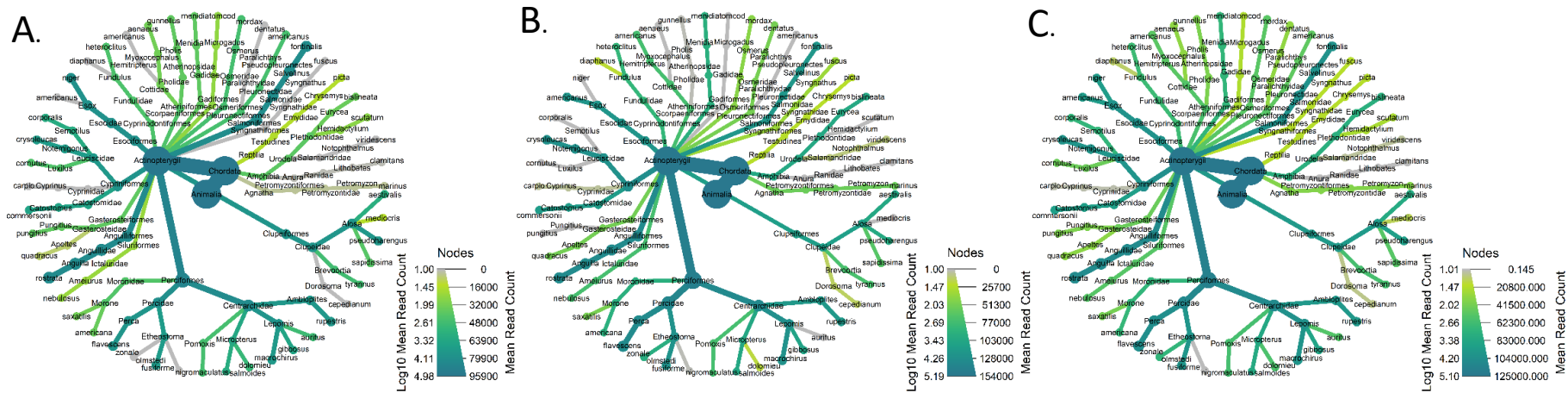


Figure 2.9 Taxonomic heat trees of aquatic vertebrate communities detected via eDNA metabarcoding across the Jones River watershed in 2020 (A.), 2021 (B.), and both years combined (C.). Trees were generated using the *Metacoder* R package and depict mean read count per taxon, with line thickness scaled to abundance and color indicating  $\log_{10}$ -transformed mean read count (green = higher abundance). Central nodes represent higher-level taxonomic groupings (e.g., *Chordata*), branching outward to genus and species levels. These visualizations highlight differences in taxonomic richness and relative abundance between years.

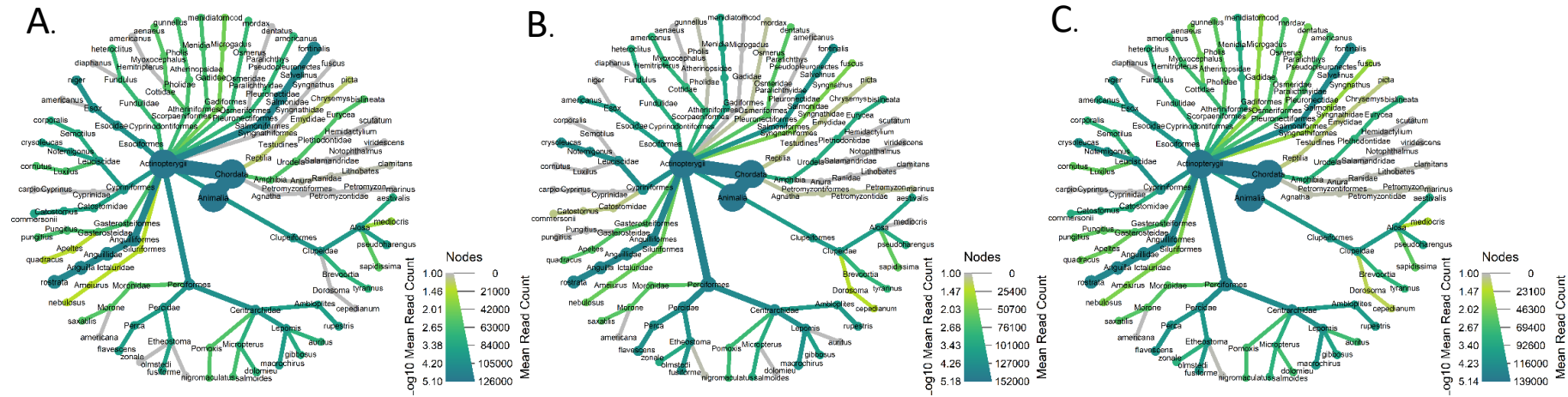


Figure 2.10. Taxonomic heat trees of aquatic vertebrate communities detected via eDNA metabarcoding at downstream sites in the Jones River watershed for 2020 (A.), 2021 (B.), and both years combined (C.). Plots display mean read count values per taxon, with line thickness reflecting abundance and node/edge color scaled by  $\log_{10}$ -transformed mean read count (green = higher abundance). Tree structure spans from the phylum (*Chordata*) to species level.

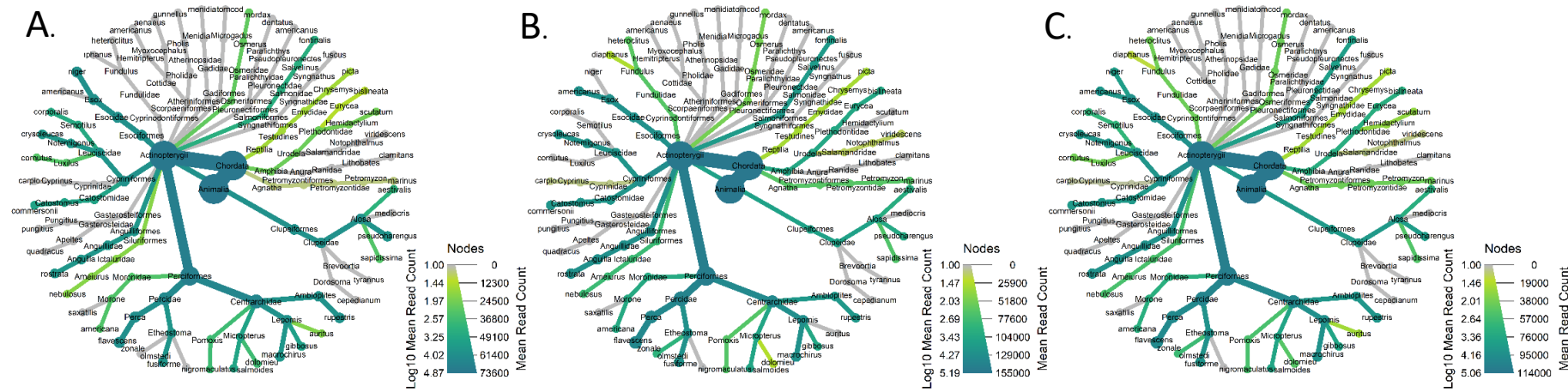


Figure 2.11. Taxonomic heat trees of aquatic vertebrate communities detected via eDNA metabarcoding at upstream sites in the Jones River watershed for 2020 (A.), 2021 (B.), and both years combined (C.). Tree structures represent the phylogenetic hierarchy from phylum to species level, with line and node thickness proportional to mean read count per taxon. Node color reflects log<sub>10</sub>-transformed mean read counts, with darker green indicating higher abundance.

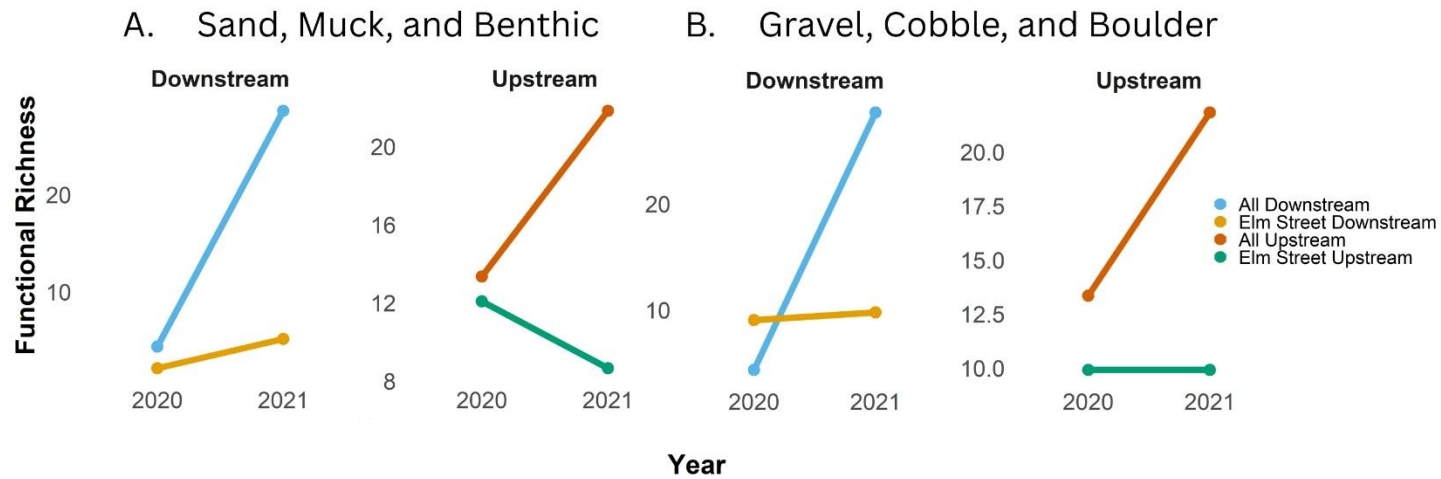


Figure 2.12. Changes in functional richness across upstream and downstream mainstem sites of the Jones River between 2020 and 2021, categorized by substrate-associated trait groups. A. Functional richness of taxa with sand, muck, and benthic substrate preferences. B. Functional richness of taxa associated with gravel, cobble, and boulder substrates. Lines represent mean values for grouped sites: all downstream (blue), all upstream (orange), Elm Street Downstream (yellow), and Elm Street Upstream (green).

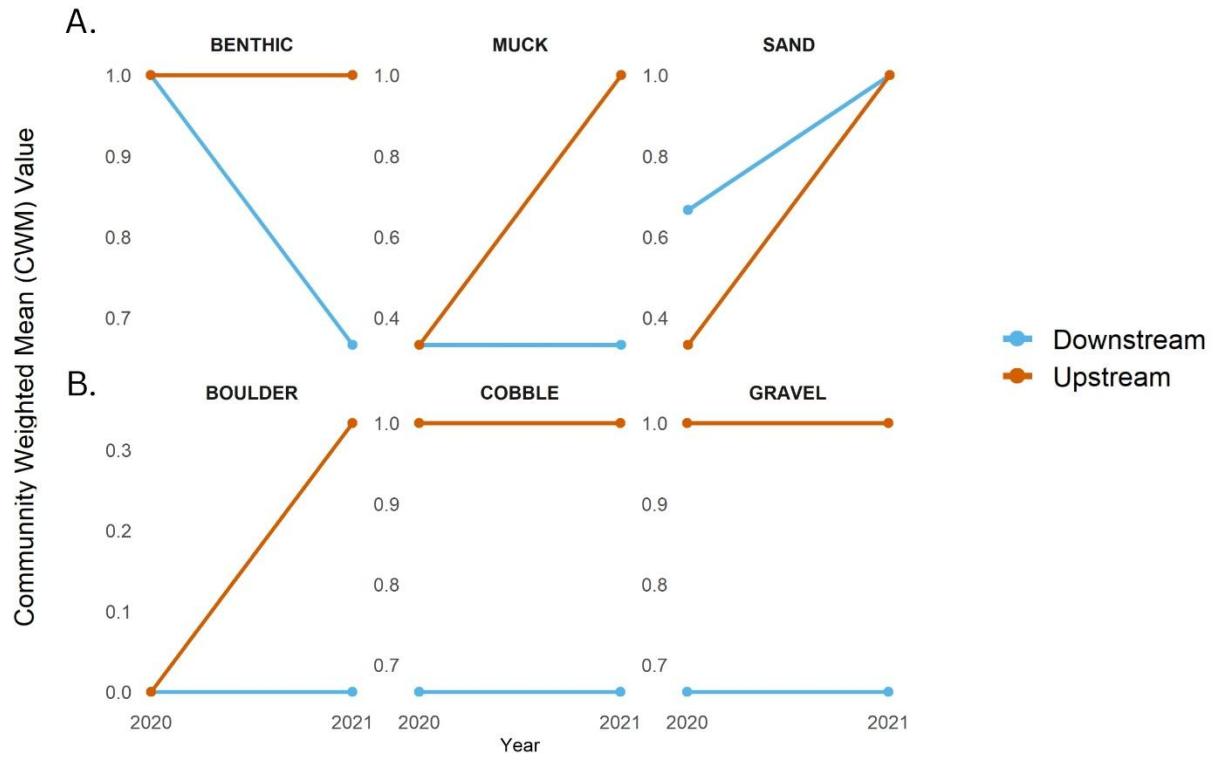


Figure 2.13. Community Weighted Mean (CWM) trait values for substrate-associated species in upstream and downstream mainstem sites of the Jones River, 2020–2021. A. Traits associated with soft substrates (benthic, muck, and sand). B. Traits associated with hard substrates (boulder, cobble, and gravel). Lines represent average CWM values for downstream (blue) and upstream (orange) sites.

## CHAPTER 3

### **Environmental DNA for Fisheries Management: Enhancing Abundance Monitoring with Spatial, Temporal, and Environmental Insights**

#### **Introduction**

Environmental DNA (eDNA) has emerged as a valuable tool in biodiversity monitoring, offering a non-invasive, cost-effective method to assess species presence and abundance across diverse ecosystems (Diaz-Ferguson and Moyer 2014; Evans et al. 2017; Plough 2018; Stoeckle 2020; Yates et al. 2019). By detecting genetic material shed by organisms into their environments, eDNA sampling provides sensitivity and accessibility, particularly in aquatic systems where traditional methods can be time-intensive, invasive, and resource-demanding (Andres et al. 2021; Yates et al. 2019). As global ecosystems face mounting pressures from anthropogenic activities and climate change, eDNA methods present a timely and scalable solution for monitoring biodiversity and informing conservation efforts (Hajibabaei 2022; Stein et al. 2024).

The application of eDNA for abundance estimation in conservation remains limited by knowledge gaps and methodological challenges (Thalinger et al. 2021; Schenekar 2022; Hajibabaei 2022; Stein et al. 2024). Uncertainties regarding the relationship between eDNA concentrations and organism abundance, the influence of biological and environmental variables on eDNA persistence, and the lack of standardized sampling protocols have limited its widespread adoption (Yates et al. 2019; Troth 2021).

Addressing these gaps is essential to transitioning eDNA methods from experimental tools to reliable frameworks for fisheries management (Cristescu and Hebert 2018; Thalinger et al. 2021; Schenekar 2022).

Diadromous fishes represent an ideal case study for refining eDNA techniques.

Anadromous river herring, which include alewife (*Alosa pseudoharengus*) and blueback herring (*A. aestivalis*), are ecologically and economically critical fish species but face significant monitoring challenges (Hare et al. 2021). Traditional methods to monitor river herring include electronic resistivity counters (e-counters), video monitoring, visual surveys, electrofishing, and net sampling. E-counters provide automated counts of migrating fish but cannot differentiate between species, while visual surveys and video monitoring can identify species but require infrastructure to install and power, as well as substantial staff and processing time (Nelson et al. 2011). Net sampling and electrofishing provide detailed biological data including species, length, and weight measurements, but are prone to undercounting in high abundances, labor-intensive and can cause stress to fish (Sheppard and Bednarski 2015). Additionally, all these methods are geographically constrained to specific sampling locations, hindering their scalability for broad-scale population assessments (Nelson et al. 2011; Sheppard and Bednarski 2015). Furthermore, the morphological similarity between alewife and blueback herring complicates species-specific monitoring efforts (Dalton et al. 2022; Hare et al. 2021).

This study aims to address several key gaps in eDNA research by calibrating eDNA signals to e-counter fish counts using 2021 river herring spawning migration in a southern New England watershed as a case study. Non-mechanistic and mechanistic models, respectively, were used to answer the questions: (1) can site-level eDNA

concentrations predict fish abundance when correlated directly with fish counts from traditional methods, and (2) does incorporating known spatial and hydrological drivers of eDNA transport and degradation improve ecological predictions of fish relative abundance? The results were used to develop a scalable framework for integrating eDNA into fisheries management. Outcomes demonstrate the potential for eDNA abundance monitoring to complement and enhance traditional fisheries monitoring methods, providing actionable insights for conservation and management in the face of global environmental change.

## **Methods**

### **Study System**

The Monument River, a 6-km-long, first-order system located in eastern Massachusetts (41.773516° N, 70.562659° W), flows through three, glacially-formed ponds before reaching the Cape Cod Canal (Figure 3.1). During the spring spawning season, adult river herring (both alewife and blueback herring) enter the Monument River from the Cape Cod Canal and ascend three fish ladders before reaching their upstream freshwater spawning habitats, which include four relatively long and shallow (max depth of ~ 14m) interconnected ponds: Great Herring Pond, Little Herring Pond, Beal's Pond, Benoit's Pond (Table 3.1, Figure 3.1 and 3.2). The spring adult spawning run has been monitored by the Massachusetts Division of Marine Fisheries (MA DMF) using electronic resistivity counters (e-counters) since 1984 (Nelson et al., 2011). Based on population monitoring and historical harvest records (Belding, 1921), the Monument River is considered one of the most productive river herring runs in Massachusetts with a mean annual run size of 174,175 fish, and annually ranging between 68,639 (2011) and up to 671,838 (2000) fish

since monitoring began in 1980 (Dalton et al., 2022; Reback et al., 2005; Sheppard and Bednarski, 2015).

### **Electronic Herring Counter Data Collection**

Monitoring was conducted by the Massachusetts Division of Marine Fisheries (MA DMF) using an e-counter (Model 1601; Smith-Root) installed at the upstream side of the second fish ladder in the Monument River. The counting apparatus (86.4-cm length, 127-cm width, 76.2-cm height) consisted of eight white PVC circular counting tunnels (50.8-cm length, 10.16-cm diameter) outfitted with three stainless steel electrodes following the design specifications of Liscom and Volz (1975). The counter recorded the number of fish passing upstream daily throughout the spring spawning migration. E-counter sensitivity and depth was adjusted as needed throughout the migration period to improve resolution and to maintain flow rates between 1.0 and 1.5 m/s, which fell within the acceptable velocity range for river herring passage (Haro et al. 2004; Castro-Santos 2005).

### **eDNA Sample Collection**

Duplicate 500 mL water samples ( n = 18 samples per site) and a single “blank” sample (n = 9 field blanks per site) were collected using 500 mL PET plastic water bottles (Nestle Pure Life, Aberfoyle Ontario) twice weekly between March 29 to May 27, 2021 (n = 9 weeks) at four sites within the Monument River watershed including: Little Herring Pond, Great Herring Pond, Benoits Pond, and a concrete pool site downstream of the Benoits Pond site (Figure 3.1). Following protocols established by Holmes et al. (2021), blank samples were collected in the field before primary sample collection occurred. All samples and blanks were handled using gloves, and all equipment was

sterilized between collections to prevent cross-contamination. Collected samples were immediately placed in sealed containers and put on ice until storage under sterile conditions in a -20°C freezer.

### **Environmental Data Collection**

Water temperature data (°C) was collected daily by biologists and technicians from the MA DMF using mercury thermometers. Basin volumes for study sites were primarily derived from the Massachusetts Department of Environmental Protection (MA DEP) *Massachusetts Integrated List of Waters* database (MA DEP, 2012). For ponds where data were unavailable in the MA DEP database, basin volume was estimated by multiplying the pond's surface area (measured in square meters) by its average depth (measured in meters), a common method for calculating pond volume in ecological studies (Wetzel, 2001). Surface area measurements were sourced from publicly available geographic datasets or determined using satellite imagery.

Distances from the electronic counter to each sampling site were calculated using Google Earth Pro (Google, Mountain View, CA). Measurements were based on the most direct waterway path connecting each site to the counter. These measurements provide critical spatial and environmental context for analyzing the relationship between eDNA signals and fish counts during their annual spawning migration.

### **eDNA Filtration**

Frozen eDNA bottles were thawed for approximately 12 to 16 hours at room temperature before being filtered using techniques outlined by Laramie et al. (2015). Briefly, all filtration equipment was sterilized with a 50% bleach solution and rinsed with distilled

water before drying in a sterile hood. Samples (including a laboratory blank using distilled water) were then filtered using an Air Cadet 115V vacuum pump (part number: 07532-40, Cole Palmer), aluminum filter manifold (part number: 180310-01, Steritech Corporation), and 47 mm, 0.8µm cellulose nitrate filters (part number: 7188-004, Whatman) were used as the filtration apparatus. In cases of filter clogging, samples were processed using sequential filtration, and volumes were recorded to monitor filtration efficiency. After filtration was complete, the cellulose nitrate filter paper for each sample was folded and stored in a microcentrifuge tube containing 95% ethanol and placed in a -80°C freezer until DNA extraction.

### **DNA Extraction**

DNA extraction was done using investigator lyse and spin basket kits (Qiagen, Hilden, Germany) and tissue extraction kits (DNeasy Blood and Tissue, Qiagen) following a modified protocol established by Holmes et al. (2021). The extraction process treated each site-specific sample independently. A PCR inhibitor removal kit (OneStep, Zymo Research, Irvine, CA) step was included to reduce the presence of PCR inhibitors observed in pilot amplifications. Extraction success was assessed by measuring DNA yield and purity using a spectrophotometer (NanoDrop, Thermo Fisher Scientific, Waltham, MA).

### **DNA Sample Preparation**

Quantitative PCR (qPCR) was used to amplify gene sequences and estimate eDNA concentrations for river herring detections in all samples. Immediately prior to qPCR experiments, extracted DNA samples were processed through a 96-well PCR inhibitor

removal kit (OneStep, Zymo Research) to minimize the presence of impurities and PCR contaminants. The resulting 96-well elution plates contained approximately 50  $\mu\text{L}$  of "clean" DNA sample per well. Four wells were left blank in each elution plate to allow for downstream addition of positive and negative control samples. Positive control samples were prepared from custom gene fragments (gBlock, Integrated DNA Technologies, Coralville, IA) of target gene sequences specific to each species (Table 3.2). All gene fragments arrived at 250 ng concentration, and were diluted to a final concentration of  $1 \times 10^6$  copies per mL using 0.5 mg/mL Poly (A) buffer in Tris EDTA (TE). Fifteen  $\mu\text{L}$  of river herring diluted gene fragment was added to two wells on each elution plate. Molecular-grade water (30  $\mu\text{L}$ ) was added in place of sample DNA to two wells of each elution plate to serve as negative control samples.

### **qPCR Assay Design**

A qPCR assay was developed for river herring that targeted both alewife and blueback herring. Each qPCR reaction contained 3.8  $\mu\text{L}$  of purified DNA samples. Mastermix was prepared for the target species using TaqMan Environmental Master Mix 2.0, Applied Biosystems, Foster City, CA; 1X final concentration, custom forward primer, custom reverse primer, and MGB probe sequences (0.5  $\mu\text{M}$ , 0.5  $\mu\text{M}$ , 0.1  $\mu\text{M}$  concentrations, respectively). Purified DNA samples and prepared mastermix were aliquoted into 384-well qPCR plates using an automated liquid-handling robot (MagEx STAR, Hamilton, Reno, NV). The liquid-handling system allowed for high-throughput qPCR sample preparation with a final reaction volume of 10  $\mu\text{L}$  in each well. Each 96-well elution plate containing purified sample DNA was processed through the Hamilton robot twice to

allow for duplicate qPCR results for each sample. Species-specific primer and probe sequences are detailed in Table 3.2.

The prepared 384-well qPCR plates were amplified using real-time PCR detection systems (CFX384 Touch, Bio-Rad, Hercules, CA). Thermal cycling parameters utilized included an initial enzyme activation step at 95°C for 10 minutes, followed by 40 cycles of 95°C for 15 seconds (denaturation phase) and 60°C for 1 minute (annealing phase).

### **Conversion of $C_q$ Values**

Initial qPCR experiments containing 10-fold serial dilutions of each species gBlock Fragment, starting at 10,000 copies per mL, were conducted to produce standard curves. Each standard curve correlated the qPCR  $C_q$  (also denoted as  $C_t$ ) value to an estimated genome copy equivalent (GCE) value for each species tested. Each sample  $C_q$  value was compared to the corresponding species standard curve equation to estimate gene copy numbers contained in each original purified DNA sample.

### **Calibrating eDNA and Traditional Methods**

Un-altered fish counts from e-counters were chosen as the abundance metric for statistical analyses. Raw counts were deemed similar to other fish abundance metrics (density, biomass) in a meta-analysis of eDNA abundance calibration efforts (Lacoursière-Roussel et al., 2016; Baldigo et al., 2017). The number of individual fish detected by the e-counter at the river herring count station, located between the Benoit's Pond and the downstream pool sites, was binned into daily, previous day (day prior to eDNA sampling date), two-day (previous day and day of sample collection), three-day

(two previous days and day of sampling), four-day, five-day, and cumulative (all previous sampling days and day of combined) fish categories.

To evaluate the minimum temporal sampling effort required to reliably capture the dynamics of the river herring run in the Monument River, subsets of consecutive temporal replicates were selected from the full set of available timepoints at each site. These reduced-replication models were compared to full models incorporating all temporal replicates to assess how the number of sampling events influenced model performance. This analysis was conducted across four sites: Little Herring Pond, Great Herring Pond, Benoit's Pond, and the Downstream Concrete Pool. The total number of temporal replicates included for each replication scenario included three-day, six-day, and nine-day intervals, and correlations between log-transformed mean eDNA GCE scores and log-transformed daily fish counts were calculated for each scenario. These intervals were selected by choosing evenly spaced intervals that were less than the smallest number of temporal replication at any individual site ( $n=10$ ). Sites were analyzed in order of their spatial position within the watershed, from upstream to downstream.

For each collection site and date combination, the mean GCE was calculated for duplicate water samples. To determine the best time interval for fish counts, we compared the fish e-counter fish counts to mean GCE values at each eDNA collection site using simple linear regression. The combination with the highest  $R^2$  value was chosen as the best time interval for a given site. Both GCE means and binned e-counter fish counts were log transformed and had a corrective factor of +1.1 added to account for zeroes in the dataset.

To test if eDNA signals collected through time and space accurately predicted the abundance of river herring fish counts generated by e-counters, data were analyzed at

both site specific ( $n = 4$ ) and watershed scales (all sites combined) using the same temporal bin category determined previously.

### **Spatial, Biological, and Environmental Effects**

A linear mixed-effects model was used to evaluate whether eDNA signals collected across space and time predicted fish counts during the spawning migration period. The response variable was the log-transformed mean eDNA GCE value, with log-transformed 2-day binned fish counts, water temperature ( $^{\circ}\text{C}$ ), flow (cfs), basin surface area ( $\text{km}^2$ ), and distance from the fish counter (km) included as fixed effects. Pond identity was included as a random intercept to account for potential non-independence of repeated measures within sites. All predictors were rescaled prior to analysis to improve model interpretability.

Model assumptions were evaluated through residual versus fitted plots and Q-Q plots. Although minor deviations from normality were observed in the tails, residuals were generally homoscedastic and symmetrically distributed. A Dredge Function (R Package: MuMIn (version 1.47.5)) was used to compare models by assigning Akaike Information Criterion (AIC) values to all possible model combinations. The final model with the lowest AIC value included log-transformed mean eDNA GCE value as the response variable, with log-transformed 2-day binned fish counts, basin surface area ( $\text{km}^2$ ), and distance from the fish counter (km) included as fixed effects, with pond identity and sampling week included as random effects. To account for river herring eDNA shed rate ( $1.63 \times 10^{-3}$  (ng/L)/h) and decay rate ( $(2.64 \times 10^{-6}$  (ng/L)/h; Gibbons et al. 2021), we adjusted the final eDNA GCE score using the equation:

Adjusted eDNA GCE score =  $\log \text{eDNA GCE}((\text{river herring shed rate} * \text{hours elapsed})/(\text{eDNA decay rate}))$

### **Mechanistic Allocation of Fish Abundance from eDNA in a Hydrologically Connected Pond System**

A mechanistic scaling and allocation approach was developed to estimate site-specific fish abundances from environmental DNA (eDNA) signals across the three hydrologically connected freshwater ponds. The model leveraged eDNA samples collected at each site in conjunction with fish counts recorded at a single downstream e-count station. Modeling was performed on both a two-day rolling window of fish counts and a cumulative-to-date time series.

For each pond, eDNA concentrations were log-transformed using the function  $\log(\text{eDNA} + 1.1)$  to stabilize variance and manage zero values. The log-transformed eDNA signal was then scaled to account for morphometric and spatial characteristics of each pond. Specifically, scaled eDNA values were calculated as:

$$\text{eDNA}_{\text{adj},i} = \frac{\log(\text{eDNA}_i + 1.1) \times A_i^{\alpha_i}}{\log(D_i + 1.1)}$$

Where  $A_i$  is the surface area of pond  $i$ ,  $D_i$  is the linear distance from pond  $i$  to the downstream fish counter, and  $\alpha_i$  is a site-specific exponent derived via inverse proportional surface area, or sensitivity analysis minimizing model AIC. In the inverse proportional surface area approach, exponents  $\alpha_i$  were defined as  $1 - p_i$ , where  $p_i$  is the proportional surface area of site  $i$  relative to the total surface area of all ponds. This scaling reflects the hypothesis that smaller ponds contribute disproportionately stronger

eDNA signals per unit surface area due to reduced dilution and confinement of biomass. For example, Benoits Pond, which represented only 1% of the total surface area, was assigned an exponent of 0.99, while Great Herring Pond, covering 83% of the total area, was assigned an exponent of 0.17. This adjustment accounts for eDNA dilution dynamics and degradation, consistent with known hydrological behavior and species movement ecology (Jane et al., 2015; Carraro et al., 2020). Sensitivity analysis was performed by evaluating a grid of exponent combinations for each pond (0.01 to 1.5 in 0.05 increments), fitting linear mixed-effects models at each combination, and selecting the exponent set that minimized AIC while maximizing conditional  $R^2$ .

The adjusted signals were then used to proportionally allocate the observed fish count to each pond. Fish abundances  $Fish_i$  were estimated via:

$$Fish_i = \left( \frac{eDNA_{adj,i}}{\sum_j eDNA_{adj,j}} \right) \times N_{window}$$

Where  $N_{window}$  is the total number of fish recorded at the downstream counter over the two-day or cumulative sampling window. A nested allocation scheme was applied to reflect the hydrological reality of the system: fish were first allocated to Benoits Pond, the most downstream site, based on its proportional contribution to the total adjusted eDNA signal. The remaining unallocated fish were then distributed between the two upstream ponds, GHN and LHP, in proportion to their respective  $eDNA_{adj}$  values. This structure ensured that fish were not over-assigned to upstream ponds, which would violate the directional flow of eDNA and fish movement.

The resulting fish abundance estimates were log-transformed as  $\log(\text{Fish}_i + 1.1)$ , and site-specific generalized linear models were fitted using either quadratic (to account for non-linear trends for two-day data) or linear (for cumulative data) temporal terms. For the two-day dataset, models followed:  $\log(\text{eDNA}_i) \sim \log(\text{Fish}_i) + \log(\text{Fish}_i^2) + \text{Julian}_i + \text{Julian}_i^2$ . For cumulative datasets, the model structure was simplified:  $\log(\text{eDNA}_i) \sim \log(\text{Fish}_i)$ , as the cumulative data structure accounted for time in the model.

To cross validate outputs from mechanistic models, linear mixed-effects models were fit to evaluate the combined predictive capacity across all sites and sampling weeks, where the two-day formula was:  $\log(\text{eDNA}) \sim \log(\text{Fish}) + (1|\text{site}) + (1|\text{week})$ ; and the cumulative formula was:  $\log(\text{eDNA}) \sim \log(\text{Fish}) + (1|\text{site})$ . Model performance was evaluated using marginal and conditional  $R^2$ , AIC, and visual goodness-of-fit comparisons. See Model Formula table (Table 3.3) for full model formula combinations. Figures illustrating mechanistically derived proportional fish allocations trends in eDNA and estimated fish abundance across sites were generated using the same data used to construct these models (Figures 3.3 and 3.4).

This framework rests on the assumption that eDNA signal strength is reflective of contemporary fish occupancy within each pond, and that transport is primarily unidirectional with measurable decay across distance (Pilliod et al., 2014; Yates et al., 2019). The use of surface area scaling reflects the biology of the target species—river herring—which occupy and spawn in shallow littoral zones (Hare et al., 2021).

All analyses were conducted in R (v4.3.2) using the `dplyr`, `lme4`, `ggplot2`, and `lubridate` packages.

## Results

eDNA amplification success for field samples varied, with a combined success rate of 51% for laboratory replicates. For 16% of samples, one replicate amplified and the other did not. Samples with only one amplified replicate were not averaged, and included as a singular sample in the final datasets. When both duplicates failed to amplify for a given date at a given site, it, along with its paired e-count values, were removed from the dataset. Field blanks showed no amplification indicating no contamination present.

### Calibrating eDNA and Traditional Methods

Because amplification success varied across sites, some sites had more sampling events than others. Number of dates eDNA samples successfully amplified ranged from 11 at Great Herring Pond to 16 at Benois Pond and Concrete Pool (Table 3.4). Sites with a higher number of sampling events generally showed stronger statistical performance, with higher  $R^2$  values and lower p-values, reflecting the importance of repeated sampling for improving model reliability (Table 3.5). The two-day binned approach yielded consistently significant p-values and high  $R^2$  values across all time-steps examined, only being outperformed by single day fish counts at the Great Herring Pond site and the previous day fish count narrowly outperforming the two-day fish count at Benois Pond. For site-specific models, Benois Pond had the strongest relationship between eDNA and fish counts, with the previous day's fish count as the top predictor ( $R^2 = 0.94$ ,  $p < 0.001$ ). The downstream Pool site also performed well, with a two-day binned fish count as the best predictor ( $R^2 = 0.83$ ,  $p < 0.0001$ ). Great Herring Pond performed moderately, with the single-day fish count as the best predictor ( $R^2 = 0.53$ ,  $p = 0.01$ ). Little Herring Pond

had the weakest correlation, with a two-day binned fish count as the top predictor ( $R^2 = 0.36$ ,  $p = 0.03$ ) (Table 3.6).

We observed that log-transformed eDNA signals closely track two-day binned (Figure 3.5) and cumulative fish counts (Figure 3.6) over short (weekly) to longer term (~2 months) time scales. Larger temporal bins (three + days) performed worse than smaller temporal bins across all sites. Fish count signals were closely mirrored by eDNA signals. As fish counts increased or decreased over the course of the migratory season, eDNA signal responded in real time. For full temporal bin results see supplementary materials Table 1A.

Several combinations of consecutive eDNA sampling events were tested to determine the minimum number of eDNA sampling events needed to capture the dynamics recorded by the e-counter counts in the river herring run in the Monument River. A clear positive trend in correlation with increasing sampling events and e-counter counts was observed (Table 3.7). At nine temporal replicates, all sites had significant correlations between log-transformed mean eDNA GCE scores and log-transformed daily fish counts.

### **Spatial, Biological, and Environmental Effects**

The best-performing multiple linear model used the two-day fish count as the response variable, and incorporated eDNA GCE scores, the distance from the e-counter, and surface area as predictor variables (AIC score = 203.1,  $R^2 = 0.74$ ,  $p < 0.001$ ) (Table 3.8).

The best-performing watershed scale linear model, used log-transformed eDNA GCE scores as the predictor and two-day binned fish counts as the response variable, explained 58% of the variance ( $R^2 = 0.58$ ,  $p < 0.001$ ).

Log-transformed eDNA GCE had the largest effect size (0.77,  $p < 0.001$ ), making it the most influential predictor in the model (Table 3.7). Distance from the e-counter had a significant negative effect ( $p < 0.001$ , effect size =  $-4.6E-04$ ), reflecting the inverse relationship between proximity to the counter and eDNA-fish count correlations. Surface area exhibited a smaller but significant effect ( $p = 0.009$ , effect size =  $-8.4E-07$ ), likely reflecting the dilution effect in larger basins. In contrast, water temperature, although included in the model, did not significantly contribute to predicting fish counts ( $p = 0.18$ , effect size =  $6.81E-02$ ).

### **Mechanistic Allocation of Fish Abundance from eDNA in a Hydrologically Connected Pond System**

Mechanistic and non-mechanistic eDNA models were evaluated for their ability to predict fish abundance across three connected ponds; Benois Pond, Great Herring Pond, and Little Herring Pond. Mechanistic models using surface area- and distance-adjusted eDNA signals to allocate fish relative abundance over a 2-day window yielded strong to moderate site-specific fits. Sensitivity analysis showed that scaling all three ponds using uniform  $\alpha_i$  values of 0.01 performed best out of all  $\alpha_i$  value combinations tested for both 2-day and cumulative mechanistic model approaches. Linear mixed models using mechanistic model derived fish abundance estimates and sensitivity analysis optimized  $\alpha_i$  values explained 95.4% of variance at Benois Pond ( $R^2 = 0.954$ ,  $p = 0.001$ ), 73% at Great Herring Pond ( $R^2 = 0.73$ ,  $p = 0.1$ ), and 60.9% at Little Herring Pond ( $R^2 = 0.609$ ,  $p = 0.24$ ). The corresponding models which used  $\alpha_i$  values derived from the inverse proportionally scaled surface area of a given pond showed similarly high performance at

Benoits Pond ( $R^2 = 0.94$ ) and Little Herring Ponds ( $R^2 = 0.63$ ,  $p=0.22$ ) but reduced explanatory power at Great Herring ( $R^2 = 0.69$ ,  $p=0.14$ ).

Mechanistic cumulative models including time terms were assessed the same way the two-day fish count window, and performed well across all sites. Models using  $\alpha_i$  values derived from sensitivity analysis explained 99% of the variance at Benoits Pond ( $R^2 = 0.99$ ), 81% at Great Herring Pond, and 98% at Little Herring Pond, with all models significant at  $p < 0.001$ . The corresponding models which used  $\alpha_i$  values derived from the inverse proportionally scaled surface area of a given pond also achieved high explanatory power ( $R^2 = 0.98-0.78$ ), with slightly higher AIC values (Table 3.3).

Non-mechanistic models using unadjusted eDNA concentrations showed reduced predictive performance compared to mechanistic alternatives. When temporal terms were excluded, the model explained 81% of the variance at Benoits Pond ( $R^2 = 0.81$ ,  $p = 0.003$ ,  $AIC = 29.9$ ), but only 33% at Great Herring Pond ( $R^2 = 0.33$ ,  $p = 0.24$ ) and 9% at Little Herring Pond ( $R^2 = 0.09$ ,  $p = 0.72$ ). Inclusion of quadratic Julian day term markedly improved the Benoits Pond model ( $R^2 = 0.96$ ,  $p = 0.001$ ,  $AIC = 18.3$ ), but yielded more modest gains at Great Herring Pond ( $R^2 = 0.66$ ,  $p = 0.17$ ,  $AIC = 37.6$ ) and Little Herring Pond ( $R^2 = 0.54$ ,  $p = 0.34$ ,  $AIC = 43.4$ ). Despite this improvement in explanatory power, performance remained consistently lower than mechanistic models, and did not yield statistically significant results particularly for Great Herring and Little Herring Ponds.

When aggregating across all three basins, the highest performing model used cumulative mechanistic eDNA values with surface area scaling ( $R^2 = 0.97$ ,  $p < 0.001$ ,  $AIC = 70.27$ ),

closely followed by the cumulative sensitivity-optimized model ( $R^2 = 0.95$ ,  $AIC = 63.24$ ). Two-day models also performed well, with the sensitivity-optimized variant outperforming the surface area-scaled version ( $R^2 = 0.93$  vs  $0.81$ ). Both non-mechanistic combined models were less predictive, with  $R^2$  values of  $0.76$  (with time) and  $0.64$  (without time), and substantially higher AIC values (Table 3.3).

Temporal trends and proportional allocations corresponding to these models are visualized in figures 3.3 and 3.4.

## **Discussion**

The general strong relationship between eDNA GCE scores and independently determined river herring counts supports previous findings that eDNA concentrations can consistently and accurately reflect species' relative abundances in aquatic systems (Takahara et al., 2012; Shelton et al., 2019; Yates et al., 2019). In addition, findings aligned with more recent work showing that temporal replication—repeated sampling across key biological windows—substantially improves correlations between eDNA signals and traditional monitoring data (Levi et al., 2019; Searcy et al., 2021; Fowler et al., 2024; Ogburn et al., 2023; Capo et al., 2019; Doi et al., 2017; Yates et al., 2019; Rosset et al., 2017). The variability among locations in the relationship to the fish counts also support claims that eDNA transport and detectability is strongly shaped by spatial and physical factors within a watershed (Yates et al., 2019; Drummond et al., 2021). The strength of eDNA-fish count correlations varied across individual sites and at the watershed scale, and were best explained by spatial aspects like lake surface area and distance from the fish counter. These two spatial variables likely capture key dilution,

eDNA dispersal, and fish dispersal dynamics that govern eDNA detectability in this system.

Other environmental variables known to influence eDNA signal persistence and detection were analyzed but ultimately excluded from final models. Flow and temperature were evaluated as fixed effects but did not significantly improve eDNA-based predictions of fish abundance. Flow was measured at a single point near the fish ladder and did not capture spatial variability across the watershed, particularly in lentic habitats where hydrology is driven more by wind, stratification, and inflow/outflow dynamics than by discharge alone (Shogren et al., 2017; Conant et al., 2019). Although water temperatures ranged from 7.5 °C to 23.5 °C—conditions known to influence eDNA degradation and shedding (Strickler et al., 2015; Fry & Hart, 1948)—temperature effects may have been masked by stronger spatial or biological drivers. Future work incorporating vertical profiles and finer temporal resolution may be necessary to detect temperature effects in more stratified or isolated systems (Mächler et al., 2018; Harrison et al., 2019).

By knowing the estimated maximum number of river herring within the system at a given downstream location and time point, integrating hydrological principles, eDNA transport, degradation dynamics (Jane et al., 2015; Shogren et al., 2017; Harrison et al., 2019; Van Driessche et al., 2022; Carraro et al., 2024), and spatially explicit biological expectations, such as river herring aggregations in littoral and pelagic lake habitats (Devine et al., 2021; Yates et al., 2019), mechanistic models generated ecologically plausible and internally consistent site-level relative abundance estimates from a single e-count station. While models based on cumulative fish counts performed best overall in the mechanistic model comparisons, likely due to the additive nature of eDNA transport and persistence

downstream (Carraro et al., 2020), the two-day models performed nearly as well and offered complementary insights. The two-day binning window may more accurately reflect real-time fish presence and eDNA shedding associated with active migration and spawning events, whereas cumulative models likely captured downstream signal accumulation across longer time periods. Both approaches provide potentially actionable information for natural resource managers interested in knowing more about how river herring are using these connected habitats.

Mechanistic scaling using either sensitivity-optimized or surface area-optimized exponents ( $\alpha_i$ ) revealed further tradeoffs in how fish abundance was allocated across sites. Models optimized via sensitivity analysis consistently allocated a greater proportion of fish to Benoit's Pond, and outperformed surface area-based models in predictive accuracy. In contrast, models using surface area-derived exponents allocated most fish to Great Herring Pond, consistent with known habitat usage and spawning patterns of river herring in this system. The alpha ( $\alpha$ ) values in these mechanistic models serve as scaling exponents that adjust the influence of site-specific DNA inputs on predicted fish abundance, effectively modulating how eDNA signal strength is interpreted across space. In the sensitivity-scaled model, setting all  $\alpha$  values to a uniform, low constant ( $\alpha = 0.01$ ) acted as a conservative normalization factor, minimizing the influence of large spatial or volumetric differences between ponds. In contrast, the surface area-scaled model used  $\alpha_i$  values derived from the inverse of each pond's proportional surface area, meaning that smaller ponds (e.g., Benoit's Pond) received greater scaling of their eDNA values than larger ponds. This approach reflects the assumption that eDNA concentrations are naturally higher in smaller waterbodies due to reduced dilution and more confined

biomass. Both mechanistic frameworks outperformed linear mixed models that relied solely on distance from the e-count station and pond surface area as fixed effects, highlighting the value of customized, site-specific correction factors grounded in physical and ecological data. From a management perspective, the choice between sensitivity-scaled and surface area-scaled models reflects a tradeoff between aligning with biological expectations of fish habitat use and accounting for physical processes that govern eDNA production, transport, and decay; selecting between them might ultimately depend on whether the primary interest lies in tracking fish distribution or understanding the environmental behavior of eDNA itself—both of which offer valuable, but distinct, insights for conservation and monitoring efforts.

Cross-validation analyses revealed a marked improvement in the correlation between eDNA concentrations and fish abundance after applying mechanistically derived, site-specific fish counts. This enhancement supports the internal coherence and ecological validity of the mechanistic outputs, suggesting that the model effectively redistributes relative abundance estimates in a biologically and hydrologically meaningful way. Such results lend credence to the use of eDNA mechanistic models for spatially explicit abundance estimation in connected systems.

Interestingly, time series comparisons of mechanistically adjusted eDNA signals and modeled fish relative abundances revealed divergence peaks along a log transformed y-axis where eDNA signals peaked well above fish count values. These peak divergences may indicate spawning activity, where eDNA values are larger than the number of fish in a given pond, possibly derived from additional genetic material being shed into the environment during spawning (Rosset et al., 2017). If mechanistic model derived time

series comparisons are in fact reflecting spawning events within connected ponds, this observation could suggest that eDNA has the potential to provide novel insights into the timing of key life history events of target species. However, persistent underestimation of eDNA signals in Great Herring Pond relative to observed fish counts likely reflects physical eDNA transport dynamics, such as wind-driven mixing or DNA sedimentation, that are not currently accounted for in the model. However, further empirical validation is needed. Installing an additional resistivity fish counter between Little Herring Pond and Great Herring Pond would provide a critical opportunity to test model predictions and confirm the accuracy of inter-basin abundance assignments. Such validation efforts are essential given the ongoing need to refine eDNA-based inference frameworks and assess their limits in dynamic, lotic-lentic systems (Hajibabaei, 2022; Carraro et al., 2018; Carraro & Altermatt, 2024).

At the time of writing, qPCR primers and probes which can distinguish alewife from blueback herring do not exist (Dalton et al., 2022). Therefore, combining eDNA with weekly biological sampling at the fish ladder can help resolve species composition and seasonal shifts (Plough et al., 2018; Goldberg et al., 2015). Biological sampling data collected by the MA DMF showed that the Monument River Herring run is dominated by alewife in the first two weeks of the sampling window, with the following two-week window comprised of a mix of alewives and blueback herring, and the last two weeks of the run dominated primarily by blueback herring (pers. Communication, MA DMF). If biological sampling data are compared to the mechanistic temporal patterns of river herring count numbers and eDNA signals, three distinct peaks occur between the connected Benois Pond and Great Herring Pond (between Julian dates 115-125, 130-140,

and 140-147, respectively), and only two distinct peaks occur in the most upstream Little Herring Pond (between Julian date 115-125 and 130-140). This could be a signal that Alewives are making it into Benois Pond, Great Herring Pond, and Little Herring Pond, but Blueback Herring might be prioritizing only Benois Pond and Great Herring Pond for spawning, as Little Herring Pond lacked the final peak, and Blueback herring are known to have been present within this system in higher numbers during that window.

Ultimately, the ability to reconstruct watershed-scale fish distributions from a single traditional observation point underscores the promise of eDNA for monitoring ephemeral migration events and spatial occupancy dynamics in near real-time. While continued refinement and validation are essential, these findings demonstrate that well-calibrated, mechanistically informed eDNA models can provide ecological insights into species abundance across connected aquatic systems (Cristescu & Hebert, 2018; Spear et al., 2021). By enabling spatially resolved relative abundance estimates with minimal field infrastructure, this approach offers a scalable and cost-effective enhancement to traditional monitoring networks, particularly in systems where access, funding, or staffing are limited. As climate change accelerates phenological shifts and alters species distributions, tools that can reliably detect and model biological responses across space and time are increasingly vital (Visser & Both, 2005; Antão et al., 2022). The mechanistic framework presented here provides a foundation for next-generation biomonitoring strategies that are both data-efficient and ecologically grounded, with broad applications for conservation, fisheries management, and ecosystem restoration.

## Tables

Table 3.1. Basin surface areas and distances from fish counter. Surface areas and spatial data for four ponds and pools near the fish counter in the Monument River Watershed, Massachusetts, USA. Sites are ordered largest to smallest.

Site No.	Site Name	Lake Surface Area (m <sup>2</sup> )	Distance from Counter (m)
1	Great Herring Pond	1,695,693	1867
2	Little Herring Pond	327,807	4828
3	Benoits Pond	16,188	1.5
4	Concrete Pool	178	44

Table 3.2. qPCR assay components for river herring detection. Gene target, synthetic gene block, primer sequences, and probe used for species-specific detection of river herring (alewife and blueback herring) targeting the ND2 mitochondrial gene. gBlock refers to a synthetic double-stranded DNA fragment used as a positive control in qPCR assays. FAM = 6-carboxyfluorescein (fluorescent reporter dye).

Species	Gene Target	gBlock Gene Sequence	Forward Primer 5'-3'	Reverse Primer 5'-3'	Probe 5'-3' (Fluorophore)
River Herring	ND2	ACAATGTTGGCTCAACCAA AACTATCACCCCTCACCTCA GCCTGAACTAAAGCCCC ACCCTGACCGCACTGGCCT GCCTTATTCTTCTCTCCTTA GGAGGCTTACCCCACTAA CCGGATTCATGCCTAAATG ACTAATTCTCCAAGAAGTC ACCAGCCAGGGATTTCTC TCACTGCCACCGTGATAGC	TTGGCTCAACCA AACTATCACCC TCA	ACGGTGGCAGT GAGAGGAAATC CC	TGCCTTATTCTTCT CTCCTTAGGAGGC (FAM)

Table 3.3. Summary of model performance metrics across sites, temporal windows, and scaling approaches. Models were constructed to evaluate the relationship between observed eDNA concentrations and predicted fish counts across three hydrologically connected ponds (Benoits Pond, Great Herring Pond, and Little Herring Pond) using either a two-day or cumulative sampling window. Mechanistic models incorporated scaling of eDNA concentrations by surface area and distance, using either sensitivity-optimized or proportional surface area-derived exponents. Non-mechanistic models used raw downstream fish counts without spatial correction. Model type, R<sup>2</sup> values, P-values, and AIC scores are presented for each configuration.

Site	Two-Day or Cumulative	Scaling Method	Mechanistic?	Model Type	R Squared	P value	AIC
Benoits Pond	2 day	sensitivity	yes	multiple linear model	0.95	0.001	19.5
Great Herring Pond	2 day	sensitivity	yes	multiple linear model	0.73	0.1	35.3
Little Herring Pond	2 day	sensitivity	yes	multiple linear model	0.619	0.24	41.8
Benoits Pond	2 day	surface area	yes	multiple linear model	0.94	0.002	21.8
Great Herring Pond	2 day	surface area	yes	multiple linear model	0.69	0.14	36.6
Little Herring Pond	2 day	surface area	yes	multiple linear model	0.63	0.22	41.3
Benoits Pond	cumulative	sensitivity	yes	multiple linear model	0.99	<0.001	0.6
Great Herring Pond	cumulative	sensitivity	yes	multiple linear model	0.81	<0.001	24.4
Little Herring Pond	cumulative	sensitivity	yes	multiple linear model	0.98	<0.001	1.7
Benoits Pond	cumulative	surface area	yes	multiple linear model	0.98	<0.001	2.1
Great Herring Pond	cumulative	surface area	yes	multiple linear model	0.78	<0.001	25.4
Little Herring Pond	cumulative	surface area	yes	multiple linear model	0.98	<0.001	3.3
Benoits Pond	2 day	NA	no	multiple linear model	0.96	0.001	18.3
Great Herring Pond	2 day	NA	no	multiple linear model	0.66	0.17	37.6
Little Herring Pond	2 day	NA	no	multiple linear model	0.54	0.34	43.4
Combined Watershed	2 day	sensitivity	yes	multiple linear model	0.93	<0.001	111.1
Combined Watershed	2 day	surface area	yes	multiple linear model	0.81	0.01	116.4
Combined Watershed	cumulative	sensitivity	yes	multiple linear model	0.95	<0.001	63.2
Combined Watershed	cumulative	surface area	yes	multiple linear model	0.97	<0.001	70.3
Combined Watershed	2 day	NA	no	linear mixed model	0.76	0.01	162.5

Table 3.4. Sampling and amplification success across sites. Total number of sampling dates and number of successful amplifications (in at least one of two replicates) per site during the 2021 river herring monitoring period. Sites are ordered from most amplification success to least success. Successful amplification is defined as detectable target DNA in at least one of two qPCR replicates.

Site	Dates Sampled	Dates with Successful Amplification
Benoits Pond	18	18
Concrete Pool	18	16
Little Herring Pond	18	12
Great Herring Pond	18	11

Table 3.5. Correlation strength and statistical significance of eDNA-based relative abundance estimates across trial temporal sampling windows.  $R^2$  values and associated p-values for correlations between eDNA signal and fish counts across increasing temporal sampling windows (3, 6, and 9 days). Sites are listed from furthest upstream (Little Herring Pond) to furthest downstream (Concrete Pool).

Site	3-day replication		6-day replication		9-day replication	
	$R^2$	p-value	$R^2$	p-value	$R^2$	p-value
Little Herring Pond	0.94	0.16	0.54	0.09	0.50	0.03
Great Herring Pond	0.99	0.05	0.68	0.04	0.49	0.03
Benoits Pond	0.56	0.46	0.89	0.01	0.92	<0.001
Concrete Pool	0.35	0.60	0.64	0.06	0.81	<0.001

Table 3.6. Best-performing temporal bin models for predicting eDNA signal. Top predictive model results for each site based on temporal binning of fish count data. Sites are ordered from furthest upstream (Little Herring Pond) to furthest downstream (Concrete Pool). For full model results, see Supplementary Table 1A. Top predictors were selected based on the strongest correlation ( $R^2$ ) between fish count metrics and eDNA concentrations for each site.

Site	Top Predictor	$R^2$	p-value
Little Herring Pond	2-day binned fish count	0.36	0.03
Great Herring Pond	Single-day fish count	0.53	0.01
Benoits Pond	Previous-day fish count	0.94	<0.0001
Concrete Pool	2-day binned fish count	0.83	<0.0001

Table 3.7. Effect sizes and significance of predictors in a multiple linear regression model estimating log-transformed 2-day fish counts. Model results ( $R^2 = 0.75$ , adjusted  $R^2 = 0.73$ ,  $p < 0.001$ ) for predicting river herring abundance using environmental and spatial covariates. Log-transformed eDNA concentration (GCE) and distance from the fish counter were significant predictors of fish abundance. Non-significant environmental variables were left out of final models.

Variable	Effect Size	p-value
Distance from counter (m)	$4.3 \times 10^{-4}$	<0.001
Basin volume ( $m^3$ )	$1.07 \times 10^{-7}$	0.02
Water temperature ( $^{\circ}C$ )	$6.81 \times 10^{-2}$	0.18
Flow (Cubic Feet per Second, CFS)	0.21	0.55
Log mean eDNA GCE	0.77	<0.001

Table 3.8. AIC model selection and performance metrics for predicting 2-day binned river herring counts. Top five multiple linear regression models ranked by Akaike Information Criterion (AIC) for predicting watershed-scale fish counts. Models include combinations of environmental, spatial, and biological covariates. Lower AIC and  $\Delta$ AIC values indicate stronger model performance. AIC = Akaike Information Criterion;  $\Delta$ AIC = difference from best model (rank 1).

<b>Model Rank</b>	<b>Intercept</b>	<b>Basin Volume</b>	<b>Distance from Counter</b>	<b>2-Day Fish Count</b>	<b>Water Temp.</b>	<b>Flow (CFS)</b>	<b>Df</b>	<b>Log Likelihood</b>	<b>AIC</b>	<b><math>\Delta</math>AIC</b>
1	1.30	$-1.26 \times 10^{-7}$	-0.001	0.89	—	—	5	-95.92	203.1	0.0
2	0.89	$-1.25 \times 10^{-7}$	-0.001	0.86	0.04	—	6	-95.56	204.9	1.8
3	1.15	—	-0.001	0.88	—	—	4	-99.57	207.9	4.9
4	0.68	—	-0.001	0.84	0.05	—	5	-99.16	209.5	6.5
5	0.99	$-1.57 \times 10^{-7}$	—	0.84	—	—	4	-106.86	222.5	19.5

## Figures

Figure 3.1. Map of the Monument River watershed. Red dots signify sampling locations for the upstream reaches of the watershed. Northmost sampling location was the outflow of Little Herring Pond into Great Herring Pond. Downstream sampling location for Great Herring Pond occurred at the outflow of Great Herring Pond, which flowed into Benoit's Pond.



Figure 3.2. Map of downstream sampling locations within the Monument River watershed. Benois Pond location was at the top of the fish ladder which flowed downstream into the Concrete Pool sampling location. The Monument River then flowed under a highway, into Cape Code Canal.

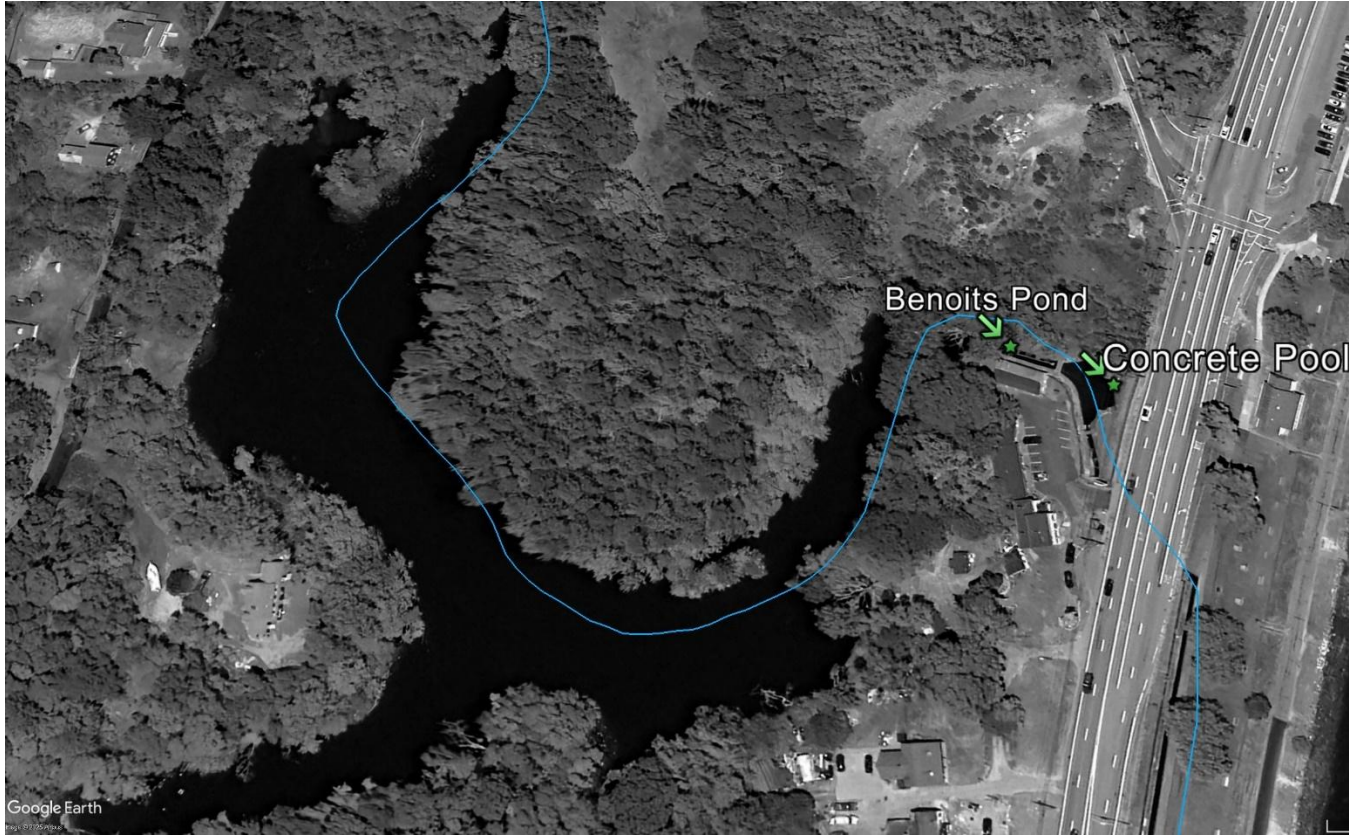


Figure 3.3. Proportional allocation of river herring across three connected ponds over time based on mechanistic model outputs. Panel A shows results from the sensitivity-optimized model using uniform  $\alpha$  values ( $\alpha = 0.01$ ) to scale log-transformed eDNA concentrations and generate two-day binned fish count estimates across sites. Panel B displays results from the inverse surface area-scaled model, where  $\alpha$  values were derived as  $1 - p_i$ , with  $p_i$  representing each site's proportional surface area. Both panels show the proportion of total predicted fish abundance by site across Julian days, with Benois Pond (blue), Great Herring Pond (green), and Little Herring Pond (orange).

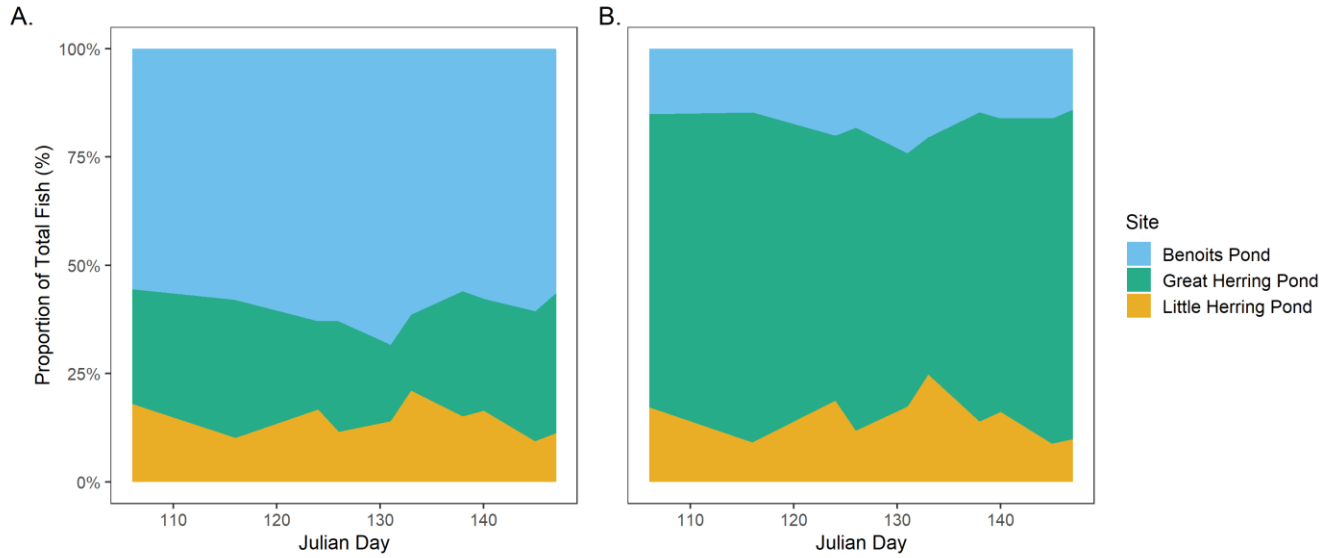


Figure 3.4. Comparison of predicted fish counts and eDNA concentrations across three connected ponds over time using two mechanistic scaling approaches. Panel A shows time series of two-day binned predicted fish counts (blue) and scaled eDNA concentrations (orange) generated using a sensitivity-optimized mechanistic model with uniform  $\alpha$  values ( $\alpha = 0.01$ ) across sites. Panel B presents the same metrics derived from the inverse surface area–scaled model, where  $\alpha$  values were calculated as  $1 - p_i$ , with  $p_i$  representing each pond’s proportional surface area.

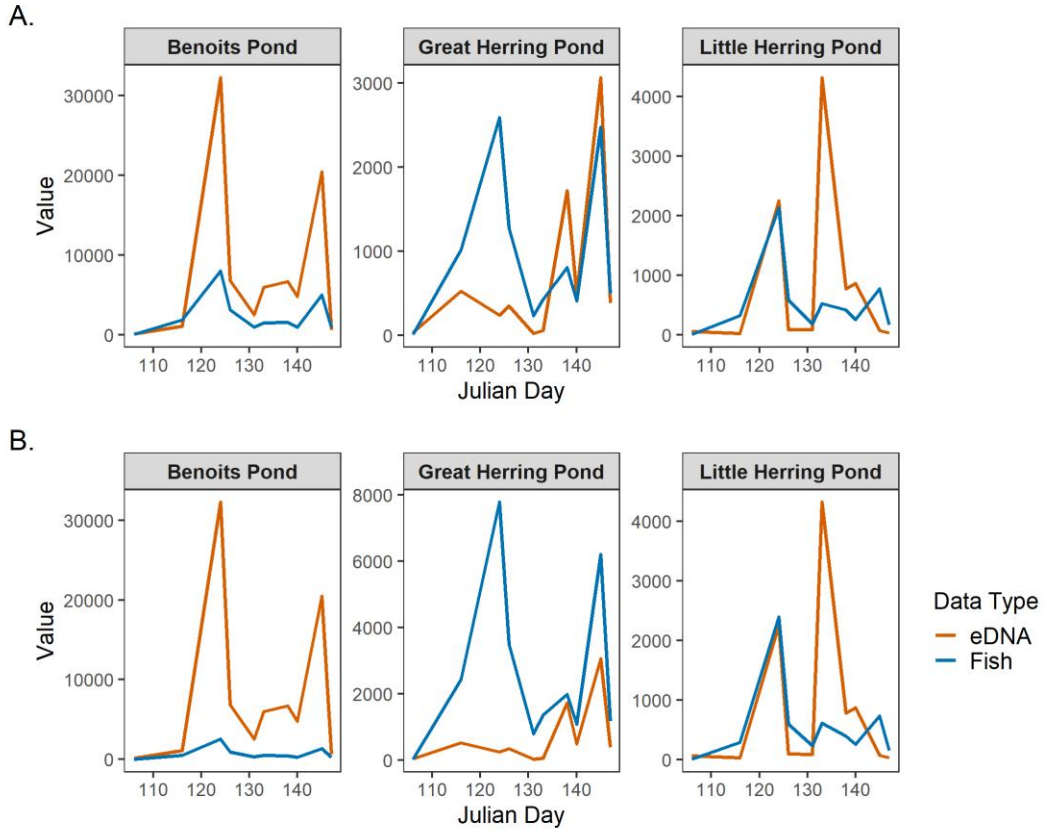


Figure 3.5. Temporal alignment of log-transformed eDNA gene copy equivalent (GCE) scores (green lines) and binned two-day fish count totals (orange lines) across four monitoring locations during the 2021 spring migration season. Panel A represents the Benois Pond sampling location. Panel B represents the Concrete Pool sampling location. Panel C represents the Great Herring Pond sampling location. Panel D represents the Little Herring Pond sampling location. All eDNA GCE scores are being compared to the single e-counter station located between the Benois Pond and Concrete Pool sampling locations.

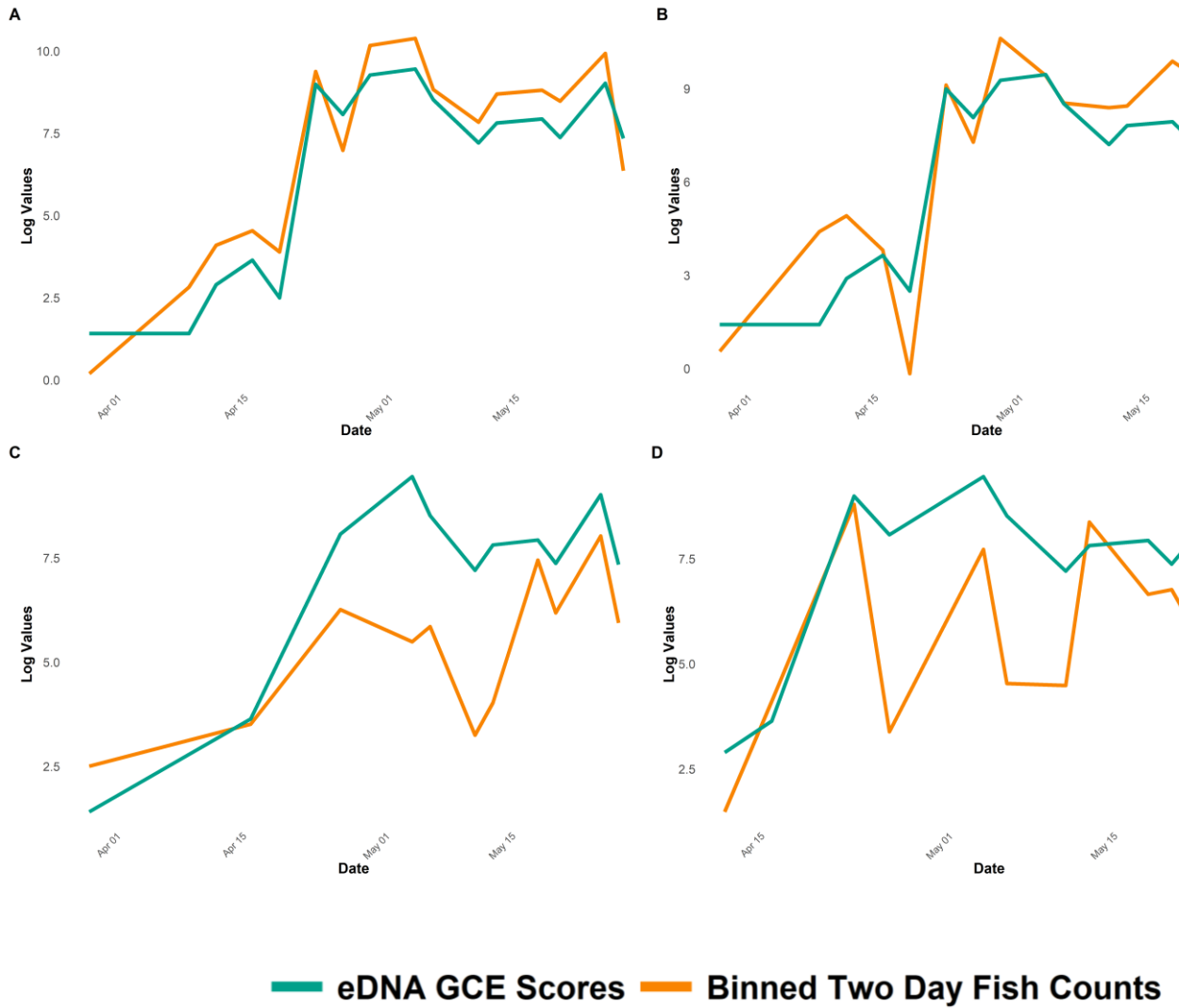
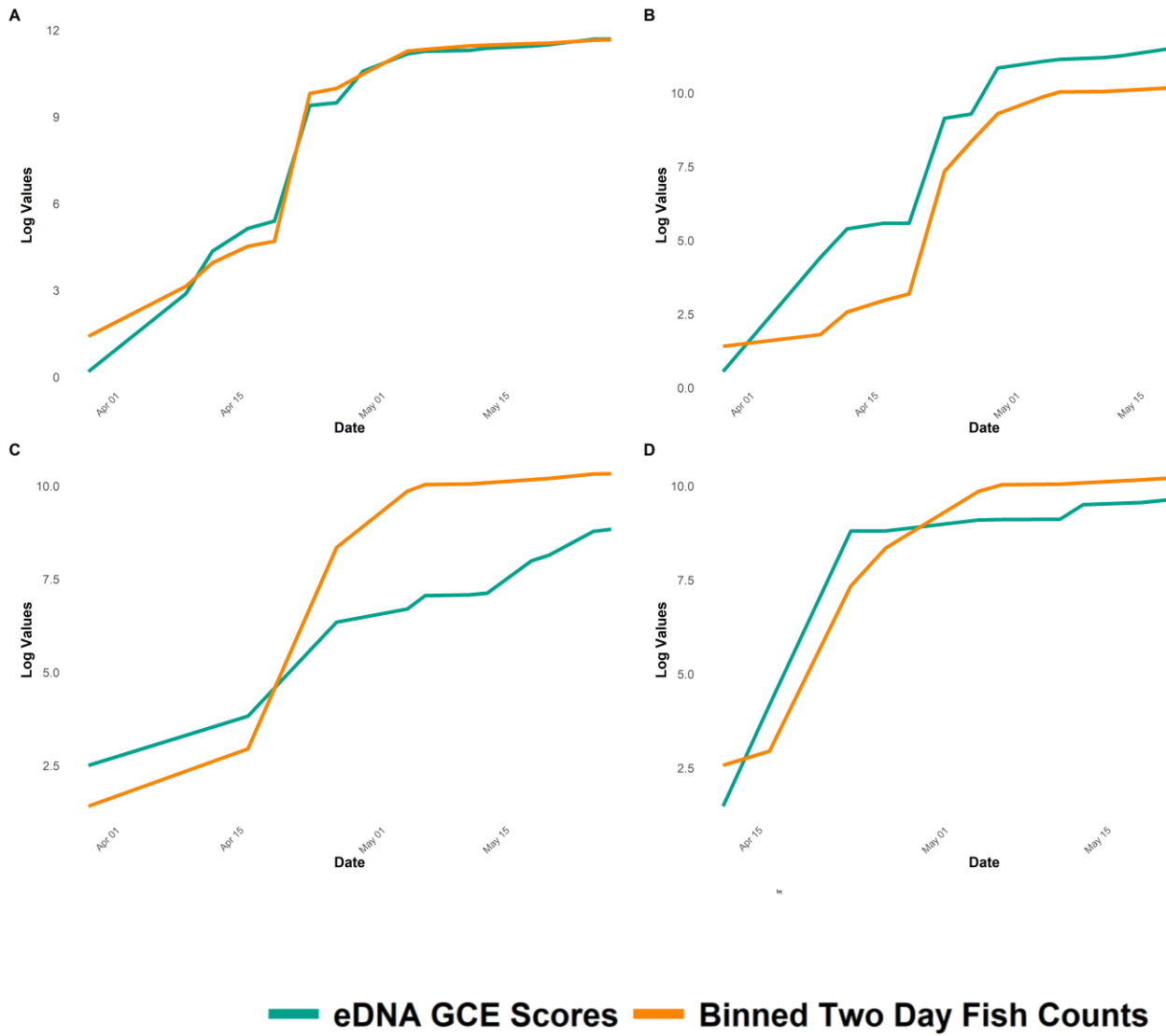


Figure 3.6. Cumulative log-transformed eDNA gene copy equivalent (GCE) scores (green lines) and cumulative fish counts (orange lines) across four sampling locations during the 2021 spring migration season. Panel A corresponds to the Benois Pond sampling location, Panel B to the Concrete Pool, Panel C to Great Herring Pond, and Panel D to Little Herring Pond. All cumulative eDNA scores are plotted against the fish counts recorded at a single stationary electronic fish counter located downstream between Benois Pond and the Concrete Pool.



## CHAPTER 4

### **Towards a Unified Approach for Fisheries Abundance Estimation: Integrating eDNA and Traditional Methods through Detection Probability**

#### **Introduction**

Since the late 19th century, when Petersen (1896) first applied mark-recapture techniques to estimate plaice (*Pleuronectes platessa*) populations in Danish waters, researchers have sought to understand the abundance of species of interest, and how to track populations through time and space (Hjort, 1914; Baranov, 1918; Schaefer, 1954; Ricker, 1954).

Despite significant methodological advances over the past century, a fundamental challenge persists in fisheries research that seeks to understand a given species abundance: different species, environments, and management questions require different techniques, each with their own metrics, associated costs, and methodological differences and biases. This diversity of approaches has complicated efforts to standardize abundance monitoring across systems and to discuss abundance-based monitoring efforts between related fields, particularly as new technologies emerge and are incorporated into existing management frameworks (Bonar et al., 2009; Pope & Willis, 1996).

Abundance carries different meanings across closely related fields (Table 4.1). In fisheries science, absolute abundance refers to the total number of individuals in a population, while relative abundance typically refers to an index proportional to true abundance, such as catch-per-unit-effort (CPUE) from surveys using a variety of methods, from seine and trawl nets to electrofishing and counting devices (Shelton et al., 2022). In contrast, ecologists may use relative abundance to describe a species'

proportion within a community rather than relative to its absolute number (Zinger et al., 2021). Similarly, in environmental DNA (eDNA) research (using genetic signals shed by targeted organisms derived from environmental samples to passively assess biodiversity metrics), abundance can refer to gene copy estimates (GCE), cycle quantification ( $C_q$ ) values, metabarcoding read counts, or experiments examining the relationship between eDNA concentrations and relative abundance estimates derived from more traditional techniques. These different methods for calculating abundance create further terminological confusion when attempting to calibrate eDNA with abundance from other sampling methods (Rourke et al., 2022; Yates et al., 2019). These inconsistent definitions have led to methodological challenges and misinterpretations when integrating techniques across disciplines (Thalinger et al., 2021).

The field of eDNA-based abundance estimation has been dominated by debates over whether molecular signals can reliably correlate with traditional abundance metrics (Lacoursière-Roussel et al., 2016; Yates et al., 2019). Recent studies have demonstrated that eDNA concentration can strongly predict fish abundance and biomass across diverse systems when properly calibrated (Pochardt et al., 2020; Rourke et al., 2022; Yamamoto et al., 2020). For instance, eDNA concentration strongly correlated with fish abundance in a study on river herring, where flow-corrected eDNA concentration exhibited a Spearman's correlation coefficient of 0.86 with daily sonar fish counts, highlighting the potential of high-frequency eDNA sampling as a reliable and cost-effective alternative for fish enumeration (Fowler et al., 2024). The conversation should now shift from questioning *whether* eDNA can serve as a proxy for abundance to determining *how* to effectively implement it within existing monitoring frameworks.

To address this implementation gap, it must be recognized that all relative abundance indices—both traditional and eDNA-based—are fundamentally shaped by their ability to capture and detect target species presence. Traditional fisheries methods such as electrofishing, fyke netting, visual counts, and electronic resistivity counters each have well-documented biases affecting their accuracy. Electrofishing efficiency varies substantially by species and habitat, often failing to detect up to 50% of individuals present (Nelson., 2019; Price & Peterson, 2010). Electronic resistivity counters consistently underestimate fish passage during peak migration periods by up to 30% (Rasmussen et al., 2022; Sheppard & Bernardski 2017), while video monitoring efficacy decreases with higher fish densities and in turbid conditions (Hiebert et al., 2000). Similarly, eDNA detection is influenced by environmental factors such as flow rate, temperature, and microbial activity (Barnes & Turner, 2016; Curtis et al., 2021), with high flows potentially reducing eDNA concentrations by a factor of 10 or more (Curtis et al., 2021). However, surprisingly little attention has focused on how the biases in traditional methods might affect eDNA calibration efforts. When a traditional metric provides a poor estimate of relative abundance but eDNA more accurately reflects reality, the inevitable misalignment between methods could be interpreted as a failure of eDNA methodologies rather than a limitation of the reference technique.

In this chapter, I shift the narrative from questioning eDNA's capabilities to providing a framework for its functional implementation into management by examining both eDNA and traditional abundance estimation techniques through the common lens of one of their shared sources of potential error, which could lead to bias: detection probability. Drawing from occupancy modeling frameworks (MacKenzie et al., 2006; Dorazio & Erickson,

2018), I argue that detection probability—the likelihood of detecting a species when it is present—offers a standardized metric for comparing and calibrating different monitoring approaches. Through case studies pairing eDNA and traditional relative abundance techniques (fyke net, video, electronic resistivity, backpack electrofishing), I demonstrate how understanding the influence that detection probability has across environmental DNA and traditional relative abundance estimating methodologies can guide method selection and integration. These four techniques provide a suite of traditional-method case-studies that are currently used to measure relative abundance in anadromous fish species, each with potential sources of error and factors that influence the detection probability.

Understanding the detection biases inherent in each method can facilitate more effective resource allocation and improve monitoring accuracy. For fisheries managers faced with declining budgets, limited personnel, and expanding monitoring needs, this unified framework provides a practical approach to method selection based on species-specific and system-specific considerations. By centering the conversation around relative and absolute abundance and quantifying the role of detection probability in method performance, I aim to move beyond methodological debates and towards more integrated, efficient, and accurate monitoring effort.

## **Methods**

### **Study Areas and Study Species**

This study was conducted across seven coastal river systems in southeastern Massachusetts, which support spawning populations of anadromous fishes of

conservation concern. These rivers span a range of hydrological conditions—from lentic pond outlets to intertidal estuarine channels—providing a gradient of environmental contexts for comparing traditional monitoring methods and eDNA-based approaches.

The Monument River (Bourne, MA) connects Great Herring Pond to the Cape Cod Canal and serves as a primary migratory corridor for river herring (*Alosa pseudoharengus* and *A. aestivalis*). In this system, river herring were monitored using an electronic fish counter positioned at the uppermost fish ladder. Alewife and blueback herring are anadromous species that migrate from marine habitats to freshwater lakes and ponds each spring to spawn (Bigelow & Schroeder, 1953). Although morphologically and ecologically similar, the two species differ in their preferred spawning temperatures and peak migration timing, contributing to their staggered occupancy of freshwater habitats (Bigelow & Schroeder, 1953).

Electrofishing surveys targeting American shad (*Alosa sapidissima*) were conducted in two inland tributaries of the North River: The Indian Head River and South River. These larger-bodied clupeids typically spawn in flowing freshwater reaches with gravel or cobble substrates and ascend rivers during the spring migration to spawn above head-of-tide obstructions (Bigelow & Schroeder, 1953).

Rainbow smelt (*Osmerus mordax*), a smaller-bodied, coldwater species, were surveyed using fyke nets in the Fore, Jones, and Weweantic rivers. Smelt migrate from marine environments to spawn in intertidal riffles during late winter and early spring and are known to prefer small freshwater tributaries with gravelly substrates for spawning (Bigelow & Schroeder, 1953). Unlike the other two species, which ascend fish ladders

and spawn in pond or riverine habitats, smelt spawning activity is more spatially restricted and often occurs close to the estuarine interface.

Together, these three species represent distinct life histories, migration timings, and spawning habitats, allowing for a broad evaluation of how eDNA performs relative to traditional survey methods across ecological contexts.

### **Traditional Monitoring Methods**

#### *Electronic Herring Counter: River Herring*

River herring abundance was monitored by the Massachusetts Division of Marine Fisheries (MA DMF) using a Smith-Root Model 1601 electronic fish counter installed at the second fish ladder in the Monument River, at the outflow of Benois Pond. The counter consisted of eight PVC tunnels outfitted with stainless steel electrodes and was operated from March 17 to June 8, 2021. Daily upstream passage was recorded throughout the migration season, with adjustments made to counter sensitivity and depth to maintain optimal passage velocities (1.0–1.5 m/s) in accordance with river herring swimming capabilities (Haro et al., 2004; Castro-Santos, 2005).

#### *Video Monitoring: River Herring*

MA DMF operated a video camera system at the Morey's Bridge Dam fish ladder in Taunton, MA to monitor river herring entering Lake Sabbatia. Video was recorded continuously from March 29 to May 28, 2021 and reviewed on weekdays by trained biological technicians. For each fish observed, species, direction of movement, date, and time were recorded. This site represents the first accessible lentic spawning habitat for river herring migrating through the Mill River.

### *Electrofishing: American Shad*

American shad were sampled via single pass backpack electrofishing surveys in the Indian Head River (5,560 m<sup>2</sup> transect) and South River (1,390 m<sup>2</sup> transect) from May 3 to June 22, 2021. Sampling occurred three times per week at or near low tide, adjusted based on predicted tidal delays relative to Damons Point (NOAA tide station) on the North River. Catch-per-unit-effort (CPUE) was calculated as the number of fish per minute of electrofishing effort, and both mean CPUE indices and raw fish counts were used to estimate relative abundance.

### *Fyke Nets: Rainbow Smelt*

A single fyke net was deployed at each site (Fore, Jones, and Weweantic Rivers) to capture rainbow smelt from February 22 to May 12, 2021, encompassing the full spawning period. Nets were checked Tuesday, Wednesday, and Thursday of every weekday within the monitoring period. Nets featured 1.2 × 1.2 m square wings and a 7-hoop codend, with 7 mm mesh throughout. Nets were deployed at mid-channel intertidal locations downstream of known spawning areas and were checked three times per week. All captured individuals were measured and enumerated to estimate run size and seasonal abundance.

## **Environmental DNA Methods**

### *eDNA Sample Collection*

Paired, duplicate water samples and a single "blank" sample were collected in conjunction with traditional techniques using 500 mL water bottles (Nestle Pure Life) twice weekly. Samples paired with electronic resistivity counters were collected between

March 29 to May 27, 2021 (n = 9 weeks) at four sites within the Monument River watershed including: Little Herring Pond, Great Herring Pond, Benoits Pond, and a location downstream of Benoits Pond. Samples paired with fyke nets were collected between March 23<sup>rd</sup> 2021 and May 6<sup>th</sup> 2021. Samples paired with the video count survey were collected between March 30<sup>th</sup>, 2021 and May 28<sup>th</sup>, 2021. Samples paired with electrofishing surveys were collected between May 3<sup>rd</sup> 2021, and June 22<sup>nd</sup>, 2021. All samples were collected following protocols established by Holmes et al. (2021). Single blank samples were collected every eDNA sampling date before eDNA sample collection occurred in the field. All samples and blanks were handled using gloves, and all equipment was sterilized between collections to prevent cross-contamination. Collected samples were immediately placed in sealed containers, put on ice, and stored under sterile conditions in a -20°C freezer.

#### *eDNA Processing and Analysis*

Frozen eDNA samples were thawed for 12-16 hours at room temperature before filtration following techniques outlined by Laramie et al. (2015). All filtration equipment was sterilized with a 50% bleach solution, rinsed with distilled water, and dried in a sterile hood. Samples (including a laboratory blank using distilled water) were filtered using an Air Cadet 115V vacuum pump (Cole Palmer, part number: 07532-40), aluminum filter manifold (Steritech Corporation, part number: 180310-01), and 47 mm, 0.8 µm cellulose nitrate filters (Whatman, part number: 7188-004). In cases of filter clogging, sequential filtration was used, and volumes were recorded to monitor filtration efficiency. After filtration, the cellulose nitrate filter for each sample was folded and stored in a microcentrifuge tube containing 95% ethanol at -80°C until DNA extraction.

DNA extraction was performed using Qiagen Investigator Lyse & Spin Basket Kit (Cat. No. 19598) and DNeasy Blood and Tissue kits (Cat. No. 69504) following a modified protocol established by Holmes et al. (2021). A ZYMO Research OneStep™-PCR Inhibitor Removal kit ((Zymo Research, Cat. No. D6035)) was used to reduce PCR inhibitors observed in pilot amplifications. Extraction success was assessed by measuring DNA yield and purity using a NanoDrop spectrophotometer (Thermo Fisher Scientific). Quantitative PCR (qPCR) was used to amplify gene sequences and estimate eDNA concentrations for river herring in all samples. The resulting 96-well elution plates contained approximately 50 µL of purified DNA sample per well, with four wells left blank for controls. Positive control samples were prepared from custom gBlock Gene Fragments (Integrated DNA Technologies) of target gene sequences specific to each species. These fragments (starting at 250 ng concentration) were diluted to  $1 \times 10^6$  copies per mL using 0.5 mg/mL Poly (A) buffer in Tris EDTA (TE), with 15 µL added to two wells on each elution plate. Molecular-grade water (30 µL) was added to two wells as negative controls.

A qPCR assay was developed for river herring that targeted both alewife and blueback herring. Each qPCR reaction well contained 3.8 µL of purified DNA samples. Mastermix was prepared using TaqMan™ Environmental Master Mix 2.0 (Applied Biosystems; 1X final concentration), custom forward primer, custom reverse primer, and TaqMan™ MGB Probe (Applied Biosystems) at concentrations of 0.5 µM, 0.5 µM, and 0.1 µM, respectively. A Hamilton MagEx STAR liquid-handling robot aliquoted purified DNA samples and prepared mastermix into 384-well qPCR plates with a final reaction volume

of 10  $\mu$ L per well. Each 96-well elution plate was processed twice to allow for duplicate qPCR results for each sample.

The 384-well qPCR plates were amplified using BioRad CFX384 Touch Real-Time PCR Detection Systems. Thermal cycling parameters included an initial enzyme activation step at 95°C for 10 minutes, followed by 40 cycles of 95°C for 15 seconds (denaturation) and 60°C for 1 minute (annealing).

To convert cycle quantification ( $C_q$ ) values to gene copy numbers, standard curves were created using 10-fold serial dilutions of each species' gBlock Fragment, starting at 10,000 copies per mL. Each sample's  $C_q$  value was compared to the corresponding standard curve equation to estimate gene copy equivalents (GCE) in the original purified DNA sample.

## **Statistical Analyses**

### *Data Preparation*

Raw fish count was selected as the relative abundance metric across all analyses of traditional monitoring techniques, as previous studies have shown that raw counts perform similarly to other fish relative abundance metrics (e.g., density, biomass, CPUE) in eDNA relative abundance calibration efforts (Lacoursière-Roussel et al., 2016; Baldigo et al., 2017). For each site and collection date, the mean GCE was calculated from the raw GCE score of each laboratory replicate ( $N=2$ ) for each of the individual field sample replicates ( $N=2$ ). Each field replicate was treated as an independent sampling event across all sites and sampling dates. Both GCE means and fish count values were log-transformed with a corrective factor of +1.1 added to account for zeros in the dataset.

This corrective factor was chosen based on preliminary data distributions to ensure log transformation compatibility.

### *Relative Abundance Estimation Using Bayesian Hierarchical Models*

To evaluate the predictive relationship between eDNA abundance and traditional fish count data, a Bayesian hierarchical models implemented in JAGS via R2jags in R using Markov Chain Monte Carlo (MCMC) sampling was employed (Plummer, 2003; Su & Yajima, 2021). These models accounted for imperfect detection across eDNA and traditional techniques, spatial and temporal structure, species-specific responses, and methodological differences across fisheries monitoring techniques.

Model selection was guided by the distributional characteristics of traditional abundance data: Gamma Regression Models were used for electronic fish counter data, which were strictly positive and right-skewed.; Gaussian Regression Models were applied to video-based fish count data, which were approximately normally distributed.; Hurdle Gamma Models were applied to fyke net data, electrofishing data, and the combined method dataset (fyke net, electrofishing, video, and electronic counter), which exhibited zero inflation and right-skewed distributions

Each model included log-transformed eDNA concentrations (GCE) as a predictor of traditional fish abundance, while incorporating random effects to control for site-specific variability. For each method  $m$  at site  $i$  and time  $j$ , the general model structure was:

For Gamma models:  $y_{i,j,m} \sim \text{Gamma}(\text{shape}, \text{rate} = \text{shape}/\mu_{i,j,m})$

For Gaussian models:  $y_{i,j,m} \sim \text{Normal}(\mu_{i,j,m}, \sigma^2)$

For Hurdle Gamma models:  $z_{i,j,m} \sim \text{Bernoulli}(\pi_{i,j,m})$

$z_{i,j,m} \sim \text{Bernoulli}(\pi_{i,j,m}) y_{i,j,m} | z_{i,j,m} = 1 \sim \text{Gamma}(\text{shape}, \text{rate} = \text{shape}/\mu_{i,j,m})$

Where:

$$\text{logit}(\pi_{i,j,m}) = \alpha_0 + \alpha_1 \cdot \log(\text{eDNA}_{i,j}) + \alpha_{\text{site}[i]}$$

$$\log(\mu_{i,j,m}) = \beta_0 + \beta_1 \cdot \log(\text{eDNA}_{i,j}) + \beta_{\text{site}[i]}$$

To regularize estimates and prevent overfitting, weakly informative priors were assigned:

Fixed effects:  $\alpha_0, \alpha_1, \beta_0, \beta_1 \sim \text{Normal}(0, 10)$

Random effect standard deviations:

$\alpha_0, \alpha_1, \beta_0, \beta_1 \sim \text{Normal}(0, 10) \sigma_{\text{site}} \sim \text{Half-Cauchy}(0, 2.5)$

Gamma shape parameters:  $\text{shape} \sim \text{Gamma}(0.01, 0.01)$

MCMC models were run with three chains of 5,000 iterations (1,000 burn-in, thinning = 10). Model convergence was confirmed using Gelman-Rubin diagnostics ( $\hat{R} < 1.1$ ), effective sample size (>1000), and trace plots.

### *Detection Probability Estimation Using Bayesian Occupancy Models*

To estimate detection probabilities for eDNA and traditional methods, a Bayesian hierarchical occupancy model that explicitly accounted for imperfect detection across methods, sites, and sampling replicates was implemented. This approach allowed to compare methods using a uniform metric and infer true species presence while incorporating detection uncertainty.

For each site  $i$ , sampling week  $j$ , and replicate  $k$ , the model was structured as follows:

1. Latent Occupancy State  $z_{i,j} \sim \text{Bernoulli}(\psi_i)$
2. Detection Probability for eDNA and Traditional Methods:

eDNA:

$$z_{i,j} \sim \text{Bernoulli}(\psi_i) y_{i,j,k,\text{eDNA}} \sim \text{Bernoulli}(p_{i,j,\text{eDNA}} \cdot z_{i,j})$$

$$\text{Traditional: } y_{i,j,k,\text{trad}} \sim \text{Bernoulli}(p_{i,j,\text{trad}} \cdot z_{i,j})$$

where:  $\text{logit}(p_{i,j,\text{eDNA}}) = \alpha_{\text{eDNA}} + \beta \cdot y_{i,j,k,\text{trad}} + \varepsilon_i$

$$\text{logit}(p_{i,j,\text{trad}}) = \alpha_{\text{trad}} + \gamma \cdot y_{i,j,k,\text{eDNA}} + \varepsilon_i$$

The parameter  $\beta$  represents the effect of traditional method detection on eDNA detection probability, while  $\gamma$  represents the effect of eDNA detection on traditional method detection probability. The site-specific random effect  $\varepsilon_i$  accounts for location-specific variation in detection rates. Priors were weakly informative to allow flexibility while constraining estimates to biologically reasonable values: Occupancy probability:  $\psi_i \sim \text{Beta}(1, 1)$ . Detection probability intercepts:  $\alpha_{(\text{eDNA})}, \alpha_{(\text{trad})} \sim \text{Normal}(0, 1.5)$ . Detection probability effects:  $\beta, \gamma \sim \text{Normal}(0, 1.5)$ . Site random effects:  $\varepsilon_i \sim \text{Normal}(0, \sigma_{(\text{site})})$ . Site standard deviation:  $\sigma_{(\text{site})} \sim \text{Half-Cauchy}(0, 2.5)$ . MCMC models were run with three chains of 5,000 iterations (1,000 burn-in, thinning = 10). Convergence diagnostics ( $\hat{R} < 1.1$ , effective sample size >1000) were verified.

### *Comparison of Detection Probabilities*

Posterior samples of detection probabilities ( $p_{(\text{eDNA})}$  and  $p_{(\text{trad})}$ ) were extracted from the MCMC simulations and summarized for each site and method as posterior means with 95% credible intervals (CIs). These credible intervals represent the range of plausible

values for each detection probability, incorporating uncertainty from the posterior distribution.

To compare detection probabilities between eDNA and traditional methods, we computed the posterior probability that eDNA detection was higher at each site:

$$P(p_{\text{eDNA},i} > p_{\text{trad},i}) = \frac{\sum I(p_{\text{eDNA},i,s} > p_{\text{trad},i,s})}{S}$$

where  $I()$  is an indicator function and  $S$  is the number of posterior samples. A probability near 1.0 suggests higher detection efficiency for eDNA, whereas a probability near 0.0 indicates superior detection by traditional methods.

The width of credible intervals between eDNA and traditional methods was also compared to assess the precision of detection probability estimates. For each site, the width of the 95% credible interval was calculated as the difference between the upper and lower bounds. Narrower credible intervals indicate higher precision in the detection probability estimates. A paired t-test was performed to compare the mean credible interval width differences between techniques. A bar plot with eDNA and traditional credible interval widths for combined sites was also generated.

In addition to Bayesian comparisons, a frequentist analysis to compare the relationship between eDNA and traditional detections was conducted. A chi-squared test of independence was performed to assess whether eDNA and traditional detections were related. A logistic regression model was used to evaluate the influence of traditional method detection on eDNA detection probability.

Finally, to directly compare detection probabilities between methods, the site-level proportions of detection as well as mean detection probabilities for both eDNA and traditional methods was extracted and plotted by site and traditional monitoring type. A paired t-test was performed to compare the mean difference in detection probabilities between method types. A box plot comparing detection probabilities across methods (combined) was created to show detection probabilities and variability between eDNA and traditional methods. After confirming the normality of differences using a Shapiro-Wilk test, we tested whether eDNA detection probabilities were significantly different from traditional method detection probabilities across all sites.

## **Results**

### **Relative Abundance Calibration Using Bayesian Hierarchical Models**

The combined traditional methods dataset (fyke net, electrofishing, video, and electronic counter) yielded a Hurdle Gamma model with an intercept of -0.27 (95% CI: 0.101, 0.2) and an effect on log-transformed eDNA GCE scores of 0.15. This model demonstrated strong fit (Bayesian  $R^2 = 0.71$ , Bayesian p-value = 1) with successful convergence (Rhat = 1). Posterior estimates of model parameters are summarized in Table 4.2.

For Lake Sabbatia video monitoring data, the Gaussian regression model estimated an intercept of 4.5 (95% CI: 0.002, 0.33) with an effect on log-transformed eDNA GCE scores of 0.17. This model showed a strong fit (Bayesian  $R^2 = 0.953$ , Bayesian p-value = 0.97) with full convergence (Rhat = 1).

The Monument River electric resistivity fish count data, analyzed with a Gamma regression model, produced an intercept of 0.86 (95% CI: 0.067, 0.151) and an effect on

log-transformed eDNA GCE scores of 0.11. The model fit was robust (Bayesian  $R^2 = 0.76$ , Bayesian p-value = 1) with confirmed convergence (Rhat = 1).

For electrofishing data, the Hurdle Gamma model estimated an intercept of -1.65 (95% CI: 0.135, 0.267) and an effect of 0.20 on log-transformed eDNA GCE scores, with an included and significant site/week spline term of -5.95. This model demonstrated strong fit (Bayesian  $R^2 = 0.77$ , Bayesian p-value = 1) with full convergence (Rhat = 1).

The fyke net data yielded a Hurdle Gamma model with a non-significant intercept of 1.06 (95% CI: -0.04, 0.01) and a minimal effect of -0.01 on log-transformed eDNA GCE scores. While the model converged successfully (Rhat = 1), it showed a lower Bayesian  $R^2$  (0.73) and non-significant Bayesian p-value (0.15).

Overall model convergence was confirmed by Gelman-Rubin diagnostic values (Rhat) of 1.0 for most parameters, and had a range between 1.0 and 1.2. Effective sample sizes (n.eff) were generally high (>1,000). The occupancy model's Deviance Information Criterion (DIC) was 3650.7 with 23.6 estimated effective parameters, indicating reasonable fit.

### **Detection Probability Estimation Using Bayesian Occupancy Models**

The Bayesian hierarchical occupancy model estimated site- and method-specific detection probabilities across sampling locations and gear types. The model revealed meaningful site-level variation in detection probabilities, with the standard deviation of the site-level random intercept estimated at 0.85 (95% CI: 0.27, 1.86). When traditional methods failed to detect a species, the baseline probability of eDNA detection was estimated at -0.37 (95% CI: -1.3, 0.53).

Traditional detections strongly predicted eDNA detection success, with an estimated effect size of 1.97 (95% CI: 1.19, 2.79). This corresponds to an odds ratio of approximately 7.2, meaning eDNA detection was 7.2 times more likely to detect a species when traditional methods also detected a species.

### **Site-Specific Comparisons of Detection Probabilities**

Comparison of detection probabilities across seven sites revealed generally comparable efficiencies between eDNA and traditional methods (Table 4.3). Most sites showed overlapping 95% credible intervals between methods, suggesting no statistically significant differences. However, eDNA detection probabilities consistently showed narrower credible intervals compared to traditional methods, indicating greater precision in eDNA-based estimates. This difference was most pronounced at sites using fyke nets (Jones River, Fore River, and Weweantic), where traditional methods exhibited substantially higher uncertainty. While traditional methods yield more variable detection estimates across sites, eDNA provides more consistent detection probability across diverse environmental contexts.

At Lake Sabbatia, eDNA demonstrated a mean detection probability of 0.76 (95% CI: 0.46, 0.93), comparable to traditional video monitoring's 0.78 (95% CI: 0.08, 1.00). For fyke net comparisons at Fore River and Jones River, eDNA showed mean detection probabilities of 0.70 (95% CI: 0.41, 0.90) and 0.72 (95% CI: 0.43, 0.91), respectively, similar to traditional method values of 0.64 (95% CI: 0.06, 0.99) and 0.70 (95% CI: 0.07, 0.99).

At the Weweantic River, eDNA detection probability (0.70, 95% CI: 0.36, 0.92) was higher than traditional fyke net detections (0.58, 95% CI: 0.04, 1.00), though credible intervals overlapped. Bayesian posterior probability analysis did not yield strong evidence that eDNA was consistently more effective than traditional methods at any site. However, the comparison of credible interval widths suggests that eDNA detection probabilities exhibited lower uncertainty across sites, indicating greater stability in estimates compared to traditional methods.

### **Frequentist Validation of Detection Relationships**

A frequentist logistic regression model supported our Bayesian findings, with an estimated effect size for traditional detection of 1.99 (SE = 0.83,  $p = 0.02$ ). This corresponds to an odds ratio of 7.3, indicating eDNA detection was approximately 7.3 times more likely to also detect a species when traditional methods detected a species (Table 4.6). A chi-squared test further confirmed this significant relationship ( $\chi^2 = 4.73$ ,  $p = 0.03$ ).

The results of the paired t-test comparing detection probabilities between eDNA and traditional methods indicated a statistically significant difference between eDNA and traditional methods ( $t = 3.305$ ,  $df = 6$ ,  $p = 0.02$ ), with eDNA detection probabilities averaging 5.32 percentage points higher than traditional methods. The 95% confidence interval (CI: 1.38% – 9.25%) provided additional evidence that eDNA consistently outperformed traditional methods in terms of detection probability (Figure 4.8).

When traditional methods failed to detect a species, eDNA maintained detection capabilities. The mean posterior probability of eDNA detection in these cases was 0.39

(95% CI: 0.29, 0.50), closely matching the empirical probability of 0.37 (95% CI: 0.26, 0.49). This provides evidence for the potential complementary value of eDNA in monitoring programs.

The hierarchical Bayesian model incorporating site-level variability confirmed a strong relationship between traditional and eDNA detection (effect size 1.97, 95% CI: 1.19, 2.79), with all posterior samples supporting a positive effect (posterior probability of  $\beta > 0 = 1.00$ ).

## **Discussion**

### **Calibration and Detection**

The outcome of the Bayesian hierarchical model calibrating eDNA relative abundance to traditional relative abundance monitoring methods are consistent with the strong correlations found between eDNA and traditional relative abundance metrics reported in previous studies (Pochardt et al., 2020; Rourke et al., 2022; Yates et al., 2019), with the notable exception of fyke net surveys. Further, eDNA effectively detects species presence even when traditional methods fail, with an estimated 39% detection probability in such cases. Both Bayesian and frequentist analyses confirm a strong positive relationship between traditional and eDNA detections, indicating that while traditional methods remain valuable, eDNA offers an important complementary detection tool.

A critical insight from this study is that eDNA calibration is inherently constrained by the detection biases of the reference method. The inconsistency of fyke net results aligns with documented lower detection probabilities (Stevens et al., 2024) and selectivity biases (Turner et al., 2021), which may have been further exacerbated by the low-abundance

conditions of the systems included in the present study. The proximity of eDNA sampling locations (50 meters downstream) could have also influenced detection, as inadequate water mixing near source populations has been shown to impact eDNA dispersion (Porto-Hannes et al., 2023; Sansom et al., 2024). The Bayesian Hurdle Gamma model examining eDNA GCE scores in relation to electrofishing-based fish counts revealed a significant negative effect of site, suggesting location-specific detection constraints. This may reflect differences in sampling efficiency between the two rivers, as the Indian Head River is larger than the South River, yet both were sampled using a single-pass electrofishing approach—potentially limiting detectability in the larger system. Given that single-pass electrofishing may detect less than 50% of individuals present (Price & Peterson, 2010) and fyke nets exhibit variable capture efficiencies (Dunlop et al., 2010), these methodological limitations introduce inherent challenges when calibrating eDNA against imperfect reference datasets.

Detection probabilities derived from Bayesian hierarchical occupancy models that explicitly accounted for imperfect detection across methods, sites, and sampling replicates were not significantly different between eDNA and traditional methods, although eDNA based methods consistently had the same as or greater detection probabilities when compared to traditional methods in this study. However, frequentist analyses (paired t-test) of the same posterior distribution-derived detection probabilities found significant differences between methods, showing eDNA estimates had significantly narrower confidence intervals, indicating greater precision. Bayesian models yielded more conservative conclusions than frequentist, as they incorporated the full posterior distributions and site-level variability into models. At the same time, Bayesian

approaches provided valuable flexibility in addressing uncertainties by remaining robust to smaller datasets and effectively accounting for variability across monitoring techniques (Nelson et al., 2019; Dorazio & Erickson, 2018; Shelton et al., 2022). Additionally, the non-independence between eDNA and traditional methods, coupled with eDNA's ability to detect species 39% of the time when traditional methods failed, highlights its value in reducing false negatives (Spear et al., 2021). Rather than continuing to evaluate eDNA methods solely on its ability to reflect ecological and biological significance—an area where substantial evidence already supports its efficacy—attention can shift toward optimizing its use (Deiner et al., 2016; Diaz-Ferguson & Moyer., 2014; Lacoursière-Roussel et al., 2016; Yates et al., 2019; Pochardt et al., 2020; Evans et al., 2017; Rourke et al., 2022; Shelton et al., 2022; Harrison et al., 2023; Liu et al., 2024). By understanding the shared sources of inherent bias between eDNA and traditional sampling techniques, its application can be refined to maximize the strengths of both methods, minimize their respective limitations, and improve the accuracy of presence and relative abundance-based observations in ecosystem monitoring.

### **Monitoring and Management**

For the systems evaluated in this study, eDNA provides a noninvasive tool for indexing species relative abundance and detecting shifts in community composition, but its ecological interpretation is inherently dependent on sampling strategy, system-specific knowledge, and monitoring objectives. eDNA can track species migration patterns at the same (for medium and high counts of diadromous fishes) or higher resolution (at low relative abundance sites) than traditional relative abundance techniques. Unlike traditional methods, which capture a discrete snapshot of local relative abundance at the

time of sampling, eDNA integrates signals from multiple biological processes, offering possible insight into immigration, emigration, and life history transitions when targeted with standardized, objective-based sampling strategies. For instance, temporal eDNA sampling has been successfully used to infer spawning events, with seasonal peaks in genetic material corresponding to known reproductive periods in freshwater mussels (*Buldotskia iwakawai*) (Wu et al., 2024). Similarly, eDNA has been leveraged to track migration phenology, distinguishing between peak upstream movements of closely related diadromous species such as river herring and American shad (Fowler et al., 2024). However, the success of these approaches depends on a well-designed spatiotemporal sampling framework, where repeated, high-resolution sampling is aligned with species phenology and environmental conditions (Fowler et al., 2024; Pochardt et al. 2019). By refining eDNA applications toward operationalized ecological monitoring, researchers and managers can maximize its utility for tracking species responses to environmental change, identifying critical migration windows, and assessing population dynamics with greater precision than some traditional monitoring methods.

Several potential use-case scenarios emerge from these findings. Systems with lower relative abundances of target species, similar to fyke net and single-pass electrofishing surveys, may benefit from pairing their methods with eDNA given the higher detection probabilities in these conditions demonstrated in this study. This integration could improve monitoring efficiency, particularly for rare and endangered species, invasive and non-indigenous species, species experiencing contracting or expanding ranges, or during early and late migration phases (Stevens et al., 2024). The increased sensitivity of eDNA methods could help build regionalized or local Time of Year (ToY) restrictions used by

town, state, and federal agencies that oversee restoration action and infrastructure improvement permitting. The native range of rainbow smelt (*Osmerus mordax*) is known to be contracting, likely due to anthropogenic stressors such as fishing pressure and climate change (Kovak et al., 2013). The Weweantic River in southeastern Massachusetts is at the southernmost extent of the modern rainbow smelt range; implementing seasonal and annual eDNA monitoring at this location could provide critical information about local extinctions of this fish south of Cape Cod, given how effective eDNA was found to be in this study.

The narrower credible interval widths of eDNA detection probabilities could inform management decision-making, especially when data is limited. Additionally, watershed, regional, and national-scale monitoring networks could strategically incorporate eDNA sampling to complement traditional surveys at fish passage structures. This combined approach might bolster efforts by organizations like the Atlantic States Marine Fisheries Commission (ASMFC), and would be able to shed light on coast-wide movement and migration for highly migratory diadromous, coastal, and pelagic species (Cairns et al., 2022; Carraro et al., 2021). However, it is essential that the well-documented limitations of eDNA methods are acknowledged in any monitoring framework (Cristescu & Hebert, 2018). Traditional capture-based techniques, such as electrofishing, netting, and trap-based surveys, remain necessary to collect biological data that eDNA cannot provide. These include key demographic and life-history traits such as age and growth (through otolith, scale, or spine analysis), size and body condition, sex, fecundity, and physiological state (Bonar et al., 2009). Such information is critical for stock assessments, reproductive studies, and understanding population structure and viability—

data that eDNA, while powerful for detection and distribution, cannot yet capture. Integrating eDNA with traditional methods can therefore provide a more holistic understanding of population health and ecological dynamics, combining broad-scale surveillance with fine-scale biological resolution.

### **Future Research**

Future research opportunities exist to incorporate occupancy modeling across multiple watershed locations, leveraging eDNA qPCR, ddPCR, and metabarcoding to improve species distribution mapping (Carraro et al., 2021). A critical next step is to compare detection probabilities among qPCR, ddPCR, metabarcoding, and other next-generation sequencing (NGS) approaches, potentially through a meta-analysis of existing paired studies. Environmental variables like streamflow could also be integrated into abundance models, as variable flow conditions in streams can lead to tenfold differences via dilution or concentration of eDNA signals (Curtis et al., 2021), while fish activity can increase eDNA shedding thirtyfold (Thalinger et al., 2021). Given that eDNA shedding rates scale with body size and metabolic activity (Maruyama et al., 2014; Thalinger et al., 2021), future applications may extend to estimating ontogenetic shifts, such as juvenile recruitment timing, by analyzing size-specific shedding dynamics in species like alewife and blueback herring in both lab and field environments.

Density of DNA per unit volume of water directly correlates with the density of target species within a given system (Yates et al., 2021). Having interannual environmental data for a specific system will help us better understand and differentiate biological drivers from specific environmental drivers of eDNA signal detection, persistence, and behavior, giving us a holistic, ecosystem level understanding of a system (Deiner et al., 2015).

Future efforts could pair eDNA-based relative abundance monitoring with already established long-term surveys like volunteer river herring counts, which are common throughout coastal Atlantic states in the U.S. and prone to detection imprecision, as well as extend monitoring to sites where traditional approaches are not implemented (Nelson, 2006; TR-25 protocol guidelines). This approach could provide more accessible and reliable insights into seasonal run dynamics while also offering additional biological and ecological information, depending on how eDNA is incorporated into the monitoring framework (Nelson, 2006). Finally, advanced statistical approaches such as artificial intelligence hold promise for eDNA monitoring, with machine learning algorithms improving eDNA-based abundance estimates by 25–40% over traditional statistical methods (Li et al., 2023).

This study demonstrates that detection probability provides a unifying framework for comparing different relative abundance monitoring methods, calculated from either detection/non-detection data using Bayesian and frequentist techniques. This approach offers a simple means of standardization across diverse methodologies, and a partial solution (lab standardization aside) to common challenges facing eDNA implementation in fisheries management (Cristescue 2018; Hajibabaei 2022; Harrison et al., 2019; MacKenzie et al. 2006; Mathieu et al 2020; Ruppert et al 2019; Yates et al., 2019).

This study provides evidence that eDNA can be applied in fisheries management contexts to determine abundance in system-specific surveys. Yet, eDNA is not a universal solution but rather a context-dependent tool that can enhance existing monitoring regimes or establish entirely new, cost-effective ones. By focusing on detection probability as a unifying metric, researchers and managers can make informed decisions about when,

where, and how to integrate eDNA into their monitoring toolkits. As eDNA sampling protocols continue to evolve (Andres et al., 2021; McCauley et al., 2024) and analytical approaches become more sophisticated (Nelson et al., 2022; Guri et al., 2024; Carraro et al., 2024), the integration of eDNA with traditional monitoring can be used to improve aquatic monitoring and management.

## Tables

Table 4.1. Abundance metrics used in eDNA monitoring and fisheries management. This table summarizes 16 abundance metric types commonly used in eDNA-based ecological studies and fisheries science. Each metric is defined and contextualized with examples of its application in eDNA studies and its relevance to fisheries-based decision-making. Metrics range from absolute and relative abundance to model-based, functional, and method-specific abundance estimates. Several metrics, such as gene copy number or normalized read counts, are specific to qPCR or metabarcoding workflows.

<b>Abundance Type</b>	<b>Definition</b>	<b>Application in eDNA</b>	<b>Fisheries-Based Applications</b>
<b>Absolute Abundance (AA)</b>	Total number of individuals in a study area	Rare in eDNA; requires calibration against direct fish counts using species-specific shedding rates. Used with qPCR and ddPCR.	Used in stock assessments and population models to estimate total fish numbers in a region.
<b>Relative Abundance (RA)</b>	Proportion of species in a system, an index of AA	Common in eDNA qPCR and metabarcoding where sequence read counts provide proportional abundance estimates.	Helps in fishery-independent surveys and long-term monitoring of fish populations.
<b>Biomass-Based Abundance</b>	Mass of species per unit area	eDNA concentration (copies/L) is used as a biomass proxy, qPCR based approaches often calibrated against experimental mesocosm studies.	Supports fish stock management and biomass-based fisheries quotas.
<b>Detection-Based Abundance</b>	Based on presence-absence data & detection probability	Used in occupancy modeling to infer species occurrence rather than true abundance.	Applied in habitat suitability models and species distribution modeling.
<b>Catchability-Adjusted Abundance</b>	RA based abundance corrected for survey method bias	Used in Bayesian eDNA models that integrate traditional surveys with eDNA estimates.	Helps refine catch per unit effort (CPUE) and improve survey calibration.
<b>Community-Level Abundance</b>	RA based abundance assessed at an ecosystem level	Used in metabarcoding studies to compare species read abundance across sites.	Supports ecosystem-based fisheries management (EBFM) and biodiversity assessments.
<b>Functional Abundance</b>	Abundance based on ecological roles	Applied in functional diversity studies to assess ecosystem functions rather than individual counts.	Helps understand trophic dynamics and functional redundancy in fish communities.
<b>Spatiotemporal Abundance</b>	AA or RA based abundance changes across time and space	Requires hydrodynamic modeling of eDNA transport and seasonal sampling.	Supports migration studies, seasonal fishery openings, and climate change impact assessments.
<b>Model-Based Abundance</b>	AA or RA based statistical abundance estimation	Used in Generalized Additive Models (GAMs), Bayesian hierarchical models, and zero-inflated models.	Supports fisheries forecasting and multi-species abundance modeling.
<b>Read Count Abundance</b>	Number of sequencing reads assigned to a species in a metabarcoding dataset	Used in eDNA metabarcoding as a proxy for species relative abundance, but subject to PCR biases and sequencing depth.	Helps in multi-species fisheries assessments and early detection of invasive species.

<b>Abundance Type</b>	<b>Definition</b>	<b>Application in eDNA</b>	<b>Fisheries-Based Applications</b>
<b>Gene Copy Number Abundance</b>	Number of gene copies per unit volume of water (often measured in <b>copies/L</b> )	Used in qPCR and ddPCR studies to quantify species-specific eDNA abundance.	Applied in species-specific monitoring, including endangered and commercial fish species.
<b>Sequencing Depth Abundance</b>	Total number of sequences generated per sample	Affects sensitivity and detectability of rare species in eDNA metabarcoding.	Ensures high-quality data for fisheries eDNA monitoring programs.
<b>Relative Sequence Read Abundance (RSRA)</b>	Proportion of a species' reads compared to the total number of reads in a sample	Used in metabarcoding studies to infer species dominance but does not directly equate to population size.	Helps identify dominant fish species in an ecosystem.
<b>Normalized Read Count Abundance</b>	Read count values adjusted for sequencing effort and PCR biases	Used in statistical corrections to improve relative abundance estimates in metabarcoding.	Reduces bias in fisheries eDNA assessments, especially when comparing across multiple sites.
<b>Quantitative PCR (qPCR) Cycle Threshold (Ct) Abundance</b>	The number of PCR cycles required to amplify a detectable amount of eDNA	Lower Ct values indicate higher eDNA abundance, commonly used in calibrated abundance models.	Helps estimate species-specific fish presence and abundance in target fisheries.
<b>Droplet Digital PCR (ddPCR) Absolute Quantification</b>	Direct count of eDNA copies in a sample without reliance on Ct values	Used in high-precision eDNA quantification, allowing better absolute abundance estimates.	Used in commercial fisheries to track spawning stock biomass and migration patterns.

Table 4.2. Bayesian hierarchical model results calibrating eDNA abundance to traditional fish monitoring methods. Model type and coefficients reflect the strength and direction of association between eDNA and traditional abundance data, while spline terms account for temporal or spatial variability. Posterior credible intervals (CI) and Bayesian R<sup>2</sup> values indicate model fit, and all models fully converged ( $\hat{R} = 1$ ), ensuring reliable inference. All models converged ( $\hat{R} = 1$ ). Spline terms reflect smoothed seasonal or spatial variation. CI = 95% credible interval.

Method	Model Type	N sites	Sample Size	Bulk ESS eDNA	Bulk ESS Intercept	Intercept	Log eDNA	Spline Term	CI Lower	CI Upper	Bayesian R <sup>2</sup>	p-value
Video Monitoring	Gaussian Regression	1	30	20551	20647	4.46	0.17	-14.7	0.002	0.334	0.95	0.98
Combined	Hurdle Gamma	7	391	15966	5538	-0.27	0.15	N/A	0.107	0.195	0.71	1
Electronic Counter	Gamma Regression	1	60	13683	14746	0.86	0.11	3.16	0.067	0.151	0.76	1
Electrofishing	Hurdle Gamma	2	133	23888	12677	-1.65	0.2	-5.95	0.135	0.267	0.77	1
Fyke Net	Hurdle Gamma	3	95	25578	8394	1.06	-0.01	-0.57	-0.044	0.014	0.73	0.15

Table 4.3. Site-level detection probabilities for eDNA versus traditional fish monitoring methods using Bayesian hierarchical occupancy models. The models account for imperfect detection, temporal variation, and site-level effects, generating mean detection probabilities with associated 95% credible intervals (CIs) for each method.

Site	Traditional Comparison	eDNA			Traditional		
		Mean Detection Probability	Lower 95% CI	Upper 95% CI	Mean Detection Probability	Lower 95% CI	Upper 95% CI
Fore River	Fyke	0.70	0.41	0.90	0.64	0.06	0.99
Jones River	Fyke	0.72	0.43	0.91	0.70	0.07	0.99
Weweantic River	Fyke	0.70	0.36	0.92	0.58	0.04	1.00
Lake Sabbatia	Video	0.76	0.46	0.93	0.78	0.08	1.00
Benoits Pond	Fish Counter	0.73	0.40	0.92	0.63	0.05	0.99
South River	Electrofishing	0.73	0.43	0.93	0.69	0.07	0.99
Indian Head River	Electrofishing	0.69	0.36	0.92	0.61	0.04	1.00

Table 4.4. Estimates of eDNA detection probabilities when traditional methods fail, based on empirical and Bayesian models. Empirical and Bayesian estimates of eDNA detection probabilities when traditional methods fail to detect a species. The third row presents results from a hierarchical Bayesian occupancy model assessing the influence of successful detection by traditional methods on eDNA detection ( $\beta > 0$ ). Estimates are accompanied by lower and upper bounds of the 95% credible interval (CI). Posterior probability values close to 1 indicate high certainty in positive effect direction. Posterior probability ( $\beta > 0$ ) represents the probability that the relationship between eDNA and traditional detection is positive, given the posterior distribution.

Model	Type	Parameter	Estimate	l-95% CI	u-95% CI	Posterior Probability ( $\beta > 0$ )
Bayesian Prediction	eDNA Detection Probability When Traditional Method Fails	-	0.39	0.29	0.5	-
Empirical Probability	eDNA Detection Probability When Traditional Method Fails	-	0.37	0.26	0.49	-
Hierarchical Bayesian Model	Detection Effect	Detected Traditional	1.97	1.19	2.79	1

Table 4.5. Bayesian model comparisons evaluating the relationship between eDNA and traditional detection methods, with and without site-level effects. This table summarizes results from three Bayesian modeling approaches used to assess the relationship between eDNA and traditional monitoring detections. A Bayesian logistic regression was used to quantify the strength of association between traditional detections and eDNA detection. A hierarchical Bayesian model further accounted for site-level random effects, offering a more robust inference across heterogeneous monitoring contexts. A predictive Bayesian model estimated the probability of eDNA detection when traditional methods fail. For each model, parameter estimates are accompanied by 95% credible intervals (CIs), convergence diagnostics ( $\hat{R}$ ), and interpretation.  $\hat{R}$  = model convergence diagnostic (values = 1 indicate full convergence); CI = 95% credible interval.

Model	Type	Parameter	Estimate	l-95% CI	u-95% CI
Bayesian Logistic Regression	eDNA vs. Traditional Detection	Detected Traditional	1.9	1.29	2.51
Hierarchical Bayesian Model	eDNA vs. Traditional + Site-Level Effects	Detected Traditional	1.97	1.19	2.79
Bayesian Prediction	eDNA Detection Probability When Traditional Method Fails	Mean Probability	0.39	0.29	0.5

Table 4.6. Statistical comparisons between eDNA and traditional detection methods using logistic regression, chi-squared tests, and t-tests. This table summarizes the results of multiple statistical comparisons evaluating the relationship between eDNA and traditional fish detection methods. A logistic regression model tests whether traditional detections significantly increase the likelihood of eDNA detection. A chi-squared test assesses whether the two detection methods operate independently. Two t-tests evaluate: (1) differences in credible interval widths (as a measure of uncertainty) and (2) differences in mean detection probabilities. Significant p-values ( $p < 0.05$ ) indicate statistically meaningful differences in detection performance or certainty between methods.

Model	Type	Parameter	Estimate	Std. Error	p-value	Odds Ratio
Logistic Regression	eDNA vs. Traditional Detections	Detected Traditional	1.99	0.83	0.016	7.3
Chi-Squared Test	Independence Test	X-squared	4.73	-	0.029	-
T-test	Credible Interval Width	Mean Difference (CI Widths)	-0.38	0.009	<0.001	-
T-test	Detection Probability	Mean Difference (Detection Probability)	0.026	0.008	0.026	-

## Figures

Figure 4.1. Map of the seven paired eDNA and traditional survey methods throughout coastal Massachusetts.

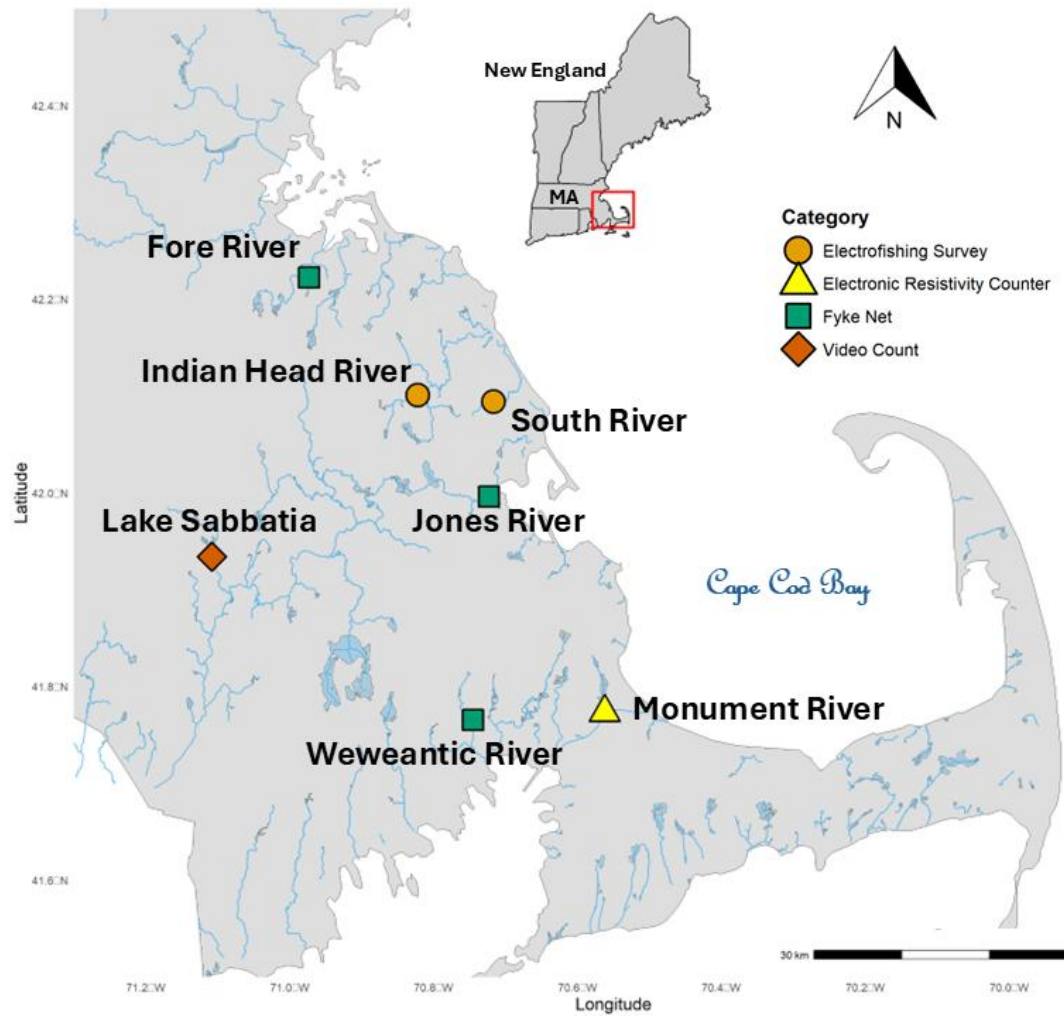


Figure 4.2. Temporal alignment of log-transformed eDNA gene copy equivalent (GCE) scores (green lines) and traditional fish counts (orange lines) targeting river herring (alewife (*Alosa pseudoharengus*) and blueback herring (*Alosa aestivalis*)) during the 2021 spring migration season at two locations within the Massachusetts waters. The left panel represents data collected at Benois Pond, where fish counts were recorded using an electronic fish counter. The right panel displays data from Lake Sabbatia, where visual observations were made using an underwater video monitoring system.

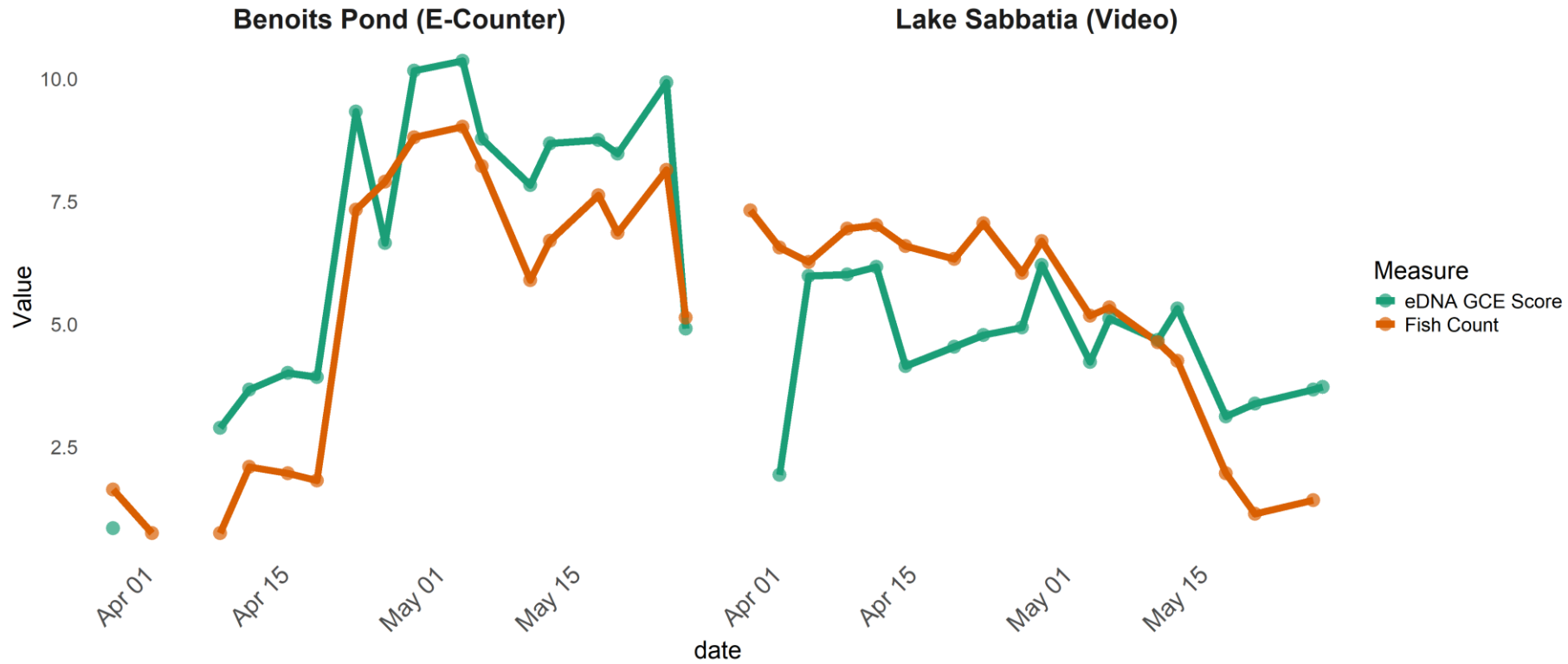


Figure 4.3. Temporal alignment of log-transformed eDNA gene copy equivalent (GCE) scores (green lines) and traditional fish counts (orange lines) targeting American shad (*Alosa sapidissima*) during the 2021 spring sampling season at two locations within the North and South River watersheds. The left panel represents data collected at Indian Head River (a tributary of the North River), and the right panel at South River, where traditional abundance estimates were obtained using single-pass electrofishing surveys.

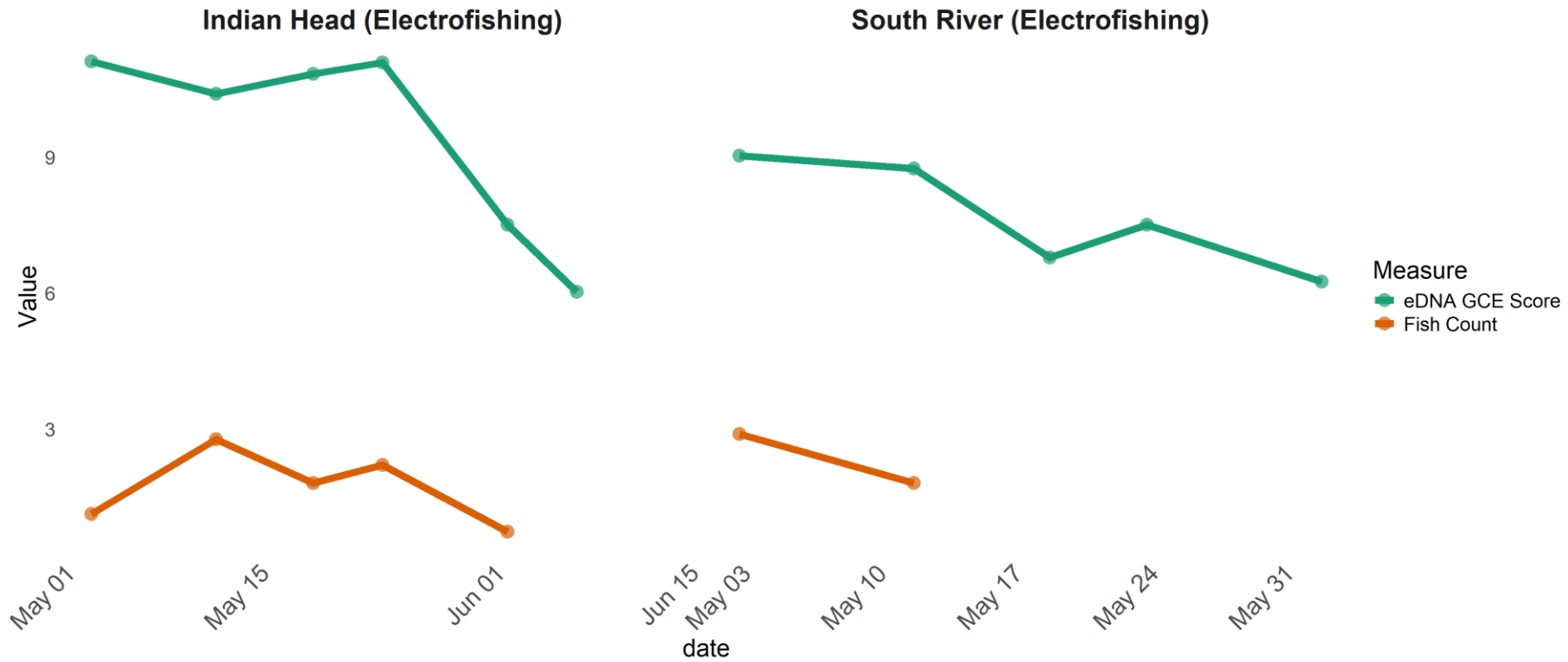


Figure 4.4. Temporal alignment of log-transformed eDNA gene copy equivalent (GCE) scores (green lines) and traditional fish counts (orange lines) during the 2021 spring spawning season at three coastal Massachusetts rivers. Traditional fish counts were obtained using fyke nets targeting rainbow smelt (*Osmerus mordax*). The left panel represents Fore River, the center panel shows Jones River, and the right panel displays data from the Weweantic River.

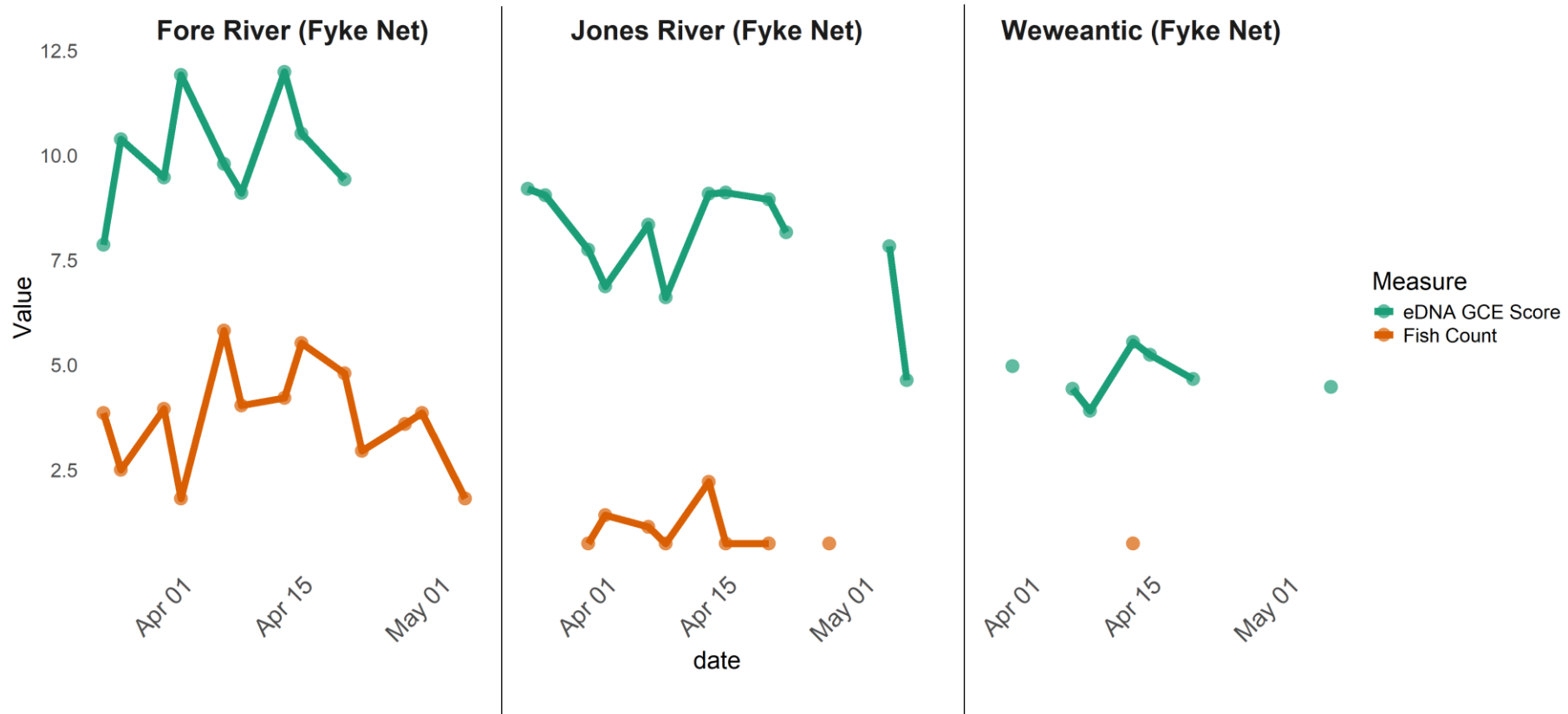


Figure 4.5. Comparison of eDNA and Traditional Fish Proportions of Detection Across Sites and Traditional Methods.

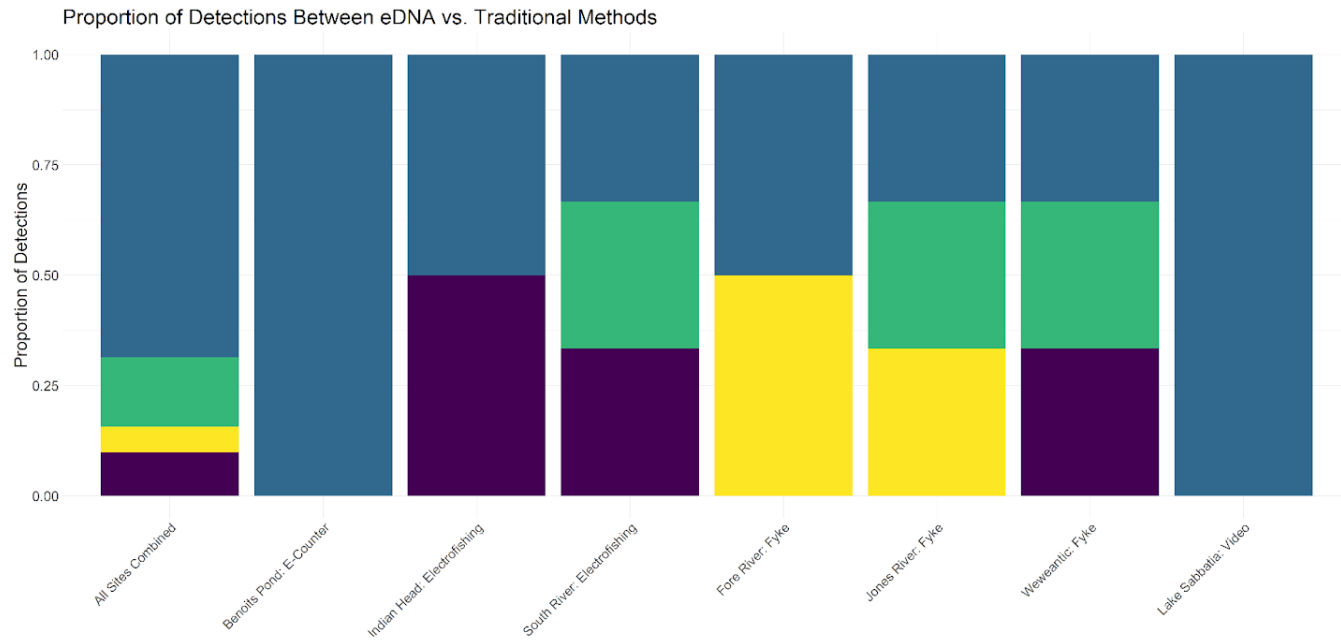


Figure 4.6: Comparison of Detection Probabilities and Credible Interval Widths Between eDNA and Traditional Sampling Methods. Bar plots comparing overall detection probabilities (left panel) and credible interval widths (right panel) between eDNA and traditional sampling methods. Mean detection probability was slightly higher for eDNA, with smaller credible intervals indicating more precise estimates. Traditional sampling methods exhibited greater uncertainty, as reflected in wider credible interval widths, suggesting higher variability in species detection. Error bars in the left panel represent 95% credible intervals.

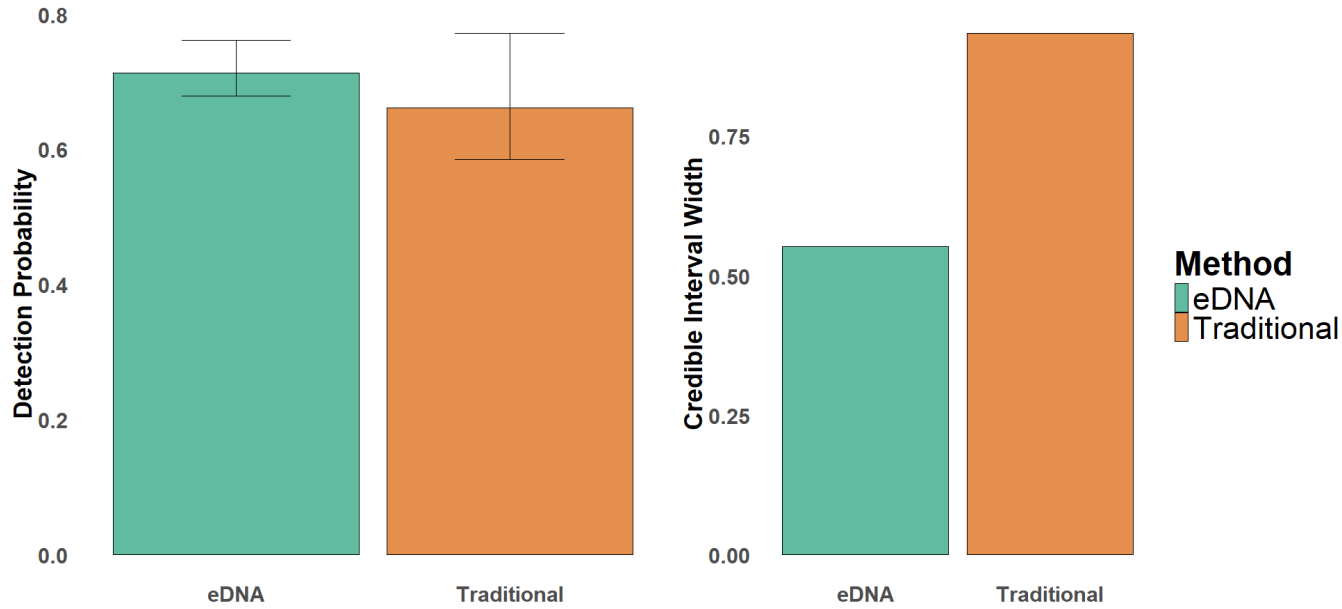


Figure 4.7. Site-Specific Comparison of Detection Probabilities and Credible Interval Widths for eDNA vs. Traditional Sampling Methods. Panel A: Bar plots comparing detection probabilities and 95% credible interval widths (panel B) across all monitored sites for eDNA-based and traditional sampling methods. Detection probabilities were generally higher and more consistent for eDNA, whereas traditional methods exhibited greater variability. Credible interval widths were consistently narrower for eDNA, indicating greater precision in detection estimates. Traditional sampling methods had wider credible intervals, suggesting increased uncertainty in species detection.

A.

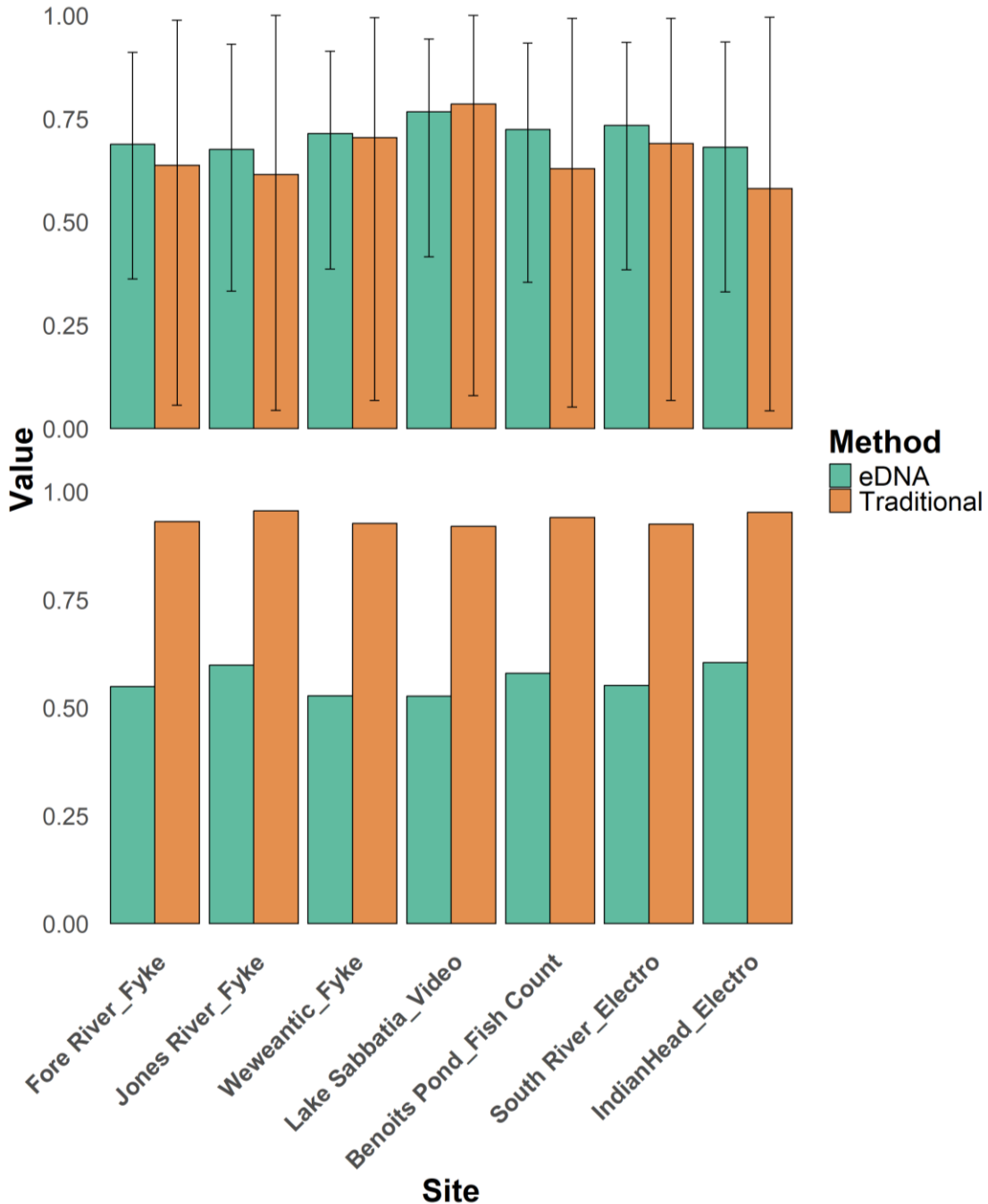


Figure 4.8. Comparison of Detection Probabilities and Credible Interval Widths for eDNA vs. Traditional Sampling Methods. Boxplots comparing detection probabilities (panel A.) and 95% credible interval widths (panel B). between eDNA-based and traditional sampling methods across monitored sites. eDNA exhibited consistently higher detection probabilities, with lower variation compared to traditional methods. In contrast, credible interval widths were significantly narrower for eDNA, indicating greater precision in detection probability estimates. Traditional methods showed greater uncertainty in both detection probability and credible interval width, reinforcing the advantage of eDNA for species detection in aquatic monitoring programs.

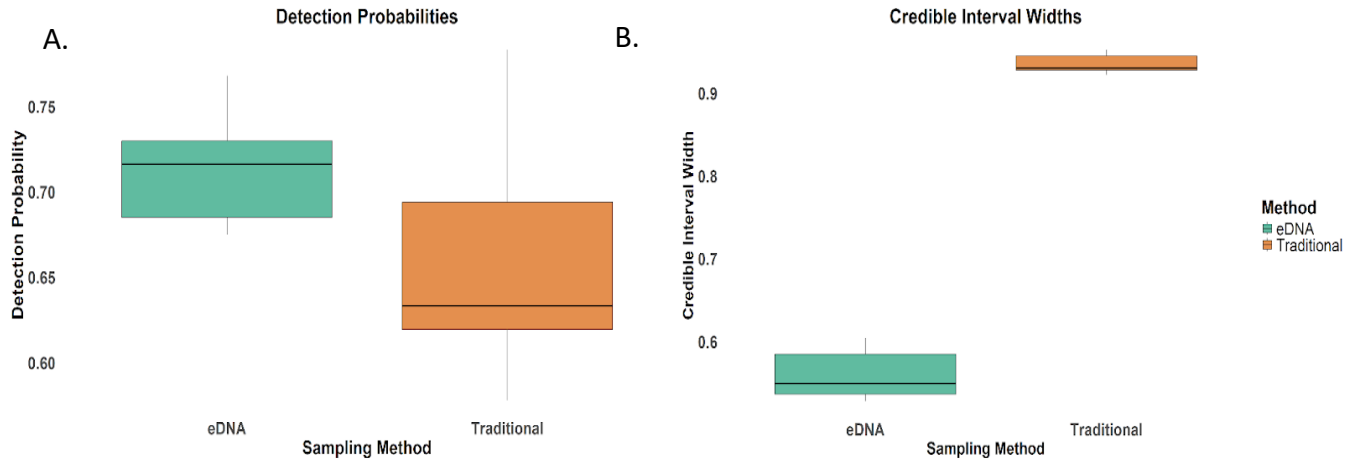
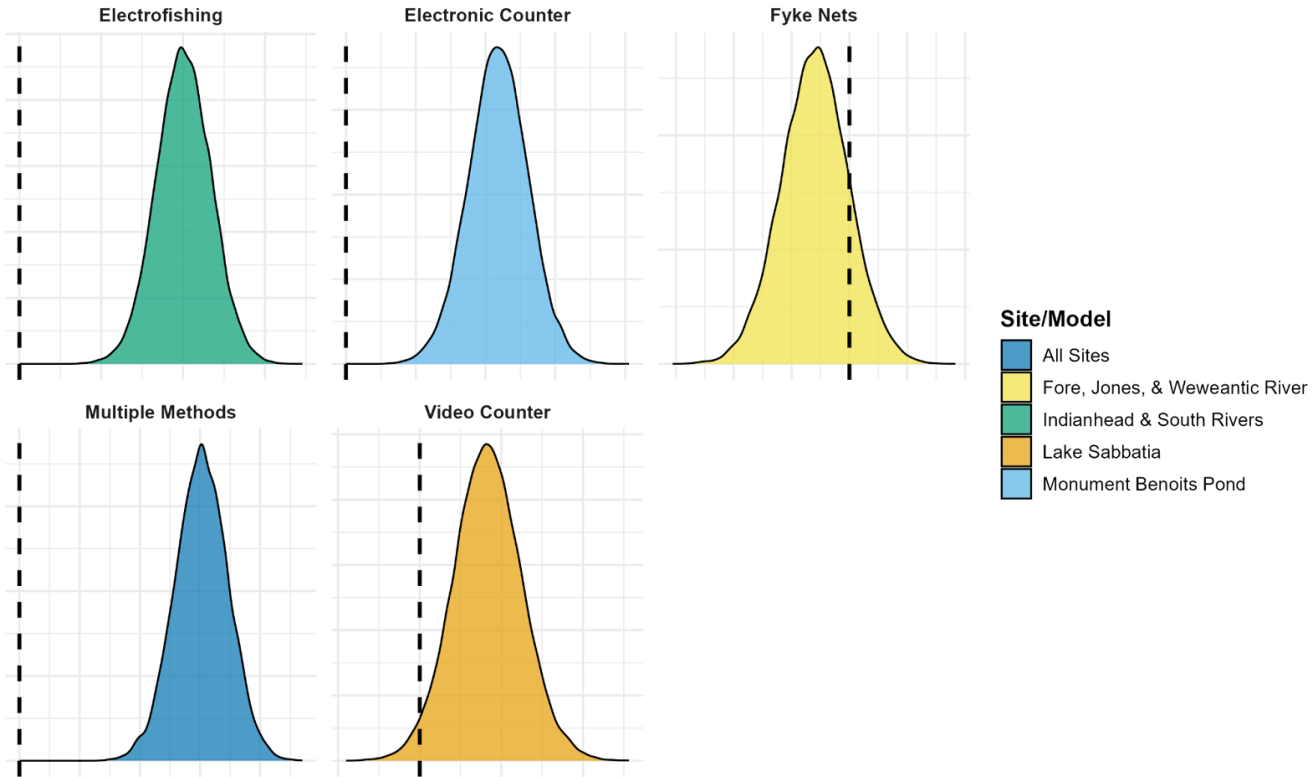


Figure 4.9. Posterior Distribution of eDNA-Based Abundance Estimates Posterior distribution plot for eDNA. Posterior distributions of model-estimated eDNA abundance across sampling sites and monitoring methods. Dashed line represents zero. The Bayesian hierarchical models incorporate site-specific random effects to account for spatial variability in detection. Higher posterior densities indicate greater certainty in relative abundance estimates. The distribution widths reflect uncertainty, with narrower intervals indicating greater model confidence.



## **CHAPTER 5**

### **CONCLUSIONS**

The overarching goal of my work is to make environmental DNA (eDNA) tools and techniques accessible, standardized, and understandable for the people, agencies, and organizations that need them most. To achieve this, I collaborated with a diverse group of project partners, helping them meet their unique monitoring goals by applying insights gained through extensive reading, critical reflection, and hands-on experience with both eDNA qPCR and metabarcoding techniques in the field.

Chapter two provided a comprehensive biodiversity assessment of the Jones River watershed - characterizing the species richness, species evenness, community composition characterization of species assemblages and functional trait characterization. This data will allow both the State of Massachusetts and the Jones River Watershed Association to have a comprehensive, watershed scale, eDNA based biodiversity baseline across 19 sites over two years within this watershed. This data also helps understand the initial response of the aquatic communities living within the Jones River watershed after a medium sized, mainstem dam removal. Patterns in diversity and species distributions revealed a complex early response to this restoration action. There was a decline in species richness from 2020 to 2021 across most sites and downstream locations. Sites grouped into the upstream category presented a more complicated set of results. Species

richness increased, while the community-weighted functional trait composition significantly decreased between 2020 and 2021 for upstream sites.

While seemingly contradictory, these results align with established ecological theory on large-scale disturbances in riverine systems (Baiser & Lockwood, 2011). Changes to natural flow regimes can trigger cascading ecological effects (Poff et al., 1997), particularly in systems undergoing abrupt transitions. The resulting reorganization phase (Holling and Gunderson, 2002) reflects a period of flux, where biotic communities respond to shifting hydrology, sediment transport, and novel habitat availability. Given the dynamic nature of this stage, observed species shifts, both upstream and downstream—are part of an expected, variable process rather than fixed trends, with ecosystem structure continuing to evolve until a new stable state is reached. Similar short-term declines in richness have been observed in other dam removal studies, where ecosystem recovery occurs over multiple years as habitat stabilizes and species redistribute (Bellmore et al., 2019). The persistence of diadromous species across both years, despite declines in other fish groups, suggests that watershed restoration efforts are successfully enhancing connectivity for migratory species, even as broader ecosystem restructuring continues. These data provide an essential baseline for tracking the magnitude, duration, and trajectory of ecological change in a post-dam removal system (Hansen & Hayes, 2012) and will support future surveys, restoration assessments, and adaptive management strategies within the Jones River watershed, and serve as a template for future metabarcoding surveys elsewhere.

Chapter three provided the foundation for calibrating eDNA qPCR derived relative abundance estimates (density of target species DNA per unit volume of water) to

traditional fisheries electronic resistivity count station relative abundance estimates (fish per hour) that were purpose built for monitoring migrating populations of river herring (Alewives (*Alosa pseudoharengus*) and blueback herring (*Alosa aestivalis*)) across four distinct locations within the monument river watershed. Results provide strong evidence that eDNA signals track daily and cumulative fish counts at both site-specific and watershed scales. Incorporating spatial variables such as basin volume and distance from counters significantly improved model performance at the watershed scale, while repeated temporal sampling enhanced both accuracy and ecological insights. Sampling broadly at multiple locations throughout the watershed helped identify optimal sampling locations to best calibrate eDNA relative abundance estimates to traditional estimates. Most importantly, however, incorporating eDNA GCE scores into a mechanistic model calibrated to a single downstream fish counter enabled estimation of relative fish abundance across multiple sites within a connected watershed. By knowing the estimated maximum number of river herring within the system at a given downstream location and time point, integrating hydrological principles, eDNA transport and degradation dynamics (Jane et al., 2015; Shogren et al., 2017; Harrison et al., 2019; Van Driessche et al., 2022; Carraro et al., 2024), and spatially explicit biological expectations, such as river herring aggregations in littoral and pelagic lake habitats (Hare et al., 2021; Yates et al., 2019), the models generated ecologically plausible and internally consistent site-level relative abundance estimates from a single e-count station. By tailoring eDNA sampling strategies to the unique characteristics of target systems, a scalable framework is provided for incorporating eDNA methods into diadromous fish stock assessments and advancing the application of eDNA in conservation management.

Chapter four provided a case arguing for a field-wide narrative shift: from questioning eDNA's capabilities to providing a framework for its functional implementation into management by examining both eDNA and traditional abundance estimation techniques through the common lens of one of their shared sources of potential bias: detection probability. Through seven case studies across four eDNA and traditional relative abundance technique pairings—eDNA vs. fyke net surveys for rainbow smelt (*Osmerus mordax*), eDNA vs. fixed video surveys and electronic resistivity counters for river herring (alewife (*Alosa pseudoharengus*) and blueback herring (*Alosa aestivalis*)), and eDNA vs. single-pass backpack electrofishing surveys for American shad (*Alosa sapidissima*)—I demonstrate how understanding the influence that detection probability has across environmental DNA and traditional relative abundance estimating methodologies can guide method selection and integration. The results presented in this study provide evidence that eDNA can be applied in fisheries management contexts to determine abundance in system-specific surveys. Results also show that detection probability provides a unifying framework for comparing different relative abundance monitoring methods, calculated from either detection/non-detection data using Bayesian and frequentist techniques. This approach offers a simple means of standardization across diverse methodologies, and a partial solution (lab standardization aside) to the singular and most persistent commentary offered from critics of eDNA implementation (Cristescue 2018; Hajibabaei 2022; Harrison et al., 2019; MacKenzie et al. 2006; Mathieu et al 2020; Ruppert et al 2019; Yates et al., 2019). Careful consideration is needed when using the term "abundance," particularly in eDNA research where it may

refer to read count abundance, DNA concentration, gene copy abundance, or calibrated estimates, etc. and in fisheries science generally.

### **Collaborators and Stakeholder Engagement**

None of the work in any of the chapters presented here, or the additional three eDNA based projects not included in this dissertation, would have been possible without input from a diverse array of project partners. Every project was the result of a co-produced, step by step process that informally followed structured decision making (SDM) guidelines (Gregory et al., 2012). Briefly, every collaborative project followed three phases. The first phase (planning phase) involved defining research and collaborative goals, gathering information from stakeholders within the community (this happened to varying degrees on each project), identifying options, role negotiation, and setting expectations and performance measures. The second (implementation) phase was characterized by the execution of our agreed upon sampling and sample processing strategies, diagnosing errors and streamlining methods, and sharing progress and timeline updates. The final (follow-through) phase involved making and communicating decisions about data processing and analysis, sharing results with project partners, jointly interpreting results, building strategies for communicating results with the broader community, assess the efficacy of planned strategies and update them accordingly for future work, and generating an agreement about final result sharing and publication.

### **Foundation for future research**

### **Lessons Learned**

Broadly speaking, two key areas emerged where improvement was clearly needed: first, the communication of expectations; and second, the development of clear, high-quality, step-by-step Standard Operating Procedures (SOPs) for both field and laboratory work. Avoidable errors occurred during critical stages of eDNA collection, including sample preparation, storage, and laboratory DNA extraction. These missteps could have been prevented through regular, structured check-ins between all collaborators—both during the initial training phase and after field and lab work began in earnest. While none of these mistakes proved fatal to the project, they underscore the importance of communication and accountability in collaborative research. I intend to carry these lessons forward into all future partnerships to ensure stronger, more resilient project outcomes.

In chapter two specifically, two years of metabarcoding data were removed due to laboratory contamination, with marine and mammalian DNA—impossible to introduce under field conditions—was detected in both field and lab blanks. Additionally, our sample preservation methods varied across years, with Longmire’s solution used in 2020–2021 and 95% ethanol in 2022–2023 due to budget constraints and reagent access issues. Longmire’s solution has been shown to better preserve eDNA for metabarcoding applications, maintaining DNA integrity while reducing degradation and contamination risks, whereas ethanol, despite its widespread use, has been associated with increased contamination potential and variable DNA retention (Turner et al., 2014; Williams et al., 2017). These findings reinforce the need for rigorous contamination controls at every step of the eDNA workflow, including dedicated pre- and post-PCR lab spaces, multiple

negative controls, and standardized decontamination protocols to ensure reliable results in restoration monitoring.

### **eDNA: from black box to repeatable science**

The expanding use of eDNA metabarcoding for biodiversity monitoring offers immense potential, but its effectiveness is often obscured by a methodological “black box.” This term describes the challenge of interpreting species detections when the decisions that shape those outcomes—ranging from field sampling to bioinformatics—are not standardized or fully transparent. Each step in the workflow introduces variability: filtration methods, preservation buffers, DNA extraction protocols, primer selection, PCR replication strategies, and sequencing platforms all influence detection sensitivity and accuracy (Sales et al., 2020). Within bioinformatics pipelines - one of the most opaque parts of the sequencing and data filtering processes - choices about denoising algorithms, filtering cutoffs, and similarity thresholds significantly affect the number and identity of detected taxa (Jackman et al. 2021). In my experience, eDNA metabarcoding techniques, including sequencing workflows, efficiency-enhancing strategies, and bioinformatic pipelines, are often closely held within individual laboratories (Dickie et al., 2018; Stein et al., 2024). These methods are rarely fully reported in the literature and are more commonly passed informally from lab member to lab member. As a result, asking two practitioners from different labs about their eDNA metabarcoding workflows will almost always reveal substantially different pipelines, even when addressing similar research questions.

To overcome this challenge and realize the full potential of eDNA metabarcoding, the field must prioritize the development of validated, standardized protocols across the

entire workflow. This includes the establishment of professional public or private laboratories capable of processing samples using reproducible and benchmarked methods, as well as community-wide agreement on best practices. A comprehensive meta-analysis of field, laboratory, and bioinformatic methodologies is urgently needed to identify effective strategies and guide standardization efforts. Moreover, full transparency in methods reporting, including detailed documentation of every step from collection to data analysis, should become a requirement, not an exception, in both peer-reviewed publications and institutional protocols.

Methodological uncertainties are rarely communicated and propagated through to ecological interpretation, where decisions about converting read counts to presence/absence or specific equations or conversions used in estimating abundance remain inconsistent. Compounding this issue is a lack of consensus in the literature on critical standards, such as the minimum number of field or technical replicates, how to distinguish true from false positives, and how to interpret MOTUs that cannot be confidently assigned to species (Cristescue et al., 2018). Without consistent and detailed reporting, comparing results across studies becomes difficult, and the full potential of eDNA metabarcoding for restoration monitoring or biodiversity assessment is diminished (Jackman et al. 2021). Moving forward, the field must prioritize the development of standardized protocols, regionally complete reference libraries, and transparent reporting practices to ensure methodological choices are clearly linked to ecological conclusions.

### **Future Research**

To enhance broader application, reliability, scalability, and conservation impact of environmental DNA (eDNA), particularly for diadromous fishes, I offer the following suggestions for future actions to improve the field of eDNA research and monitoring:

**1. Establish centralized, open-access eDNA data repositories.**

Creating unified databases will facilitate coordinated biodiversity monitoring across watersheds and support large-scale meta-analyses (Thomsen et al 2024). Such repositories would enable standardized data curation and sharing across regions, improving the comparability and reproducibility of eDNA studies.

**2. Improve transparency by fully reporting all methodological decisions.**

Many eDNA workflows—particularly in the lab and bioinformatics stages—remain opaque or unpublished (Dickie et al., 2018; Stein et al., 2024). Clear documentation of decisions around primer design, PCR replication, quality control thresholds, and filtering criteria should become a standard requirement in published eDNA studies.

**3. Conduct a global meta-analysis to identify and promote best practices across field, lab, and computational workflows.**

A synthesis of existing protocols would help identify which practices most reliably yield accurate biodiversity and abundance estimates across taxa, habitats, and geographic regions.

**4. Standardize field, laboratory, and bioinformatics protocols across agencies and institutions.**

Despite the rapid expansion of eDNA research, considerable variation exists across studies in filtration methods, preservation strategies, extraction techniques, PCR and

sequencing protocols, and bioinformatic pipelines (Sales et al., 2020; Jackman et al., 2021). A shared methodological foundation would improve interoperability between datasets and reduce uncertainty across studies.

**5. Establish purpose built, professional laboratories to implement validated, standardized workflows.**

Enabling public and private labs to conduct eDNA sample processing using rigorously validated protocols would increase consistency in results and help bridge the gap between research and monitoring applications.

**6. Evaluate detection probabilities across qPCR, ddPCR, metabarcoding, and NGS techniques.**

A comparative meta-analysis of existing paired-method studies could clarify the strengths, limitations, and ideal applications for each method type, improving decision-making in monitoring programs (Lacoursière-Roussel et al., 2016; Baldigo et al., 2017).

**7. Expand eDNA mechanistic modeling approaches and integrate environmental covariates into abundance calibration models.**

Environmental conditions—such as high flow events (Curtis et al., 2021), basin surface area, or increased fish activity (Thalinger et al., 2021)—can strongly affect eDNA detection and abundance estimates. Finding mechanistic approaches for additional habitat categories like river, stream, estuarine, and marine environments would greatly increase understanding of eDNA and environmental interactions.

**8. Generate long term (multi-year) eDNA data series.**

Pairing multi-year environmental datasets with eDNA sampling could help decouple biological signals from environmental noise, as well as elucidate interannual variation within study systems.

**9. Expand eDNA testing across hydrologically and ecologically diverse systems.**

Testing detection models across large, complex rivers and smaller tributaries will enhance generalizability. Incorporating models such as eDITH (Carraro et al., 2024) and occupancy-based approaches (Carraro et al., 2021) can improve understanding of eDNA transport, retention, and distribution dynamics.

**10. Apply strategic sampling and transitional zone monitoring to better capture eDNA gradients.**

Sampling at and around intermediate zones between habitats (e.g., along depth profiles of temperature or salinity stratified systems) could improve spatial resolution of species presence and migration/habitat use patterns, particularly in systems with known movement plasticity (Rosset et al., 2017; Rillahan & He, 2023; Legett et al., 2021).

**11. Explore both mitochondrial and nuclear eDNA approaches.**

Using both nuclear and mitochondrial targets may support population-level assessments from environmental samples. This approach could yield insights into stock structure, life history traits, and climate-linked shifts across connected freshwater-marine systems (Andres et al., 2021; McCauley et al., 2024).

**12. Expand sampling windows to capture entire life cycles, including juvenile outmigration.**

Because eDNA shedding is influenced by body size and metabolism (Maruyama et al.,

2014; Thalinger et al., 2021), seasonal changes in eDNA concentrations could reflect ontogenetic shifts and allow for tracking of juvenile development, emigration timing, or recruitment.

### **13. Integrate eDNA into existing monitoring programs to enhance cost-effectiveness and resolution.**

eDNA-based estimates can complement long-term programs like volunteer fish counts, which are widespread but often suffer from observational bias and limited spatiotemporal resolution (Nelson, 2006). A hybrid approach could increase data reach, utility, and public engagement.

The future of eDNA lies not in its technological limits, but in our ability to interpret these molecular blueprints within their environmental contexts and translate them into meaningful conservation action. Realizing this will require 1) standardization, and 2) holistic, in-depth, understanding of the hydrogeological landscape of the system of interest, incorporation of biology and ecology of species of interest, and purpose-built sampling designs that can functionally answer informed questions. Data—information—is the foundation upon which we build our understanding of the world. It fuels discovery, policy, and protection. This dissertation provides a framework for collecting and interpreting eDNA data in ways that deepen our ecological insight and justify the restoration of systems to which we are inextricably linked. In doing so, it contributes to a growing movement toward evidence-based, equitable stewardship of the natural world by those best positioned to act: conservation organizations, nonprofit groups, graduate students, tribal communities, school programs, and local, state, and federal agencies.

## BIBLIOGRAPHY

- Abbott, K. M. (2023). River restoration through dam removal: Examining ecological responses to small dam removals across Massachusetts. Dissertations. *Environmental Conservation Dissertations Collection. UMass Amherst Scholarworks*.
- Abbott, K. M., Roy, A. H., Magilligan, F. J., Nislow, K. H., & Quiñones, R. M. (2024). Incorporating climate change into restoration decisions: perspectives from dam removal practitioners. *Ecology and Society*, 29(3).
- Amano, T., & Sutherland, W. J. (2013). Four barriers to the global understanding of biodiversity conservation: wealth, language, geographical location and security. *Proceedings of the Royal Society B: Biological Sciences*, 280(1756), 20122649.
- Amarasiri, M., Furukawa, T., Nakajima, F., & Sei, K. (2021). Pathogens and disease vectors/hosts monitoring in aquatic environments: Potential of using eDNA/eRNA based approach. *Science of the Total Environment*, 796, 148810.
- Anderson, M. J., Ellingsen, K. E., & McArdle, B. H. (2006). Multivariate dispersion as a measure of beta diversity. *Ecology letters*, 9(6), 683-693.
- Andres, K. J., Sethi, S. A., Lodge, D. M., & Andrés, J. (2021). Nuclear eDNA estimates population allele frequencies and abundance in experimental mesocosms and field samples. *Molecular ecology*, 30(3), 685-697.
- Antão, L. H., Weigel, B., Strona, G., Hällfors, M., Kaarlejärvi, E., Dallas, T., ... & Laine, A. L. (2022). Climate change reshuffles northern species within their niches. *Nature Climate Change*, 12(6), 587-592.
- Balasingham, K. D., Walter, R. P., & Heath, D. D. (2017). Residual eDNA detection sensitivity assessed by quantitative real-time PCR in a river ecosystem. *Molecular Ecology Resources*, 17(3), 523–532. <https://doi.org/10.1111/1755-0998.12598>
- Baldigo, B. P., Sporn, L. A., George, S. D., & Ball, J. A. (2017). Efficacy of environmental DNA to detect and quantify brook trout populations in headwater streams of the Adirondack Mountains, New York. *Transactions of the American Fisheries Society*, 146(1), 99–111.
- Bailiff, M. D., & Karl, D. M. (1991). Dissolved and particulate DNA dynamics during a spring bloom in the Antarctic Peninsula region, 1986–1987. *Deep Sea Research Part A. Oceanographic Research Papers*, 38(8-9), 1077-1095.
- Baiser, B., & Lockwood, J. L. (2011). The relationship between functional and taxonomic homogenization. *Global Ecology and Biogeography*, 20(1), 134-144.
- Baranov, F. I. (1918). On the question of the biological basis of fisheries. *Nauchnyi Issledovatel'skii Ikhtiologicheskii Institut Izvestiia*, 1, 81-128.

- Barbarossa, V., Schmitt, R. J., Huijbregts, M. A., Zarfl, C., King, H., & Schipper, A. M. (2020). Impacts of current and future large dams on the geographic range connectivity of freshwater fish worldwide. *Proceedings of the National Academy of Sciences*, *117*(7), 3648-3655.
- Bednarek, A. T. (2001). Undamming rivers: a review of the ecological impacts of dam removal. *Environmental management*, *27*, 803-814.
- Barnes, M. A., & Turner, C. R. (2016). The ecology of environmental DNA and implications for conservation genetics. *Conservation Genetics*, *17*(1), 1–17. <https://doi.org/10.1007/s10592-015-0775-4>
- Bayer, S. R., Countway, P. D., & Wahle, R. A. (2019). Developing an eDNA toolkit to quantify broadcast spawning events of the sea scallop *Placopecten magellanicus*: moving beyond fertilization assays. *Marine Ecology Progress Series*, *621*, 127-141.
- Belding, D. L. 1921. Report on the Alewife fisheries of Massachusetts. Massachusetts Division of Fisheries and Game, Department of Conservation, 1M-6-64-938500, Boston.
- Bellmore, J. R., Duda, J. J., Craig, L. S., Greene, S. L., Torgersen, C. E., Collins, M. J., & Vittum, K. (2017). Status and trends of dam removal research in the United States. *Wiley Interdisciplinary Reviews: Water*, *4*(2), e1164.
- Bellmore, J. R., Pess, G. R., Duda, J. J., O'Connor, J. E., East, A. E., Foley, M. M., ... & Craig, L. S. (2019). Conceptualizing ecological responses to dam removal: If you remove it, what's to come?. *BioScience*, *69*(1), 26-39.
- Beng, K. C., & Corlett, R. T. (2020). Applications of environmental DNA (eDNA) in ecology and conservation: opportunities, challenges and prospects. *Biodiversity and conservation*, *29*(7), 2089-2121.
- Bernreuther, M., Herrmann, J.-P., Peck, M. A., and Temming, A. 2013. Growth energetics of juvenile herring, *Clupea harengus* L.: food conversion efficiency and temperature dependency of metabolic rate. *Journal of Applied Ichthyology*, *29*: 331–340.
- Bigelow, H. B., & Schroeder, W. C. (1953). *Fishes of the Gulf of Maine* (No. 592). US Government Printing Office.
- Biggs, C. R., Yeager, L. A., Bolser, D. G., Bonsell, C., Dichiera, A. M., Hou, Z., ... & Erisman, B. E. (2020). Does functional redundancy affect ecological stability and resilience? A review and meta-analysis. *Ecosphere*, *11*(7), e03184.
- Bloom, D. D., & Lovejoy, N. R. (2014). The evolutionary origins of diadromy inferred from a time-calibrated phylogeny for Clupeiformes (herring and allies). *Proceedings of the Royal Society B: Biological Sciences*, *281*(1778), 20132081.

- Bolyen, E., Rideout, J. R., Dillon, M. R., Bokulich, N. A., Abnet, C. C., Al-Ghalith, G. A., ... & Caporaso, J. G. (2019). Reproducible, interactive, scalable and extensible microbiome data science using QIIME 2. *Nature biotechnology*, 37(8), 852-857.
- Bonar, S. A., Hubert, W. A., & Willis, D. W. (Eds.). (2009). Standard Methods for Sampling North American Freshwater Fishes. *American Fisheries Society*.
- Brenton, P., Eby, P., Stevenson, R., & Ellwood, E. (2023). Measuring Habitat Restoration using the Darwin and "Event" Cores: Australian examples powered by BioCollect. *Biodiversity Information Science and Standards*, 7, e112083.
- Brown, J. J., Limburg, K. E., Waldman, J. R., Stephenson, K., Glenn, E. P., Juanes, F., & Jordaan, A. (2013). Fish and hydropower on the US Atlantic coast: failed fisheries policies from half-way technologies. *Conservation letters*, 6(4), 280-286.
- Buckland, M. (2017). *Information and society*. Mit Press.
- Buisson, L., Grenouillet, G., Villéger, S., Canal, J., & Laffaille, P. (2013). Toward a loss of functional diversity in stream fish assemblages under climate change. *Global change biology*, 19(2), 387-400.
- Bunt, C. M., Castro-Santos, T., & Haro, A. (2012). Performance of fish passage structures at upstream barriers to migration. *River research and applications*, 28(4), 457-478.
- Cairns, D. K., Benchetrit, J., Bernatchez, L., Bornarel, V., Casselman, J. M., Castonguay, M., ... & Zhu, X. (2022). Thirteen novel ideas and underutilised resources to support progress towards a range-wide American eel stock assessment. *Fisheries Management and Ecology*, 29(5), 516-541.
- Cantera, I., Cilleros, K., Valentini, A., Cerdan, A., Garcia-Vazquez, E., & Iribar, A. (2020). Optimizing environmental DNA sampling effort for fish inventories in tropical streams and rivers. *Scientific Reports*, 10(1), 21268. <https://doi.org/10.1038/s41598-020-78112-0>
- Cantera, I., Giachello, S., Münkemüller, T., Caccianiga, M., Gobbi, M., Losapio, G., ... & Ficetola, G. F. (2024). Describing functional diversity of communities from environmental DNA. *Trends in Ecology & Evolution*.
- Capo, E., Spong, G., Norman, S., Königsson, H., Bartels, P., & Byström, P. (2019). Droplet digital PCR assays for the quantification of brown trout (*Salmo trutta*) and Arctic char (*Salvelinus alpinus*) from environmental DNA collected in the water of mountain lakes. *PLoS One*, 14(12), e0226638. <https://doi.org/10.1371/journal.pone.0226638>
- Carpenter, S. R., Stanley, E. H., & Vander Zanden, M. J. (2011). State of the world's freshwater ecosystems: physical, chemical, and biological changes. *Annual review of Environment and Resources*, 36(1), 75-99.

- Carraro, L., Hartikainen, H., Jokela, J., Bertuzzo, E., & Rinaldo, A. (2018). Estimating species distribution and abundance in river networks using environmental DNA. *Proceedings of the National Academy of Sciences*, *115*(46), 11724-11729.
- Carraro, L., Stauffer, J. B., & Altermatt, F. (2021). How to design optimal eDNA sampling strategies for biomonitoring in river networks. *Environmental DNA*, *3*(1), 157-172.
- Carraro, L., & Altermatt, F. (2024). eDITH: An R-package to spatially project eDNA-based biodiversity across river networks with minimal prior information. *Methods in Ecology and Evolution*, *15*(5), 806-815.
- Castro-Santos, T. 2005. Optimal swim speeds for traversing velocity barriers: an analysis of volitional high-speed swimming behavior of migratory fishes. *Journal of Experimental Biology* *208*:421–432.
- Chapman, S. T. (2020). *Human Dimensions Research for Informed Decisions About Aquatic Restoration in New Hampshire: Environmental Justice in Implementation of Compensatory Mitigation* (Master's thesis, University of New Hampshire).
- Colwell, R. K., & Coddington, J. A. (1994). Estimating terrestrial biodiversity through extrapolation. *Philosophical Transactions of the Royal Society of London. Series B: Biological Sciences*, *345*(1311), 101-118.
- Conant Jr, B., Robinson, C. E., Hinton, M. J., & Russell, H. A. (2019). A framework for conceptualizing groundwater-surface water interactions and identifying potential impacts on water quality, water quantity, and ecosystems. *Journal of Hydrology*, *574*, 609-627.
- Condachou, C., Milhau, T., Murienne, J., Brosse, S., Villéger, S., Valentini, A., ... & Mouillot, D. (2023). Inferring functional diversity from environmental DNA metabarcoding. *Environmental DNA*, *5*(5), 934-944.
- Cristescu, M. E., & Hebert, P. D. (2018). Uses and misuses of environmental DNA in biodiversity science and conservation. *Annual Review of Ecology, Evolution, and Systematics*, *49*(1), 209-230.
- Curtis, A. N., Tiemann, J. S., Douglass, S. A., Davis, M. A., & Larson, E. R. (2021). High stream flows dilute environmental DNA (eDNA) concentrations and reduce detectability. *Diversity and Distributions*, *27*(10), 1918-1931.
- Dalton, R. M., Sheppard, J. J., Finn, J. T., Jordaan, A., & Staudinger, M. D. 2022. Phenological variation in spring migration timing of adult alewife in coastal Massachusetts. *Marine and Coastal Fisheries*, *14*(2), e10198.
- Daniels, J. A., Kerr, J. R., & Kemp, P. S. (2023). River infrastructure and the spread of freshwater invasive species: Inferences from an experimentally-parameterised individual-based model. *Journal of Applied Ecology*, *60*(6), 999-1009.
- Davenport, J. R., & Schiffhauer, D. E. (2000). Cultivar influences cranberry response to surface sanding. *HortScience*, *35*(1), 53-54.

- Deiner, K., Fronhofer, E. A., Mächler, E., Walser, J. C., & Altermatt, F. (2016). Environmental DNA reveals that rivers are conveyor belts of biodiversity information. *Nature Communications*, 7, 12544.
- Deiner, K., Bik, H.M., Mächler, E., Seymour, M., Lacoursière-Roussel, A., Altermatt, F., Creer, S., Bista, I., Lodge, D.M., de Vere, N., Pfrender, M.E., Bernatchez, L., 2017. Environmental DNA metabarcoding: Transforming how we survey animal and plant communities. *Mol. Ecol.* 26, 5872e5895.
- Delgado, M. L., & Ruzzante, D. E. (2020). Investigating diadromy in fishes and its loss in an-omics era. *Isience*, 23(12).
- Destoumieux-Garzón, D., Mavingui, P., Boetsch, G., Boissier, J., Darriet, F., Duboz, P., ... & Voituren, Y. (2018). The one health concept: 10 years old and a long road ahead. *Frontiers in veterinary science*, 5, 14.
- Devine, M. T., Rosset, J., Roy, A. H., Gahagan, B. I., Armstrong, M. P., Whiteley, A. R., & Jordaan, A. (2021). Feeling the Squeeze: Adult Run Size and Habitat Availability Limit Juvenile River Herring Densities in Lakes: JUVENILE RIVER HERRING DENSITIES IN LAKES. *Transactions of the American Fisheries Society*, 150(2), 207-221.
- Díaz-Ferguson, E. E., & Moyer, G. R. (2014). History, applications, methodological issues and perspectives for the use environmental DNA (eDNA) in marine and freshwater environments. *Revista de biología tropical*, 62(4), 1273-1284.
- Dickie, I. A., Boyer, S., Buckley, H. L., Duncan, R. P., Gardner, P. P., Hogg, I. D., ... & Weaver, L. (2018). Towards robust and repeatable sampling methods in eDNA-based studies. *Molecular Ecology Resources*, 18(5), 940-952.
- Dobrinkova, N., Arakelyan, A., Harutyunyan, A., & Reynolds, S. (2020). Project for an Open Source GIS Tool for Visualization of Flood Risk Analysis After Mining Dam Failures. In *Large-Scale Scientific Computing: 12th International Conference, LSSC 2019, Sozopol, Bulgaria, June 10–14, 2019, Revised Selected Papers 12* (pp. 300-308). Springer International Publishing.
- Doi, H., Inui, R., Akamatsu, Y., Kanno, K., Yamanaka, H., Takahara, T., & Minamoto, T. (2017). Environmental DNA analysis for estimating the abundance and biomass of stream fish. *Freshwater Biology*, 62(1), 30–39.
- Dorazio, R. M., & Erickson, R. A. (2018). ednaoccupancy: An r package for multiscale occupancy modelling of environmental DNA data. *Molecular ecology resources*, 18(2), 368-380.
- Doughty, C. E., Roman, J., Faurby, S., Wolf, A., Haque, A., Bakker, E. S., ... & Svenning, J. C. (2016). Global nutrient transport in a world of giants. *Proceedings of the National Academy of Sciences*, 113(4), 868-873.

- Duda, J. J., Torgersen, C. E., Brenkman, S. J., Peters, R. J., Sutton, K. T., Connor, H. A., ... & Pess, G. R. (2021). Reconnecting the Elwha River: spatial patterns of fish response to dam removal. *Frontiers in Ecology and Evolution*, *9*, 765488.
- Dunlop, K., Staby, A., van der Meeren, T., Keeley, N., Olsen, E. M., Bannister, R., & Skjæraasen, J. E. (2022). Habitat associations of juvenile Atlantic cod (*Gadus morhua* L.) and sympatric demersal fish communities within shallow inshore nursery grounds. *Estuarine, Coastal and Shelf Science*, *279*, 108111.
- Drummond, J. A., Larson, E. R., Li, Y., Lodge, D. M., Gantz, C. A., Pfrender, M. E., ... & Egan, S. P. (2021). Diversity metrics are robust to differences in sampling location and depth for environmental DNA of plants in small temperate lakes. *Frontiers in Environmental Science*, *9*, 617924.
- Eichmiller, J. J., Best, S. E., & Sorensen, P. W. (2016). Effects of temperature and trophic state on degradation of environmental DNA in lake water. *Environmental science & technology*, *50*(4), 1859-1867.
- Ellis, E. C. (2021). Land use and ecological change: A 12,000-year history. *Annual Review of Environment and Resources*, *46*(1), 1-33.
- Erete, S., Ryou, E., Smith, G., Fassett, K. M., & Duda, S. (2016, February). Storytelling with data: Examining the use of data by non-profit organizations. In *Proceedings of the 19th ACM conference on Computer-Supported cooperative work & social computing* (pp. 1273-1283).
- Evans, N. T., Shirey, P. D., Wieringa, J. G., Mahon, A. R., & Lamberti, G. A. (2017). Comparative cost and effort of fish distribution detection via environmental DNA analysis and electrofishing. *Fisheries*, *42*(2), 90-99.
- Ewels, P., Magnusson, M., Lundin, S., & Källner, M. (2016). MultiQC: summarize analysis results for multiple tools and samples in a single report. *Bioinformatics*, *32*(19), 3047- 3048.
- Fernandez, S., Arboleya, E., Dopico, E., & Garcia-Vazquez, E. (2022). Dams in South Europe: Socio-environmental approach and eDNA-metabarcoding to study dam acceptance and ecosystem health. *Wetlands Ecology and Management*, *30*(2), 341-355.
- Ficetola, G. F., Miaud, C., Pompanon, F., & Taberlet, P. (2008). Species detection using environmental DNA from water samples. *Biology letters*, *4*(4), 423-425.
- Foster, Z. S., Sharpton, T. J., & Grünwald, N. J. (2017). Metacoder: An R package for visualization and manipulation of community taxonomic diversity data. *PLoS computational biology*, *13*(2), e1005404.
- Fowler, C. M., Ogburn, M. B., Aguilar, R., Heggie, K., Legett, H. D., Richie, K. D., & Plough, L. V. (2024). Viability of high-frequency environmental DNA (eDNA) sampling as a fish enumeration tool. *Ecological Indicators*, *166*, 112384.

- Freeman, M. C., Pringle, C. M., Greathouse, E. A., & Freeman, B. J. (2003, January). Ecosystem-level consequences of migratory faunal depletion caused by dams. In *American Fisheries Society Symposium* (Vol. 35, No. January, pp. 255-266).
- Frimpong, E. A., & Angermeier, P. L. (2009). Fish traits: A database of ecological and life-history traits of freshwater fishes of the United States. *Fisheries*, 34(10), 487-495.
- Fry, F. E. J., and Hart, J. S. 1948. The relation of temperature to oxygen in the goldfish. *The Biological Bulletin*, 94: 66–77.
- Foley, M. M., Bellmore, J. R., O'Connor, J. E., Duda, J. J., East, A. E., Grant, G. E., ... & Wilcox, A. C. (2017). Dam removal: Listening in. *Water Resources Research*, 53(7), 5229-5246.
- Gamfeldt, L., & Hillebrand, H. (2008). Biodiversity effects on aquatic ecosystem functioning— maturation of a new paradigm. *International Review of Hydrobiology*, 93(4-5), 550-564.
- Gibbons, S., Roozbehi, S., Brewer, M., Rulifson, R., & Field, E. (2020, February). River Herring Edna: Developing a Method for Estimating Spawning Populations in NC. In 2020 *Southern Division-American Fisheries Society meeting*. AFS.
- Goldberg, C. S., Strickler, K. M., & Pilliod, D. S. (2015). Moving environmental DNA methods from concept to practice for monitoring aquatic macroorganisms. *Biological Conservation*, 183, 1-3.
- Goldberg, C. S., Turner, C. R., Deiner, K., Klymus, K. E., Thomsen, P. F., Murphy, M. A., & Cornman, R. S. (2016). Critical considerations for the application of environmental DNA methods to detect aquatic species. *Methods in Ecology and Evolution*, 7(11), 1299–1307.
- Goode, G. B. (1880). The use of agricultural fertilizers by the American Indians and the early English colonists. *The American Naturalist*, 14(7), 473-479.
- Gouletquer, P., Gros, P., Boeuf, G., Weber, J., Gouletquer, P., Gros, P., ... & Weber, J. (2014). The importance of marine biodiversity. *Biodiversity in the Marine Environment*, 1-13.
- Graf, W. L. (2006). Downstream hydrologic and geomorphic effects of large dams on American rivers. *Geomorphology*, 79(3-4), 336-360.
- Gregory, R., Failing, L., Harstone, M., Long, G., McDaniels, T., & Ohlson, D. (2012). *Structured decision making: a practical guide to environmental management choices*. John Wiley & Sons.
- Guri, G., Ray, J. L., Shelton, A. O., Kelly, R. P., Præbel, K., Andruszkiewicz Allan, E., ... & Westgaard, J. I. (2024). Quantifying the Detection Sensitivity and Precision of qPCR and ddPCR Mechanisms for eDNA Samples. *Ecology and Evolution*, 14(12), e70678.

- Hajibabaei, M. (2022). Demystifying eDNA validation. *Trends in Ecology & Evolution*, 37(10), 826-828.
- Hansen, J. F., & Hayes, D. B. (2012). Long-term implications of dam removal for macroinvertebrate communities in Michigan and Wisconsin rivers, United States. *River Research and Applications*, 28(9), 1540-1550.
- Hare, J. A., Borggaard, D. L., Alexander, M. A., Bailey, M. M., Bowden, A. A., Damon-Randall, K., ... & Beth Tooley, M. (2021). A review of river herring science in support of species conservation and ecosystem restoration. *Marine and Coastal Fisheries*, 13(6), 627-664.
- Haro, A., T. Castro-Santos, J. Noreika, and M. Odeh. 2004. Swimming performance of upstream migrant fishes in open-channel flow: a new approach to predicting passage through velocity barriers. *Canadian Journal of Fisheries and Aquatic Sciences* 61:1590–1601.
- Harrison, J. B., Sunday, J. M., & Rogers, S. M. (2019). Predicting the fate of eDNA in the environment and implications for studying biodiversity. *Proceedings of the Royal Society B*, 286(1915), 20191409. <https://doi.org/10.1098/rspb.2019.1409>
- Hayes, D., Fricano, G., Turek, J., Jordaan, A., Kulik, B., Baker, M., & Murray, J. (2023). Predicting response of migratory fish populations to dam removal. *Aquatic Ecosystem Health & Management*, 26(1), 79-88.
- Hiebert, S., Helfrich, L. A., Weigmann, D. L., & Liston, C. (2000). Anadromous salmonid passage and video image quality under infrared and visible light at Prosser Dam, Yakima River, Washington. *North American Journal of Fisheries Management*, 20(3), 827-832. [https://doi.org/10.1577/1548-8675\(2000\)020](https://doi.org/10.1577/1548-8675(2000)020)
- Hinlo, R., Lintermans, M., Gleeson, D., Broadhurst, B., & Furlan, E. (2018). Performance of eDNA assays to detect and quantify an elusive benthic fish in upland streams. *Biological Invasions*, 20(11), 3079–3093. <https://doi.org/10.1007/s10530-018-1760-x>
- Hitt, N. P., Eyler, S., & Wofford, J. E. (2012). Dam removal increases American eel abundance in distant headwater streams. *Transactions of the American Fisheries Society*, 141(5), 1171-1179.
- Hjort, J. (1914). Fluctuations in the great fisheries of Northern Europe, viewed in the light of biological research. *Rapports et Procès-Verbaux des Réunions du Conseil Permanent International pour l'Exploration de la Mer*, 20, 1-228.
- Holling, C. S., & Gunderson, L. H. (2002). Resilience and adaptive cycles.
- Holmes, V., Aman, J., York, G., & Kinnison, M. T. (2022). Environmental DNA detects Spawning Habitat of an ephemeral migrant fish (Anadromous Rainbow Smelt: *Osmerus mordax*). *BMC Ecology and Evolution*, 22(1), 1-13.

- Hongo, Y., Nishijima, S., Kanamori, Y., Sawayama, S., Yokouchi, K., Kanda, N., ... & Kurogi, H. (2021). Fish environmental DNA in Tokyo Bay: A feasibility study on the availability of environmental DNA for fisheries. *Regional Studies in Marine Science*, 47, 101950.
- Huang, C. S., Legett, H. D., Plough, L. V., Aguilar, R., Fitzgerald, C., Gregory, B., ... & Ogburn, M. B. (2023). Early detection and recovery of river herring spawning habitat use in response to a mainstem dam removal. *Plos one*, 18(5), e0284561.
- HumpHries, A. T., DimArchHopoulou, D., Stergiou, K. I., Tsikliras, A. C., Palomares, M. L. D., Bailly, N., ... & Pauly, D. (2023). Measuring the scientific impact of FishBase after three decades. *Cybium—Revue Internationale d’Ichtyologie*, 47, 213-224.
- Jackman, J. M., Benvenuto, C., Coscia, I., Oliveira Carvalho, C., Ready, J. S., Boubli, J. P., ... & Guimarães Sales, N. (2021). eDNA in a bottleneck: Obstacles to fish metabarcoding studies in megadiverse freshwater systems. *Environmental DNA*, 3(4), 837-849.
- Jane, S. F., Wilcox, T. M., McKelvey, K. S., Young, M. K., Schwartz, M. K., Lowe, W. H., Letcher, B. H., & Whiteley, A. R. (2015). Distance, flow and PCR inhibition: eDNA dynamics in two headwater streams. *Molecular Ecology Resources*, 15(1), 216–227. <https://doi.org/10.1111/1755-0998.12285>
- Jobling, M. 1985. Growth. In *Fish Energetics: New Perspectives*, pp. 213–230.
- Johnson, J.C., & Griffith, D.C. (2010). Environmental Social Sciences: Linking human and natural systems: *social networks, environment, and ecology*.
- Jones, A. C., Meiners, S. J., Effert-Fanta, E., Thomas, T., Smith, S. C., & Colombo, R. E. (2023). Low-head dam removal increases functional diversity of stream fish assemblages. *River Research and Applications*, 39(1), 3-20.
- Kanno, Y., Letcher, B. H., Rosner, A. L., O’Neil, K. P., & Nislow, K. H. (2015). Environmental factors affecting brook trout occurrence in headwater stream segments. *Transactions of the American Fisheries Society*, 144(2), 373-382.
- Keck, F., Blackman, R. C., Bossart, R., Brantschen, J., Couton, M., Hürlemann, S., ... & Altermatt, F. (2022). Meta-analysis shows both congruence and complementarity of DNA and eDNA metabarcoding to traditional methods for biological community assessment. *Molecular Ecology*, 31(6), 1820-1835.
- Kelly, B. J., Gross, R., Bittinger, K., Sherrill-Mix, S., Lewis, J. D., Collman, R. G., ... & Li, H. (2015). Power and sample-size estimation for microbiome studies using pairwise distances and PERMANOVA. *Bioinformatics*, 31(15), 2461-2468.
- Kondolf, G. M. (1995). Five elements for effective evaluation of stream restoration. *Restoration ecology*, 3(2), 133-136.

- Kovach, A. I., Breton, T. S., Enterline, C., & Berlinsky, D. L. (2013). Identifying the spatial scale of population structure in anadromous rainbow smelt (*Osmerus mordax*). *Fisheries Research*, 141, 95-106.
- Krabbenhoft, T. J., Myers, B. J., Wong, J. P., Chu, C., Tingley III, R. W., Falke, J. A., ... & Lynch, A. J. (2020). FiCli, the Fish and Climate Change Database, informs climate adaptation and management for freshwater fishes. *Scientific data*, 7(1), 124.
- Labiberté, E., & Legendre, P. (2010). A distance-based framework for measuring functional diversity from multiple traits. *Ecology*, 91(1), 299-305.
- Lacoursière-Roussel, A., Côté, G., Leclerc, V., & Bernatchez, L. (2016). Quantifying relative fish abundance with eDNA: a promising tool for fisheries management. *Journal of Applied Ecology*, 53(4), 1148-1157.
- Lane, N. (2007). *Aging infrastructure: Dam safety*. Congressional Research Service.
- Laramie, M. B., Pilliod, D. S., Goldberg, C. S., & Strickler, K. M. (2015). Environmental DNA sampling protocol-filtering water to capture DNA from aquatic organisms (No. 2-A13). *US Geological Survey*.
- Legett, H. D., Jordaan, A., Roy, A. H., Sheppard, J. J., Somos-Valenzuela, M., & Staudinger, M. D. (2021). Daily patterns of river herring (*Alosa* spp.) spawning migrations: environmental drivers and variation among coastal streams in Massachusetts. *Transactions of the American Fisheries Society*, 150(4), 501-513.
- Levi, T., Allen, J. M., Bell, D., Joyce, J., Russell, J. R., Tallmon, D. A., Vulstek, S. C., Yang, C., & Yu, D. W. (2019). Environmental DNA for the enumeration and management of Pacific salmon. *Molecular Ecology Resources*, 19(3), 597-608. <https://doi.org/10.1111/1755-0998.12987>
- Lewontin, R. C. (2000). *The triple helix: Gene, organism, and environment*. Harvard University Press.
- Li, X., Li, F., Min, X., Xie, Y., & Zhang, Y. (2023). Embracing eDNA and machine learning for taxonomy-free microorganisms biomonitoring to assess the river ecological status. *Ecological Indicators*, 155, 110948.
- Litchman, E., Villéger, S., Zinger, L., Auguet, J. C., Thuiller, W., Munoz, F., ... & Violle, C. (2024). Refocusing the microbial rare biosphere concept through a functional lens. *Trends in Ecology & Evolution*.
- Liu, C., Yan, M., Xiong, W., Li, N., & Gao, L. (2024). Applications of environmental DNA in the aquatic ecosystem management of East Asia. *Frontiers in Marine Science*, 11, 1473463.
- Lyon, S. W., DiBlasio, M., & Creveling, E. (2020). On using initial monitoring data to communicate restoration potentials and limitations. *Applied Environmental Education & Communication*, 19(3), 287-302.

- Mächler, E., Osathanunkul, M., & Altermatt, F. (2018). Shedding light on eDNA: neither natural levels of UV radiation nor the presence of a filter feeder affect eDNA-based detection of aquatic organisms. *PloS one*, 13(4), e0195529.
- MacKenzie, D. I., Nichols, J. D., Royle, J. A., Pollock, K. H., Bailey, L. L., & Hines, J. E. (2006). Occupancy Estimation and Modeling: Inferring Patterns and Dynamics of Species Occurrence. *Academic Press*.
- Magilligan, F. J., Graber, B. E., Nislow, K. H., Chipman, J. W., Sneddon, C. S., & Fox, C. A. (2016). River restoration by dam removal: Enhancing connectivity at watershed scales. *Elementa*, 4, 000108.
- Magilligan, F. J., Sneddon, C. S., & Fox, C. A. (2017). The social, historical, and institutional contingencies of dam removal. *Environmental Management*, 59, 982-994.
- Maruyama, A., Nakamura, K., Yamanaka, H., Kondoh, M., & Minamoto, T. (2014). The release rate of environmental DNA from juvenile and adult fish. *PloS one*, 9(12), e114639.
- Mason, C. Y. (1926). The cranberry industry in Massachusetts. *Economic Geography*, 2(1), 59-69.
- Mathieu, C., Hermans, S. M., Lear, G., Buckley, T. R., Lee, K. C., & Buckley, H. L. (2020). A systematic review of sources of variability and uncertainty in eDNA data for environmental monitoring. *Frontiers in Ecology and Evolution*, 8, 135.
- Mattocks, S., Hall, C. J., & Jordaan, A. (2017). Damming, lost connectivity, and the historical role of anadromous fish in freshwater ecosystem dynamics. *BioScience*, 67(8), 713-728.
- Mauvisseau, Q., Kalogianni, E., Zimmerman, B., Bulling, M., Brys, R., & Sweet, M. (2020). eDNA-based monitoring: Advancement in management and conservation of critically endangered killifish species. *Environmental DNA*, 2(4), 601-613.
- McCauley, M., Koda, S. A., Loesgen, S., & Duffy, D. J. (2024). Multicellular species environmental DNA (eDNA) research constrained by overfocus on mitochondrial DNA. *Science of The Total Environment*, 912, 169550.
- McCanty, S. T., Dimino, T. F., & Christian, A. D. (2021). Near-Term Changes to Reach Scale Habitat Features Following Headwater Stream Restoration in a Southeastern Massachusetts Former Cranberry Bog. *Diversity*, 13(6), 235.
- McMurdie, P. J., & Holmes, S. (2013). phyloseq: an R package for reproducible interactive analysis and graphics of microbiome census data. *PloS one*, 8(4), e61217.
- Meyer, C., Kreft, H., Guralnick, R., & Jetz, W. (2015). Global priorities for an effective information basis of biodiversity distributions. *Nature communications*, 6(1), 1-8.

- Meyer, S. T., Ebeling, A., Eisenhauer, N., Hertzog, L., Hillebrand, H., Milcu, A., ... & Weisser, W. W. (2016). Effects of biodiversity strengthen over time as ecosystem functioning declines at low and increases at high biodiversity. *Ecosphere*, 7(12), e01619.
- Miya, M. (2022). Environmental DNA metabarcoding: A novel method for biodiversity monitoring of marine fish communities. *Annual Review of Marine Science*, 14(1), 161- 185.
- Moring, J. R., & Mink, L. H. (2002). Anadromous alewives, *Alosa pseudoharengus*, as prey for white perch, *Morone americana*. *Hydrobiologia*, 479, 125-130.
- Mouton, T. L., Tonkin, J. D., Stephenson, F., Verburg, P., & Floury, M. (2020). Increasing climate-driven taxonomic homogenization but functional differentiation among river macroinvertebrate assemblages. *Global Change Biology*, 26(12), 6904-6915.
- Nelson, G. A. (2006). Guide to statistical sampling for the estimation of river herring run size using visual counts.
- Nelson, G. A., P. D. Brady, J. J. Sheppard, and M. P. Armstrong. 2011. An assessment of river herring stocks in Massachusetts. *Massachusetts Division of Marine Fisheries, Technical Report 46*, Gloucester.
- Nelson, G. A. (2019). Bias in common catch-curve methods applied to age frequency data from fish surveys. *ICES Journal of Marine Science*, 76(7), 2090-2101.
- Nevers, M. B., Byappanahalli, M. N., Morris, C. C., Shively, D., Przybyla-Kelly, K., Spoljaric, A. M., Dickey, J., & Roseman, E. F. (2020). Influence of sediment and stream transport on detecting a source of environmental DNA. *PLoS ONE*, 15(1), e0226906. <https://doi.org/10.1371/journal.pone.0226906>
- Ney, J. J., & Helfrich, L. A. (2005). Sustaining America's Aquatic Biodiversity. *Selected Freshwater Fish Families*.
- Noonan, M. J., Grant, J. W., & Jackson, C. D. (2012). A quantitative assessment of fish passage efficiency. *Fish and Fisheries*, 13(4), 450-464.
- Ogburn, M. B., Plough, L. V., Bangley, C. W., Fitzgerald, C. L., Hannam, M. P., Lee, B., ... & Weller, D. E. (2023). Environmental DNA reveals anadromous river herring habitat use and recolonization after restoration of aquatic connectivity. *Environmental DNA*, 5(1), 25-37.
- Ogram, A., Sayler, G. S., & Barkay, T. (1987). The extraction and purification of microbial DNA from sediments. *Journal of microbiological methods*, 7(2-3), 57-66.
- Oksanen, Jari, et al. "The vegan package." *Community ecology package* 10.631-637 (2007): 719.

- O'Malley, A. J., Enterline, C., & Zydlewski, J. (2017). Size and age structure of anadromous and landlocked populations of Rainbow Smelt. *North American Journal of Fisheries Management*, 37(2), 326-336.
- Ouellet, V., Collins, M. J., Kocik, J. F., Saunders, R., Sheehan, T. F., Ogburn, M. B., & Trinko Lake, T. (2022). The diadromous watersheds-ocean continuum: Managing diadromous fish as a community for ecosystem resilience. *Frontiers in Ecology and Evolution*, 10, 1007599.
- Palkovacs, E. P., Dion, K. B., Post, D. M., & Caccone, A. (2008). Independent evolutionary origins of landlocked alewife populations and rapid parallel evolution of phenotypic traits. *Molecular ecology*, 17(2), 582-597.
- Paul, J. H., Kellogg, C. A., & Jiang, S. C. (1996). Viruses and DNA in marine environments. *Microbial diversity in time and space*, 115-124.
- Perez, C. R., Bonar, S. A., Amberg, J. J., Ladell, B., Rees, C., Stewart, W. T., Gill, C. J., Cantrell, C., & Robinson, A. T. (2017). Comparison of American Fisheries Society (AFS) standard fish sampling techniques and environmental DNA for characterizing fish communities in a large reservoir. *North American Journal of Fisheries Management*, 37(5), 1010–1027. <https://doi.org/10.1080/02755947.2017.1342721>
- Persky, J. H. (1993). *Yields and water quality of stratified-drift aquifers in the southeast coastal basin, Cohasset to Kingston, Massachusetts* (No. 91-4112). US Geological Survey, Water Resources Division; Books and Open-File Reports Section.
- Pess, G. R., McHenry, M. L., Denton, K., Anderson, J. H., Liermann, M. C., Peters, R. J., ... & Hanson, K. M. (2024). Initial responses of Chinook salmon (*Oncorhynchus tshawytscha*) and steelhead (*Oncorhynchus mykiss*) to removal of two dams on the Elwha River, Washington State, USA. *Frontiers in Ecology and Evolution*, 12, 1241028.
- Pess, G. R., Quinn, T. P., Gephard, S. R., & Saunders, R. (2014). Re-colonization of Atlantic and Pacific rivers by anadromous fishes: linkages between life history and the benefits of barrier removal. *Reviews in Fish Biology and Fisheries*, 24, 881-900.
- Petersen, C. G. J. (1896). The yearly immigration of young plaice into the Limfjord from the German Sea. *Report of the Danish Biological Station*, 6, 1-48.
- Piggott, M. P., Banks, S. C., Broadhurst, B. T., Fulton, C. J., & Lintermans, M. (2021). Comparison of traditional and environmental DNA survey methods for detecting rare and abundant freshwater fish. *Aquatic Conservation: Marine and Freshwater Ecosystems*, 31(1), 173-184.

- Pilliod, D. S., Goldberg, C. S., Arkle, R. S., & Waits, L. P. (2013). Estimating occupancy and abundance of stream amphibians using environmental DNA from filtered water samples. *Canadian Journal of Fisheries and Aquatic Sciences*, 70(8), 1123–1130. <https://doi.org/10.1139/cjfas-2013-0047>
- Plough, L. V., Ogburn, M. B., Fitzgerald, C. L., Geranio, R., Marafino, G. A., & Richie, K. D. (2018). Environmental DNA analysis of river herring in Chesapeake Bay: A powerful tool for monitoring threatened keystone species. *PLoS one*, 13(11), e0205578.
- Plummer, M. (2003, March). JAGS: A program for analysis of Bayesian graphical models using Gibbs sampling. In *Proceedings of the 3rd international workshop on distributed statistical computing* (Vol. 124, No. 125.10, pp. 1-10).
- Pochardt, M., Allen, J. M., Hart, T., Miller, S. D., Yu, D. W., & Levi, T. (2020). Environmental DNA facilitates accurate, inexpensive, and multiyear population estimates of millions of anadromous fish. *Molecular Ecology Resources*, 20(2), 457-467.
- Poff, N. L., Allan, J. D., Bain, M. B., Karr, J. R., Prestegard, K. L., Richter, B. D., ... & Stromberg, J. C. (1997). The natural flow regime. *BioScience*, 47(11), 769-784.
- Poff, N. L., Olden, J. D., Merritt, D. M., & Pepin, D. M. (2007). Homogenization of regional river dynamics by dams and global biodiversity implications. *Proceedings of the National Academy of Sciences of the United States of America*, 104, 5732–5737.
- Pope, K. L., & Willis, D. W. (1996). Seasonal influences on freshwater fisheries sampling data. *Reviews in Fisheries Science*, 4(1), 57-73. <https://doi.org/10.1080/10641269609388579>
- Porto-Hannes, I., Sassoubre, L. M., Sansom, B. J., & Morris, T. J. (2023). Applying environmental DNA methods to inform detection of *Simpsonaias ambigua* under varying water velocities in a river. *Freshwater Mollusk Biology and Conservation*, 26(2), 54-68.
- Price, A. L., & Peterson, J. T. (2010). Estimation and modeling of electrofishing capture efficiency for fishes in wadeable warmwater streams. *North American Journal of Fisheries Management*, 30(2), 481-498.
- Rader, R., Bartomeus, I., Tylianakis, J. M., & Laliberté, E. (2014). The winners and losers of land use intensification: Pollinator community disassembly is non-random and alters functional diversity. *Diversity and Distributions*, 20(8), 908-917.
- Reback, K. E., Brady, P. D., McLaughlin, K. D., & Milliken, C. G. 2005. A survey of anadromous fish passage in coastal Massachusetts part 3: South Shore. *Massachusetts Division of Marine Fisheries Technical Report 17*, Gloucester.
- Riaz, T., Shehzad, W., Viari, A., Pompanon, F., Taberlet, P., & Coissac, E. (2011). ecoPrimers: inference of new DNA barcode markers from whole genome sequence analysis. *Nucleic acids research*, 39(21), e145-e145.

- Riche, N. H., Hurter, C., Diakopoulos, N., & Carpendale, S. (Eds.). (2018). *Data-driven storytelling*. CRC Press.
- Ricker, W. E. (1954). Stock and recruitment. *Journal of the Fisheries Research Board of Canada*, 11(5), 559-623. <https://doi.org/10.1139/f54-039>
- Rosset, J., Roy, A. H., Gahagan, B. I., Whiteley, A. R., Armstrong, M. P., Sheppard, J. J., & Jordaan, A. (2017). Temporal patterns of migration and spawning of river herring in coastal Massachusetts. *Transactions of the American Fisheries Society*, 146(6), 1101- 1114.
- Rourke, M. L., Fowler, A. M., Hughes, J. M., Broadhurst, M. K., DiBattista, J. D., Fielder, S., ... & Furlan, E. M. (2022). Environmental DNA (eDNA) as a tool for assessing fish biomass: A review of approaches and future considerations for resource surveys. *Environmental DNA*, 4(1), 9-33.
- Roussel, J. M., Paillisson, J. M., Tréguier, A., & Petit, E. (2015). The downside of eDNA as a survey tool in water bodies. *Journal of Applied Ecology*, 823-826.
- Roy, S. G., Uchida, E., de Souza, S. P., Blachly, B., Fox, E., Gardner, K., ... & Hart, D. (2018). A multiscale approach to balance trade-offs among dam infrastructure, river restoration, and cost. *Proceedings of the National Academy of Sciences*, 115(47), 12069-12074.
- Ruppert, K. M. (2020). Development and Assessment of an Environmental DNA (eDNA) Assay for the Rio Grande Siren and Review of eDNA Metabarcoding Applications (*Master's thesis, The University of Texas Rio Grande Valley*).
- Saito, T., & Doi, H. (2021). Temperature-dependent decay rate of environmental DNA under natural freshwater conditions. *PeerJ*, 9, e10833. <https://doi.org/10.7717/peerj.10833>
- Sales, N. G., Wangenstein, O. S., Carvalho, D. C., Deiner, K., Præbel, K., Coscia, I., ... & Mariani, S. (2021). Space-time dynamics in monitoring neotropical fish communities using eDNA metabarcoding. *Science of the Total Environment*, 754, 142096.
- Sansom, B. J., Ruiz-Ramos, D. V., Thompson, N. L., Roberts, M. O., Taylor, Z. A., Ortiz, K., ... & Klymus, K. E. (2024). Detection and transport of environmental DNA from two federally endangered mussels. *Plos one*, 19(10), e0304323.
- Schaefer, M. B. (1954). Some aspects of the dynamics of populations important to the management of the commercial marine fisheries. *Inter-American Tropical Tuna Commission Bulletin*, 1(2), 23-56.
- Schenekar, T. (2023). The current state of eDNA research in freshwater ecosystems: Are we shifting from the developmental phase to standard application in biomonitoring? *Hydrobiologia*, 850(6), 1263-1282.
- Schübeler, D. (2015). Function and information content of DNA methylation. *Nature*, 517(7534), 321-326.

- Shelton, A. O., Kelly, R. P., O'Donnell, J. L., Park, L., Schwenke, P., Greene, C., Henderson, R. A., & Beamer, E. M. (2019). Environmental DNA provides quantitative estimates of a threatened salmon species. *Biological Conservation*, 237, 383–391. <https://doi.org/10.1016/j.biocon.2019.07.003>
- Shelton, A. O., Ramón-Laca, A., Wells, A., Clemons, J., Chu, D., Feist, B. E., ... & Park, L. (2022). Environmental DNA provides quantitative estimates of Pacific hake abundance and distribution in the open ocean. *Proceedings of the Royal Society B*, 289(1971), 20212613.
- Simon Andrews, F. K., Segonds-Pichon, A., Biggins, L., Krueger, C., & Wingett, S. (2010). *FastQC: a quality control tool for high throughput sequence data*. Assessment, M. E. (2005). *Ecosystems and human well-being: wetlands and water*. World resources institute.
- Searcy, R. T., Boehm, A. B., Weinstock, C., Preston, C. M., Jensen, S., Roman, B., ... & Yamahara, K. M. (2022). High-frequency and long-term observations of eDNA from imperiled salmonids in a coastal stream: Temporal dynamics, relationships with environmental factors, and comparisons with conventional observations. *Environmental DNA*, 4(4), 776-789.
- Sellers, G. S., Jerde, C. L., Harper, L. R., Benucci, M., Di Muri, C., Li, J., ... & Hänfling, B. (2024). Optimising species detection probability and sampling effort in lake fish eDNA surveys. *Metabarcoding and Metagenomics*, 8, 121-143.
- Siddique, R., & Palmer, R. (2021). Climate change impacts on local flood risks in the US Northeast: a case study on the Connecticut and Merrimack River Basins. *JAWRA Journal of the American Water Resources Association*, 57(1), 75-95.
- Shogren, A. J., Tank, J. L., Andruszkiewicz, E. A., Olds, B., Mahon, A. R., Jerde, C. L., & Bolster, D. (2017). Controls on eDNA movement in streams: Transport, retention, and resuspension. *Scientific Reports*, 7(1), 1-11.
- Shelton, A. O., Kelly, R. P., O'Donnell, J. L., Park, L., Schwenke, P., Greene, C., Henderson, R. A., & Beamer, E. M. (2019). Environmental DNA provides quantitative estimates of a threatened salmon species. *Biological Conservation*, 237, 383–391. <https://doi.org/10.1016/j.biocon.2019.07.003>
- Sheppard, J.J., and M. S. Bednarski. 2015. Utility of Single-Channel Electronic Resistivity Counters for Monitoring River Herring Populations, *North American Journal of Fisheries Management* 35:6, 1144-1151.
- Spear, M. J., Embke, H. S., Krysan, P. J., & Vander Zanden, M. J. (2021). Application of eDNA as a tool for assessing fish population abundance. *Environmental DNA*, 3(1), 83-91.
- Spence, B. C., Tice-Lewis, M., Sorel, M. H., & Danner, E. M. (2020). Efficacy of environmental DNA sampling to detect the occurrence of an endangered endemic stream fish. *Environmental DNA*, 2(3), 307–319. <https://doi.org/10.1002/edn3.175>

- Stein, E. D., Jerde, C. L., Allan, E. A., Sepulveda, A. J., Abbott, C. L., Baerwald, M. R., ... & Thielen, P. M. (2024). Critical considerations for communicating environmental DNA science. *Environmental DNA*, 6(1), e472.
- Stevens, E. R., Hyde, J., Beesley, L. S., Gwinn, D. C., Thompson, S., Morris, L., ... & Gleeson, D. B. (2024). Fishy Business—Assessing the Efficacy of Active and Passive eDNA to Describe the Fish Assemblage of a River in Southwestern Western Australia to Support Effective Monitoring. *Environmental DNA*, 6(6), e70040.
- Stoeckle, M. Y., Adolf, J., Charlop-Powers, Z., Dunton, K. J., Hinks, G., & VanMorter, S. M. (2021). Trawl and eDNA assessment of marine fish diversity, seasonality, and relative abundance in coastal New Jersey, USA. *ICES Journal of Marine Science*, 78(1), 293-304.
- Stoeckle, B. C., Beggel, S., Cerwenka, A. F., Motivans, E., Kuehn, R., & Geist, J. (2017). A systematic approach to evaluate the influence of environmental conditions on eDNA detection success in aquatic ecosystems. *PLoS One*, 12(12), e0189119.
- Stolper, C. D., Lee, B., Riche, N. H., & Stasko, J. (2016). *Emerging and recurring data-driven storytelling techniques: Analysis of a curated collection of recent stories.*(2016).
- Strickler, K. M., Fremier, A. K., & Goldberg, C. S. (2015). Quantifying effects of UV-B, temperature, and pH on eDNA degradation in aquatic microcosms. *Biological Conservation*, 183, 85-92.
- Strik, B. C., & Poole, A. P. (1995). Does sand application to soil surface benefit cranberry production?. *HortScience*, 30(1), 47-49.
- Su, Y.-S., & Yajima, M. (2021). *R2jags: Using R to run 'JAGS'* (Version 0.7-1) [R package].
- Takahara, T., Minamoto, T., Yamanaka, H., Doi, H., & Kawabata, Z. (2012). Estimation of fish biomass using environmental DNA. *PLoS One*, 7(4), e35868. <https://doi.org/10.1371/journal.pone.0035868>
- Thalinger, B., Wolf, E., Traugott, M., & Wanzenböck, J. (2019). Monitoring spawning migrations of potamodromous fish species via eDNA. *Scientific Reports*, 9(1), 15388. <https://doi.org/10.1038/s41598-019-51398-0>
- Thalinger, B., Deiner, K., Harper, L. R., Rees, H. C., Blackman, R. C., Sint, D., ... & Bruce, K. (2021). A validation scale to determine the readiness of environmental DNA assays for routine species monitoring. *Environmental DNA*, 3(4), 823-836.
- Thomsen, P. F., Jensen, M. R., & Sigsgaard, E. E. (2024). A vision for global eDNA-based monitoring in a changing world. *Cell*, 187(17), 4444-4448.

- Tillotson, M. D., Kelly, R. P., Duda, J. J., Hoy, M., Kralj, J., & Quinn, T. P. (2018). Concentrations of environmental DNA (eDNA) reflect spawning salmon abundance at fine spatial and temporal scales. *Biological Conservation*, 220, 1–11. <https://doi.org/10.1016/j.biocon.2018.01.030>
- Ticiani, D., Larentis, C., de Carvalho, D. R., Ribeiro, A. C., & Delariva, R. L. (2023). Dam cascade in run-of-river systems promotes homogenisation of fish functional traits in a plateau river. *Ecology of Freshwater Fish*, 32(1), 147-165.
- Troth, C. R., Sweet, M. J., Nightingale, J., & Burian, A. (2021). Seasonality, DNA degradation and spatial heterogeneity as drivers of eDNA detection dynamics. *Science of the Total Environment*, 768, 144466.
- Tsuji, S., Ushio, M., Sakurai, S., Minamoto, T., & Yamanaka, H. (2017). Water temperature-dependent degradation of environmental DNA and its relation to bacterial abundance and activity. *Microbial Ecology*, 74(1), 116–126. <https://doi.org/10.1007/s00248-016-0901-x>
- Tucker, C. M., Cadotte, M. W., Carvalho, S. B., Davies, T. J., Ferrier, S., Fritz, S. A., ... & Mazel, F. (2017). A guide to phylogenetic metrics for conservation, community ecology and macroecology. *Biological Reviews*, 92(2), 698-715.
- Turner, S. M., Chase, B. C., Bednarski, M. S., Elzey, S. P., & Ayer, M. H. (2021). Evaluating the effectiveness of fyke-net sampling to characterize an anadromous rainbow smelt population in the Fore River, Massachusetts, USA. *North American Journal of Fisheries Management*, 41(6), 1789-1797.
- Van Driessche, C., Horemans, B., & Goethals, P. L. M. (2022). Environmental DNA transport in river networks: A review of key aspects and future research directions. *Environmental DNA*, 4(4), 739–753. <https://doi.org/10.1002/edn3.285>
- Villacorta-Rath, C., Gunasekera, R. M., Lanham, B. S., Huveneers, C., Clarke, L. J., & Harford, A. J. (2021). Long-distance (>20 km) downstream detection of endangered species using environmental DNA. *PeerJ*, 9, e11030. <https://doi.org/10.7717/peerj.11030>
- Vinga, S. (2014). Information theory applications for biological sequence analysis. *Briefings in bioinformatics*, 15(3), 376-389.
- Visser, M. E., & Both, C. (2005). Shifts in phenology due to global climate change: the need for a yardstick. *Proceedings of the Royal Society B: Biological Sciences*, 272(1581), 2561-2569.
- Wagner, M. J., & Moore, P. A. (2024). Longitudinal study of stream ecology pre-and post-dam removal: Physical, chemical, and biological changes to a northern Michigan stream. *Science of the Total Environment*, 912, 168848.
- Waldman, J. (2013). *Running silver: restoring Atlantic rivers and their great fish migrations*. Rowman & Littlefield.

- Watson, J. D., & Berry, A. (2009). *DNA: The secret of life*. Knopf.
- Weinbauer, M. G., Fuks, D., & Peduzzi, P. (1993). Distribution of viruses and dissolved DNA along a coastal trophic gradient in the northern Adriatic Sea. *Applied and Environmental Microbiology*, 59(12), 4074-4082.
- Wetzel, R. G. (2001). *Limnology: Lake and River Ecosystems* (3rd ed.). Academic Press.
- Wickham, H. (2011). ggplot2. *Wiley interdisciplinary reviews: computational statistics*, 3(2), 180-185.
- Wickham, H., & Bryan, J. (2023). *R packages*. " O'Reilly Media, Inc."
- Williams, M. R., Stedtfeld, R. D., Engle, C., Salach, P., Fagher, U., Stedtfeld, T., ... & Hashsham, S. A. (2017). Isothermal amplification of environmental DNA (eDNA) for direct field-based monitoring and laboratory confirmation of *Dreissena* sp. *PLoS One*, 12(10), e0186462.
- Wohl, E. (2019). Forgotten legacies: Understanding and mitigating historical human alterations of river corridors. *Water Resources Research*, 55(7), 5181-5201.
- Wolff, A., Gooch, D., Montaner, J. J. C., Rashid, U., & Kortuem, G. (2016). Creating an understanding of data literacy for a data-driven society. *The Journal of Community Informatics*, 12(3).
- Wu, J., Negishi, J. N., Izumi, H., Kanbe, T., Mizumoto, H., & Araki, H. (2024). Application of eDNA methods to evaluate abundance and reproduction of winter-breeding freshwater mussels (*Buldowskia iwakawai*) in the Ishikari River floodplain. *Hydrobiologia*, 851(3), 541-558.
- Xu, Y., Huang, F., Zhou, M., Gu, R., Zhu, J., Rong, Q., & Cai, Y. (2023). Recognizing topological attributes and spatiotemporal patterns in spotted seals (*Phoca largha*) trophic networks based on eDNA metabarcoding. *Frontiers in Marine Science*, 10, 1305763.
- Yamamoto, S., Masuda, R., Sato, Y., Sado, T., Araki, H., Kondoh, M., ... & Miya, M. (2017). Environmental DNA metabarcoding reveals local fish communities in a species-rich coastal sea. *Scientific reports*, 7(1), 40368.
- Yates, M. C., Fraser, D. J., & Derry, A. M. (2019). Meta-analysis supports further refinement of eDNA for monitoring aquatic species-specific abundance in nature. *Environmental DNA*, 1(1), 5-13.
- Yatsuyanagi, T., Ishida, R., Sakata, M. K., Kanbe, T., Mizumoto, H., Kobayashi, Y., Kamada, S., Namba, S., Nii, H., Minamoto, T., & Araki, H. (2019). Environmental DNA monitoring for short-term Reproductive migration of endemic anadromous species, Shishamo smelt (*Spirinchus lanceolatus*). *Environmental DNA*, 2(2), 130–139. [https:// doi.org/10.1002/edn3.50](https://doi.org/10.1002/edn3.50)